NASA TECHNICAL NOTE
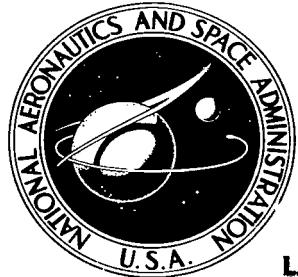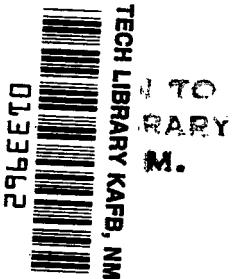
NASA TN D-8236 c.1

NASA TN D-8236

WIND-TUNNEL INVESTIGATION
OF A FOWLER FLAP AND SPOILER FOR
AN ADVANCED GENERAL AVIATION WING

John W. Paulson, Jr.

Langley Research Center
Hampton, Va. 23665

NATIONAL AERONAUTICS AND SPACE ADMINISTRATION • WASHINGTON, D. C. • JUNE 1976

1. Report No. NASA TN D-8236	2. Government Accession No.	3. Recipient's Catalog No.
4. Title and Subtitle WIND-TUNNEL INVESTIGATION OF A FOWLER FLAP AND SPOILER FOR AN ADVANCED GENERAL AVIATION WING		5. Report Date June 1976
		6. Performing Organization Code
7. Author(s) John W. Paulson, Jr.		8. Performing Organization Report No. L-10736
9. Performing Organization Name and Address NASA Langley Research Center Hampton, Va. 23665		10. Work Unit No. 505-10-11-03
		11. Contract or Grant No.
12. Sponsoring Agency Name and Address National Aeronautics and Space Administration Washington, D.C. 20546		13. Type of Report and Period Covered Technical Note
		14. Sponsoring Agency Code

15. Supplementary Notes

16. Abstract

   An investigation has been conducted in the Langley Research Center V/STOL tunnel to determine the effects of adding a Fowler flap and spoiler to an advanced general aviation wing. The wing was tested without fuselage or empennage and was fitted with approximately three-quarter-span Fowler flaps and half-span spoilers. The spoilers were hinged at the 70-percent chord point and vented when the flaps were deflected. Static longitudinal and lateral aerodynamic data were obtained over an angle-of-attack range of -8° to 22° for various flap deflections and positions, spoiler geometries, and vent-lip geometries.

   Lateral characteristics indicate that the spoilers are generally adequate for lateral control. However, the spoilers do have a region of low effectiveness when deflected less than 10° or 15°, especially when the flaps are deflected 30° or 40°. In general, the spoiler effectiveness increases with increasing angle of attack, increases with increasing flap deflections, and is influenced by vent-lip geometry. In addition, the data show that some two-dimensional effects on spoiler effectiveness are reduced in the three-dimensional case. Results also indicate the expected significant increase in lift coefficient as the Fowler flaps are deflected; when the flap was fully deflected, the maximum wing lift coefficient was increased about 96 percent.

17. Key Words (Suggested by Author(s)) Lateral control Spoilers Fowler flaps General aviation	18. Distribution Statement Unclassified – Unlimited Subject Category 08	
19. Security Classif. (of this report) Unclassified	20. Security Classif. (of this page) Unclassified	21. No. of Pages 78	22. Price* $4.75

WIND-TUNNEL INVESTIGATION OF A FOWLER FLAP AND SPOILER

FOR AN ADVANCED GENERAL AVIATION WING

John W. Paulson, Jr.
Langley Research Center

SUMMARY

An investigation has been conducted in the Langley Research Center V/STOL tunnel to determine the effects of adding a Fowler flap and spoiler to an advanced general aviation wing. The wing was tested without fuselage or empennage and was fitted with approximately three-quarter-span Fowler flaps and half-span spoilers. The spoilers were hinged at the 70-percent chord point and vented when the flaps were deflected. Static longitudinal and lateral aerodynamic data were obtained over an angle-of-attack range of -8° to 22° for various flap deflections and positions, spoiler geometries, and vent-lip geometries.

Lateral characteristics indicate that the spoilers are generally adequate for lateral control. However, the spoilers do have a region of low effectiveness when deflected less than 10° or 15°, especially when the flaps are deflected 30° or 40°. In general, the spoiler effectiveness increases with increasing angle of attack, increases with increasing flap deflections, and is influenced by vent-lip geometry. In addition, the data show that some two-dimensional effects on spoiler effectiveness are reduced in the three-dimensional case. Results also indicate the expected significant increase in lift coefficient as the Fowler flaps are deflected; when the flap was fully deflected, the maximum wing lift coefficient was increased about 96 percent.

INTRODUCTION

The development of new, thick, high-lift airfoil sections has had a profound effect on the general aviation community because these sections offer the possibility of improved performance on several new light aircraft designs. These airfoils provide higher maximum lift coefficients than the conventional 64-Series airfoils used on many general aviation aircraft. This increase in maximum lift coefficient allows the use of a smaller, more highly loaded wing with less wetted area. These developments can increase cruise performance and improve ride quality. The increased thickness of these airfoils also provides the opportunity for wing structural weight savings.

With an appropriate high-lift device such as a full-span Fowler flap, further reductions in wing area may be achieved, and the desirable low landing speeds of typical light aircraft can be maintained. Full-span flaps, however, generally preclude the use of conventional ailerons, and an alternate method of lateral control is needed. One such method would use partial span spoilers (also known as slot-lip ailerons). Several airplanes which use Fowler flaps with the advanced airfoils are already in either the design stage or early flight-test stage of development. (See ref. 1.) Some of these airplanes use the 17-percent-thick General-Aviation (Whitcomb)-1 airfoil usually referred to as the GA(W)-1. (See refs. 2 and 3.) One particular aircraft which uses this airfoil is the Advanced Technology light twin (ATLIT). (See ref. 1.) This aircraft uses nearly full-span Fowler flaps for low-speed performance and half-span spoilers for lateral control. These spoilers are vented when the flaps are extended and unvented when the flaps are retracted.

Before the original flight of the ATLIT, there was concern about the effectiveness of the spoilers at small deflections when the flaps were deflected 40° because of two-dimensional data (refs. 4 and 5). The data of reference 4 indicated that the spoilers had a region of very low effectiveness when deflected less than 10° or 15°. In addition, there was control reversal under certain conditions. If a small left spoiler deflection was given in an effort to produce a negative (left wing down) rolling moment, the result was actually a positive (right wing down) rolling moment. This investigation was undertaken to determine to what extent, if any, these two-dimensional effects were present on a three-dimensional wing.

The investigation was conducted in the Langley V/STOL tunnel by using a rectangular wing with Fowler flap and spoilers. Static forces and moments were obtained for the wing with various flap deflections and positions, spoiler deflections, spoiler cross-section geometries, and vent-lip geometries.

SYMBOLS

The data are presented in the stability-axis system shown in figure 1. The model moment center was 25 percent of the wing chord. All measurements and calculations were made in U.S. Customary Units; however, all values contained in this study are given in both SI and U.S. Customary Units. (See ref. 6.)

b   wing span (without subscript), span of flap, or vented spoiler (with subscript), m (ft)

C_D drag coefficient, $\dfrac{\text{Drag}}{q_{\infty}S}$

C_L lift coefficient, $\dfrac{\text{Lift}}{q_\infty S}$

C_l rolling-moment coefficient, $\dfrac{\text{Rolling moment}}{q_\infty S b}$

C_m pitching-moment coefficient, $\dfrac{\text{Pitching moment}}{q_\infty S \bar{c}}$

C_n yawing-moment coefficient, $\dfrac{\text{Yawing moment}}{q_\infty S b}$

C_Y side-force coefficient, $\dfrac{\text{Side force}}{q_\infty S}$

c wing chord, m   (ft)

$\bar{c}$ mean aerodynamic chord, m   (ft)

p roll rate, rad/sec

$pb/2V_\infty$ wing-tip helix angle, rad (see appendix)

q_∞ free-stream dynamic pressure, Pa   (lbf/ft^2)

R radius, percent of wing chord

S wing area, m^2 (ft^2)

V_∞ free-stream velocity, m/sec   (ft/sec)

x longitudinal dimension (see fig. 1)

$x/\bar{c}$ longitudinal distance from wing leading edge with respect to mean aerodynamic chord

y lateral dimension (see fig. 1)

z   vertical dimension (see fig. 1)

α angle of attack of model reference line, positive nose up (fig. 1), deg

δ deflection of flap or spoiler (fig. 3), deg

Subscripts:

f   flap

max   maximum

s   spoiler

APPARATUS AND PROCEDURES

This investigation was conducted in the Langley V/STOL tunnel in support of the ATLIT aircraft program to determine the general characteristics of an ATLIT-type Fowler flap and spoiler lateral-control system. An existing aspect-ratio-8.98 rectangular wing with the GA(W)-1 airfoil section was modified to accept the Fowler flap and spoiler as shown in figures 2 and 3(a). The wind-tunnel model was not intended to represent the ATLIT tapered wing exactly but rather to be a general representation of the ATLIT Fowler flap and spoiler system. Tables I and II give the coordinates of the GA(W)-1 wing section and flap section, respectively. The wing had a span of 4.01 m (13.16 ft), a chord of 0.45 m (1.46 ft), and an area of 1.79 m^2 (19.31 ft^2). When the flaps were fully deflected, the wing area was increased by 17 percent to 2.10 m^2 (22.59 ft^2). The wing root was at an incidence of 2° and the wing was linearly twisted to a tip incidence of 0°. For this investigation, the model reference line was defined to be the wing-tip chord line.

The Fowler flaps were made in four sections on each wing panel (fig. 2) but were always deflected as a unit. Each flap section was mounted on brackets to allow deflections of 0°, 10°, 20°, 30°, and 40°. Table III shows a complete listing of flap deflection and position as well as the spoiler and vent-lip geometries for this investigation. Figure 3(b) shows the flap overlap and gap dimensions corresponding to the various flap deflections and positions. The flap chord was 30 percent of the wing chord and the flap span ratio $b_f/b/2$ was 0.764.

The spoilers were made in four sections for the left wing panel only. (See fig. 2.) In order to simulate the ATLIT spoiler-span wing-span ratio, only the three outboard sections were deflected during the investigation; the inboard section (spoiler section a)

4

remained sealed at all times. The three operative spoiler sections (b, c, and d) had a span ratio $b_S/b/2$ of 0.572 and were hinged at $x/\bar{c} = 0.70$. (See figs. 2 and 3(a).) The hinge line was offset $0.015\bar{c}$ forward of the leading edge of the spoiler so that the trailing edge of the spoilers was located at $x/\bar{c} = 0.80$ when $\delta_S = 0^\circ$. This offset hinge line allowed a gap to open between the wing upper surface and the spoiler leading edge as the spoiler was deflected. (See fig. 4.) Each spoiler section was removable and could be replaced with one of three spoiler cross-section geometries (also shown in fig. 4). The vent lip (the downstream lip of the spoiler vent) as well as the spoiler geometry was varied during the test as shown in figure 5. The model installation in the V/STOL tunnel is shown in figures 6 and 7.

Most of the investigation time was concentrated on the cases with 40° flap deflection. At 40° flap deflection, the control effectiveness problem areas which were indicated in the two-dimensional data of reference 4 were examined over a spoiler-deflection range of 0° to 45° for different combinations of spoiler cross-section geometry and vent-lip geometry. Lower flap deflections were tested to obtain longitudinal and lateral data, but these tests were run by using only the triangular backed spoiler (spoiler B) and the large radius vent lip. Angle of attack ranged from -8° to wing stall.

Most of the data were obtained at a dynamic pressure of 1.44 kPa (30 lbf/ft^2); however, because of hardware constraints, some data were obtained at a dynamic pressure of 0.48 kPa (10 lbf/ft^2). Whenever the dynamic pressure was lowered to 0.48 kPa (10 lbf/ft^2), a single pair of runs was made with the identical configuration at both the high and low dynamic pressures to establish Reynolds number effects. The Reynolds numbers corresponding to these dynamic pressures are 1.49×10^6 and 0.85×10^6, respectively. It should be noted that at the lowest dynamic pressure, the Reynolds number is subcritical over a large portion of the wing chord.

Transition was fixed at 2.24 cm (0.88 in.) downstream from the leading edge for the upper surface and 4.32 cm (1.70 in.) on the lower surface (ref. 7). Data were corrected for tunnel wall effects of reference 8; no other corrections were applied.

PRESENTATION OF RESULTS

The data of this investigation have been reduced to coefficient form and are presented in the following figures:

DISCUSSION

The effects of spoiler deflection, with various flap positions, cross-section geome-tries, and vent-lip geometries, on the longitudinal and lateral characteristics of the wing are presented in figures 8 to 12. It may be seen from these data (particularly C_L and C_l plotted against α) that the vented spoiler effectiveness is very low when deflected less than 10° to 15°. In figure 13, the sequential spoiler deflections (sequences 1 and 2) confirm the trends of the previous data; the spoiler effectiveness remains low until the spoiler elements are deflected 15°. The data of figures 8 to 13 were used to construct the lift, drag, and pitching-moment curves of figure 15 with $\delta_s = 0^O$ and the rolling-moment curves of figures 16 to 18.

The effects of Reynolds number are presented in figure 14. The effects on the lon-gitudinal data were small with the typical increase in $C_{L,max}$ at the higher Reynolds number. The effects on the lateral data were somewhat inconsistent but generally not large.

Longitudinal Characteristics

The data of figure 15(a) show the longitudinal characteristics of the wing at flap deflections of 0°, 10°, 30°, and 40°. The basic wing has a design lift coefficient of 0.4 at $\alpha = 0.5^O$ and a maximum lift coefficient of 1.32 at $\alpha = 16.7^O$. At the maximum flap deflection $(\delta_f = 40^O)$, the maximum lift coefficient is increased 96 percent to 2.59 at $\alpha = 12^O$. Figure 15(b) shows the effect of moving the flap at $\delta_f = 40^O$ from $x/\bar{c} = 1.00$ to 0.96. Both lift and drag are reduced as the flap loses some effectiveness when moved beneath the trailing edge of the wing. The drag curves show the typical high drag levels associated with the large flap deflections. In addition to the high lift and drag, the flaps produce large nose-down pitching moments which must be trimmed for aircraft applications.

Lateral Characteristics

The rolling moments generated when spoiler B was deflected at various flap settings are given in figure 16. For the clean wing configuration $\left(\delta_f = 0^o, \text{fig. 16(a)}\right)$, the rolling-moment variation with spoiler deflection is reasonably linear, but somewhat less effective than that of conventional ailerons (ref. 9). At the maximum spoiler deflection of 45°, the wing-tip helix angle $pb/2V_\infty$ is 0.044; this helix angle is low according to reference 10 which states that 0.07 is an acceptable level. (The method used to calculate $pb/2V_\infty$ is discussed in the appendix.) However, a more realistic maximum deflection might be 60° or 70°; such a deflection would probably increase $pb/2V_\infty$ to a more acceptable level. This low effectiveness is apparent only with $\delta_f = 0^o$; with the flaps deflected, $pb/2V_\infty$ is significantly higher.

When the flaps are deflected 10° at $x/\bar{c} = 0.917$ (fig. 16(b)), the rolling-moment variation with spoiler deflection becomes more nonlinear and develops three rather distinct regions of effectiveness. A region of low spoiler effectiveness below $\delta_s = 15^o$ becomes apparent. A region of increasing effectiveness between $\delta_s = 15^o$ and 20° follows. Finally, the region above $\delta_s = 20^o$ shows fairly high levels of spoiler effectiveness. Although these regions are not pronounced at the 10° flap deflection, they do indicate the trends which become rather large at the 30° and 40° flap deflections.

Figure 16(b) shows that the rolling moments become more sensitive to angle of attack as the flap is deflected. The clean wing had a variation in maximum C_l from 0.045 to 0.050 at angles of attack of -4° to 8°, and the wing with $\delta_f = 10^o$ had a variation in maximum C_l from 0.056 to 0.073 at angles of attack from -4° to 8°. The wing with $\delta_f = 10^o$ and $\delta_s = 45^o$ had a $pb/2V_\infty$ ranging from 0.046 to 0.059 corresponding to the higher rolling moments. The higher $pb/2V_\infty$ is indicative of the increased control power available with the flaps deflected.

When the flaps are deflected 30° at $x/\bar{c} = 0.960$ (fig. 16(c)), the rolling-moment variation with spoiler deflection becomes very nonlinear and is segmented into three very distinct regions. These regions correspond to the regions of the data at $\delta_f = 10^o$ discussed earlier, but are much more pronounced. The region of low spoiler effectiveness below $\delta_f = 10^o$ which was of concern in the two-dimensional data is very apparent. As in the 10° flap-deflection case, the rolling moments are sensitive to angle of attack with maximum C_l varying from 0.099 to 0.122 at angles of attack of -4° and 8°. The $pb/2V_\infty$ corresponding to each of these rolling moments was 0.083 to 0.099. Here again the increased control power available with the flaps deflected was shown. Although these data are quite nonlinear, they are smooth, without reversals in slope, and appear to be adequate for lateral control.

When the flaps are deflected 40° at $x/\bar{c} = 1.00$ (fig. 16(d)), the rolling-moment variation with spoiler deflection still indicates three regions of spoiler effectiveness;

however, the data in the low effectiveness region ($\delta_S = 15^O$) show large reversals in slope. This change in spoiler effectiveness is probably caused by intermittent flow separation downstream of the vent. Above $\delta_S = 15^O$, however, the spoiler effectiveness no longer shows slope reversals. The rolling moments are still sensitive to angle of attack, and the $pb/2V_\infty$ ranging from 0.089 to 0.123 shows a further increase in control power available at $\delta_f = 40^O$. It should be noted that this configuration did have the large radius vent lip and that some of the slope reversals present at $\delta_S \leqq 15^O$ were corrected when different vent-lip geometries were used.

Effect of Vent-Lip Geometry and Flap Effectiveness

The two-dimensional models of reference 4 used vent-lip geometries which were similar to both the blunt-lip and the sharp-lip geometries used in the three-dimensional models. It was originally thought that the regions of low spoiler effectiveness and control reversals (regions of concern in ref. 4) were the result of flow separation downstream of the sharp-edged vent lips. Control reversals were defined as a change in sign of the rolling moment. (A left spoiler up control input to give a negative (left wing down) rolling moment would actually produce a positive (right wing down) rolling moment.) The two additional radius vent lips were intended to reduce these problems. As figure 17 shows, the rolling-moment data for the large and small radius vent lips and flaps deflected 40° do not show control reversals, and the data for sharp and blunt vent lips and flaps deflected 40° show only very slight control reversals. The two-dimensional control reversals evident in reference 4 are either eliminated or greatly reduced in the three-dimensional model. However, there was in all cases a region of low spoiler effectiveness below $\delta_S = 10^O$ to 15°. As shown previously in figure 16(d), the rolling-moment data for the large radius vent lip had large reversals in slope below $\delta_S = 15^O$. However, none of the other vent-lip geometries exhibited such reversals at either flap location $x/\bar{c} = 0.96$ or 1.00. In general, the spoiler effectiveness increased with increasing angle of attack both in the lower effectiveness region and at the higher spoiler deflections for all vent-lip geometries. Also, the spoiler effectiveness is higher with the blunt vent lip and with the flap located at $x/\bar{c} = 1.00$. Moving the flap from $x/\bar{c} = 0.96$ to 1.00 shows the same trend as that shown in figure 16; the spoiler effectiveness increases with increasing flap effectiveness.

Some data were obtained using other spoiler geometries on this wing. Spoiler C was similar to the spoilers used on a currently operational high performance general aviation aircraft. The third spoiler studied, spoiler A, was the T-type. The data for these spoilers with flaps deflected 40° are presented in figures 18 and 19 and show the same general characteristics of the data for spoiler B.

SUMMARY OF RESULTS

An investigation has been conducted to determine the effects of adding a full-span Fowler flap and half-span spoiler to an advanced general aviation wing. The results have shown:

1. In general, the three-dimensional data concurred with two-dimensional data of the references. The regions of decreased spoiler effectiveness are limited to spoiler deflections less than 10^0 to 15^0 and are most prominent at the highest flap deflections. However, the general effect of the three-dimensional model was to reduce many of the characteristics measured with the two-dimensional model.

2. The spoilers generally show acceptable lateral-control characteristics except for some regions of low effectiveness at small spoiler deflections.

3. The spoiler effectiveness was increased when the flap deflection was increased.

4. The spoiler effectiveness was increased when the angle of attack was increased and the flaps were deflected.

5. The spoiler effectiveness was affected by vent-lip geometry, and the blunt vent lip gave the highest rolling moment.

6. The Fowler flaps, as expected, significantly increased maximum lift coefficient; the maximum lift coefficient was increased 96 percent for the maximum flap deflection.

Langley Research Center
National Aeronautics and Space Administration
Hampton, Va. 23665
May 4, 1976

APPENDIX

COMPUTATION OF WING-TIP HELIX ANGLE

The computation of the wing-tip helix angle from steady-state lateral data depends on the ability to determine the roll-damping derivative C_{l_p}. Reference 10 gives an equation for the wing-tip helix angle

$$\frac{pb}{2V_\infty} = \frac{C_{l_\delta}}{\tau} \frac{\tau \delta_a K}{114.6 C_{l_p}}$$

where

C_{l_δ} change in rolling moment per degree of spoiler deflection

δ_a spoiler deflection in degrees

τ ratio of spoiler chord to wing chord

K correction to spoiler effectiveness because of large deflections

All these terms actually reduce to the rolling moment measured on the model with a lateral control deflected. The roll-damping derivative C_{l_p} may be estimated from reference 11 which uses a vortex-lattice type of theoretical prediction method, or C_{l_p} may be estimated from the charts in reference 10. For this report, the method of reference 11 was used. Therefore, $pb/2V_\infty$ may be written as

$$\frac{pb}{2V_\infty} = \frac{\left(C_l\right)_{measured}}{\left(C_{l_p}\right)_{calculated}}$$

REFERENCES

1. Crane, Harold L.; McGhee, Robert J.; and Kohlman, David L.: Applications of Advanced Aerodynamic Technology to Light Aircraft. [Preprint] 730318, Soc. Automot. Eng., Apr. 1973.

2. McGhee, Robert J.; and Beasley, William D.: Low-Speed Aerodynamic Characteristics of a 17-Percent-Thick Airfoil Section Designed for General Aviation Applications. NASA TN D-7428, 1973.

3. Wentz, W. H., Jr.; and Seetharam, H. C.: Development of a Fowler Flap System for a High Performance General Aviation Airfoil. NASA CR-2443, 1974.

4. Wentz, W. H., Jr.: Effectiveness of Spoilers on the GA(W)-1 Airfoil With a High Performance Fowler Flap. NASA CR-2538, 1975.

5. Wenzinger, Carl J.; and Rogallo, Francis M.: Wind-Tunnel Investigation of Spoiler, Deflector, and Slot Lateral-Control Devices on Wings With Full-Span Split and Slotted Flaps. NACA Rep. 706, 1941.

6. Mechtly, E. A.: The International System of Units — Physical Constants and Conversion Factors (Second Revision). NASA SP-7012, 1973.

7. Braslow, Albert L.; and Knox, Eugene C.: Simplified Method for Determination of Critical Height of Distributed Roughness Particles for Boundary-Layer Transition at Mach Numbers From 0 to 5. NACA TN 4363, 1958.

8. Gillis, Clarence L.; Polhamus, Edward C.; and Gray, Joseph L., Jr.: Charts for Determining Jet-Boundary Corrections for Complete Models in 7- by 10-Foot Closed Rectangular Wind Tunnels. NACA WRL-123, 1945. (Formerly NACA ARR L5G31.)

9. Paulson, John W., Jr.: Wind-Tunnel Test of a Conventional Flap and Aileron and a Fowler Flap and Slot-Lip Aileron for an Advanced General Aviation Wing. Paper 750501, Soc. Automot. Eng., Apr. 1975.

10. Perkins, Courtland D.; and Hage, Robert E.: Airplane Performance Stability and Control. John Wiley & Sons, Inc., c.1949.

11. Tulinius, J.; Clever, W.; Niemann, A.; Dunn, K.; and Gaither, B.: Theoretical Prediction of Airplane Stability Derivatives at Subcritical Speeds. NASA CR-132681, [1973].

TABLE I. - GENERAL-AVIATION (WHITCOMB)-1

AIRFOIL COORDINATES

Upper surface		Lower surface	
x/c	z/c	x/c	z/c
0.00000	0.00000	0.00000	0.00000
.00200	.01300	.00200	-.00930
.00500	.02040	.00500	-.01380
.01250	.03070	.01250	-.02050
.02500	.04170	.02500	-.02690
.03750	.04965	.03750	-.03190
.05000	.05589	.05000	-.03580
.07500	.06551	.07500	-.04210
.10000	.07300	.10000	-.04700
.12500	.07900	.12500	-.05100
.15000	.08400	.15000	-.05430
.17500	.08840	.17500	-.05700
.20000	.09200	.20000	-.05930
.25000	.09770	.25000	-.06270
.30000	.10160	.30000	-.06450
.35000	.10400	.35000	-.06520
.40000	.10491	.40000	-.06490
.45000	.10445	.45000	-.06350
.50000	.10258	.50000	-.06100
.55000	.09910	.55000	-.05700
.57500	.09668	.57500	-.05400
.60000	.09371	.60000	-.05080
.62500	.09006	.62500	-.04690
.65000	.08599	.65000	-.04280
.67500	.08136	.67500	-.03840
.70000	.07634	.70000	-.03400
.72500	.07092	.72500	-.02940
.75000	.06513	.75000	-.02490
.77500	.05907	.77500	-.02040
.80000	.05286	.80000	-.01600
.82500	.04646	.82500	-.01200
.85000	.03988	.85000	-.00860
.87500	.03315	.87500	-.00580
.90000	.02639	.90000	-.00360
.92500	.01961	.92500	-.00250
.95000	.01287	.95000	-.00260
.97500	.00609	.97500	-.00400
1.00000	-.00070	1.00000	-.00800

TABLE II.- THIRTY PERCENT c FOWLER FLAP COORDINATES

[Leading-edge radius = 0.0122c]

Upper surface		Lower surface	
x_f/c	z_f/c	x_f/c	z_f/c
0.000	-0.01920	0.000	-0.01920
.025	.00250	.025	-.02940
.050	.01100	.050	-.02490
.075	.01630	.075	-.02040
.100	.01900	.100	-.01600
.125	.01950	.125	-.01200
.150	.01820	.150	-.00860
.175	.01670	.175	-.00580
.200	.01330	.200	-.00360
.225	.00950	.225	-.00250
.250	.00530	.250	-.00260
.275	.00100	.275	-.00400
.300	-.00435	.300	-.00800

TABLE III.- CONFIGURATIONS INVESTIGATED

Spoiler geometry	Vent-lip geometry	Flap deflection and position, $\delta_f/x/\bar{c}$
Triangular back, spoiler B	Blunt	$0^o/0.713$, $20^o/0.96$, $40^o/0.96$, $40^o/1.00$
	Small radius	$40^o/0.96$
	Large radius	$10^o/0.917$, $30^o/0.96$, $40^o/0.96$, $40^o/1.00$
	Sharp	$40^o/1.00$
Triangular back, spoiler B (sequential deflection)	Large radius	$40^o/1.00$
Contoured back, spoiler C	Small radius	$40^o/0.96$
	Large radius	$40^o/0.96$
	Sharp	$40^o/1.00$
T-type back, spoiler A	Large radius	$40^o/0.96$
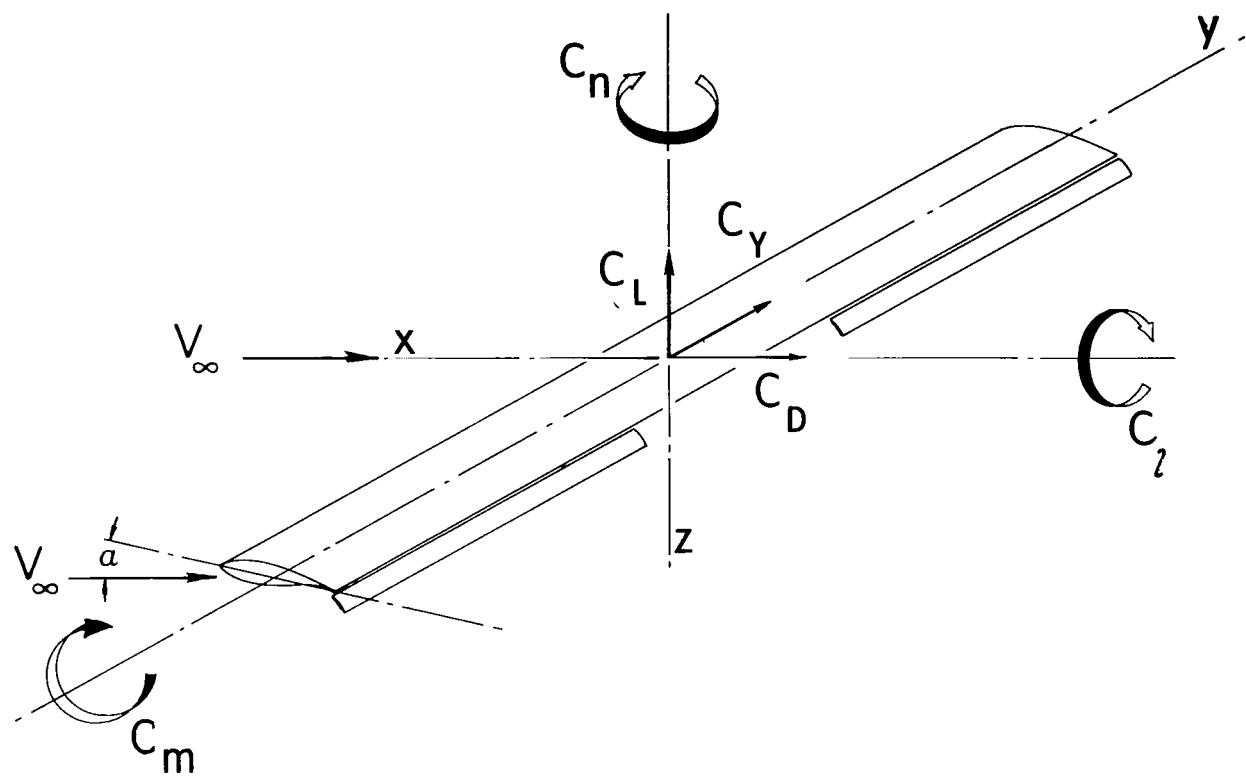
Figure 1.- Stability-axis system used in data presentation.
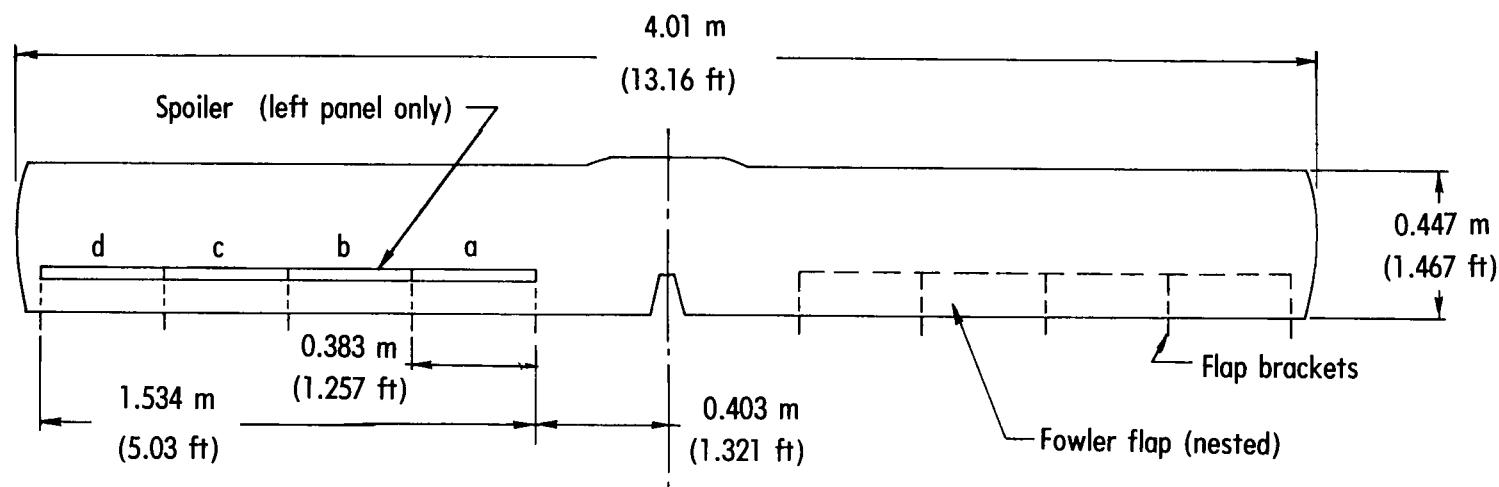
Figure 2.- Plan view of wing.

x/c = 0.7   x/c = 0.8   x/c = 1.0

x/c = 0

Spoiler

Leading-edge gap

45°

Vent

Flap nested

Vent lip

Fowler flap

40°
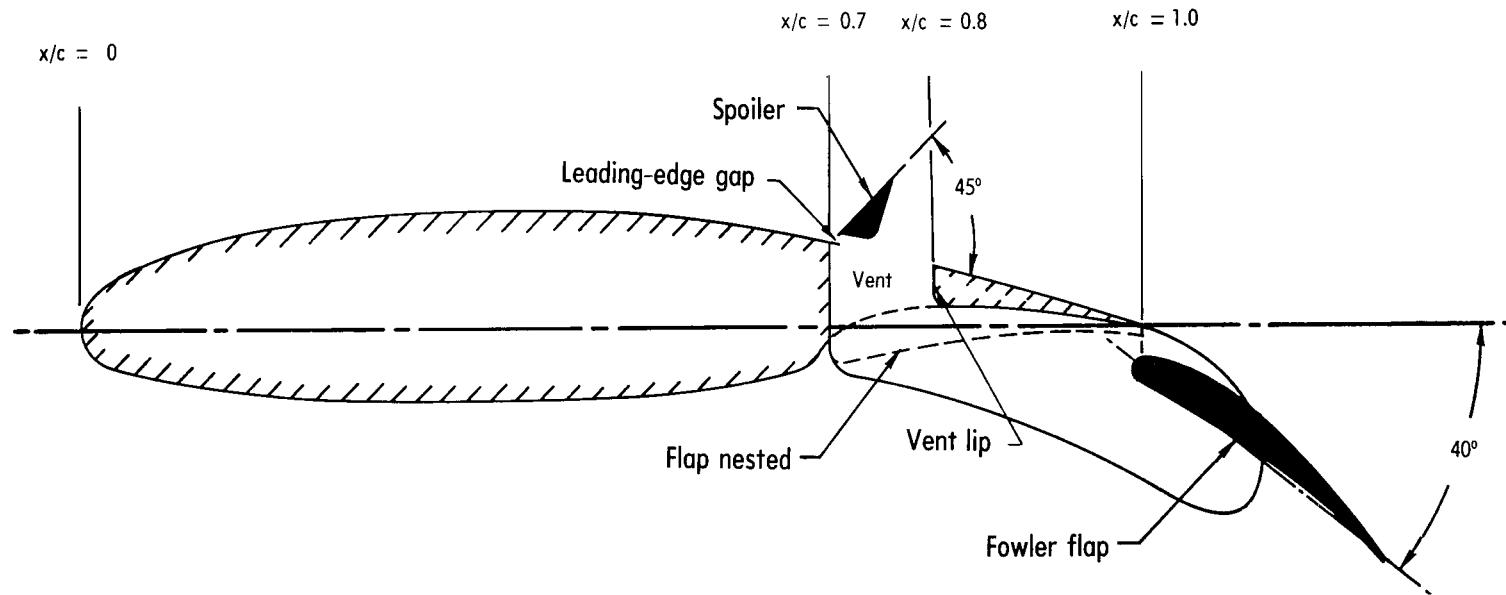
(a) GA(W)-1 airfoil with Fowler flap and spoiler.

Figure 3.- Flap deflections and positions.
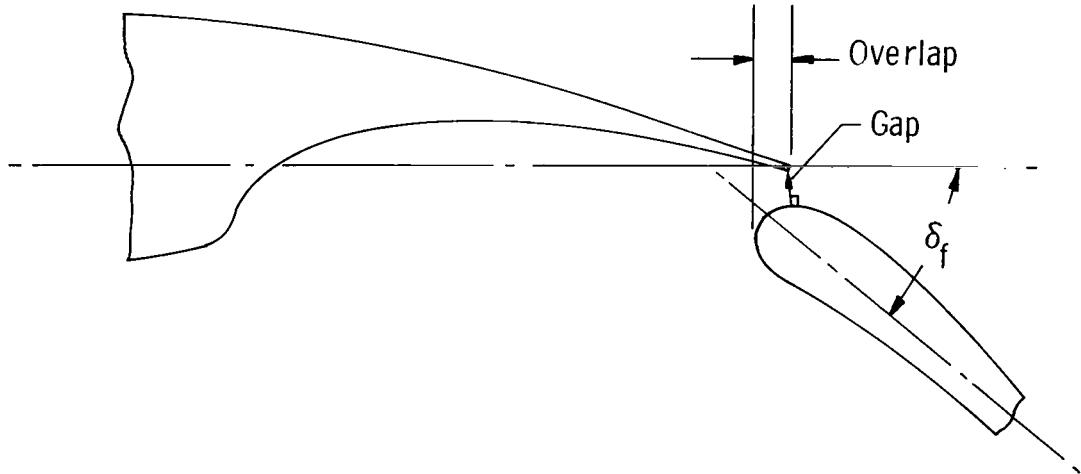
δ_f, deg	Overlap, percent $\bar{c}$	Gap, percent $\bar{c}$
0*	30.0	0
10*	9.6	3.1
20	5.3	2.6
30	5.3	3.6
40	5.3	3.6
40*	1.3	2.5

*ATLIT configurations

(b) Fowler-flap overlap and gap dimensions.

Figure 3.- Concluded.

x/c=0.70

0.100c

0.015c

0.003c

Spoiler A
T-type back

0.023c

Hinge line

0.023c

Spoiler B
Triangular back

Leading-edge gap

0.017c

Hinge

Wing upper surface

Spoiler C
Contoured back

0.007c

0.057c R

0.029c R

0.031c
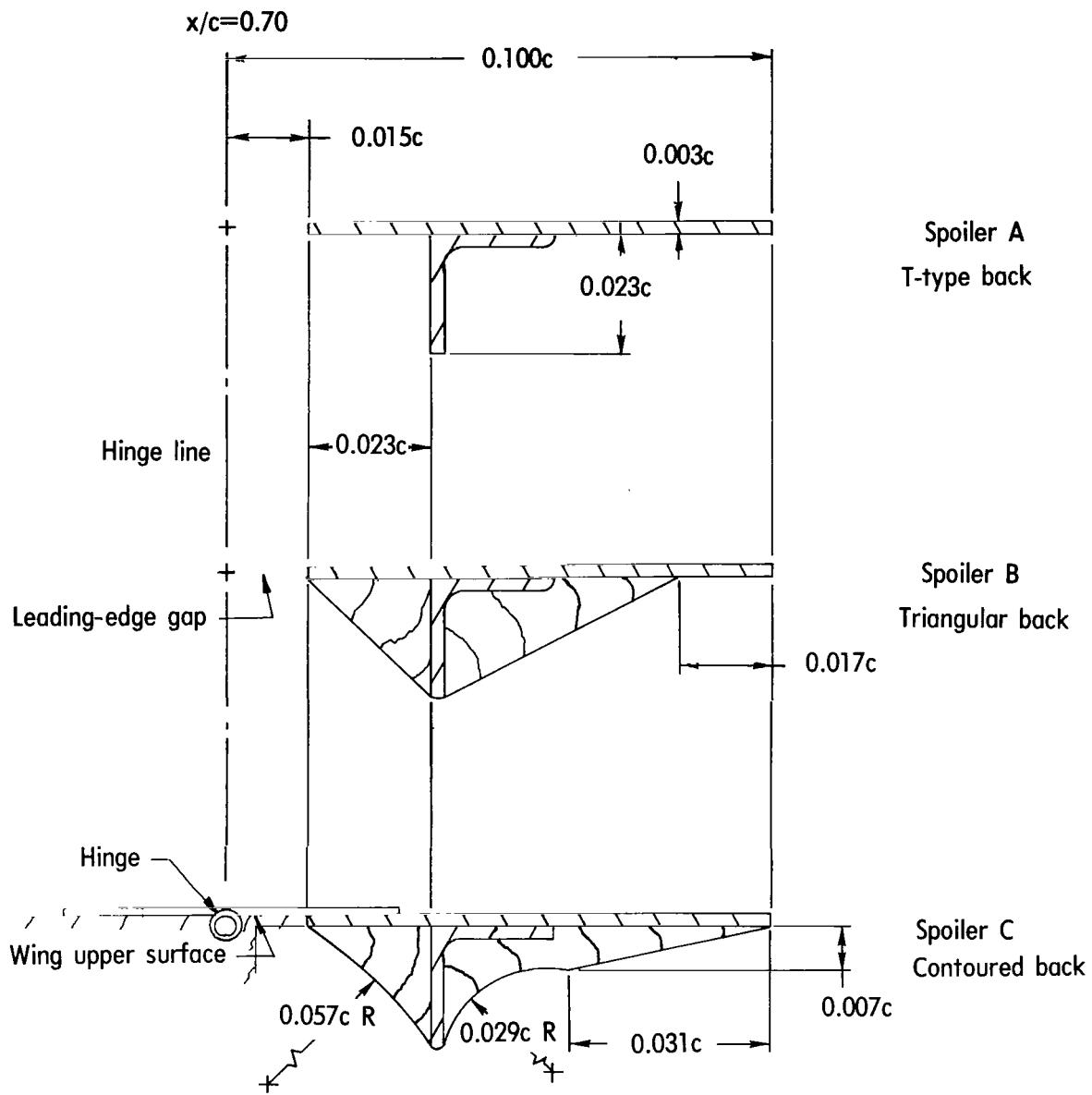
Figure 4.- Cross-section geometry of the three spoilers.

x/c = 0.80

Blunt

R = 0.011c

Small radius

R = 0.014c

Large radius

R = 0.020c

0.152 cm (0.06 in) aluminum plate

Sharp

x/c = 0.839
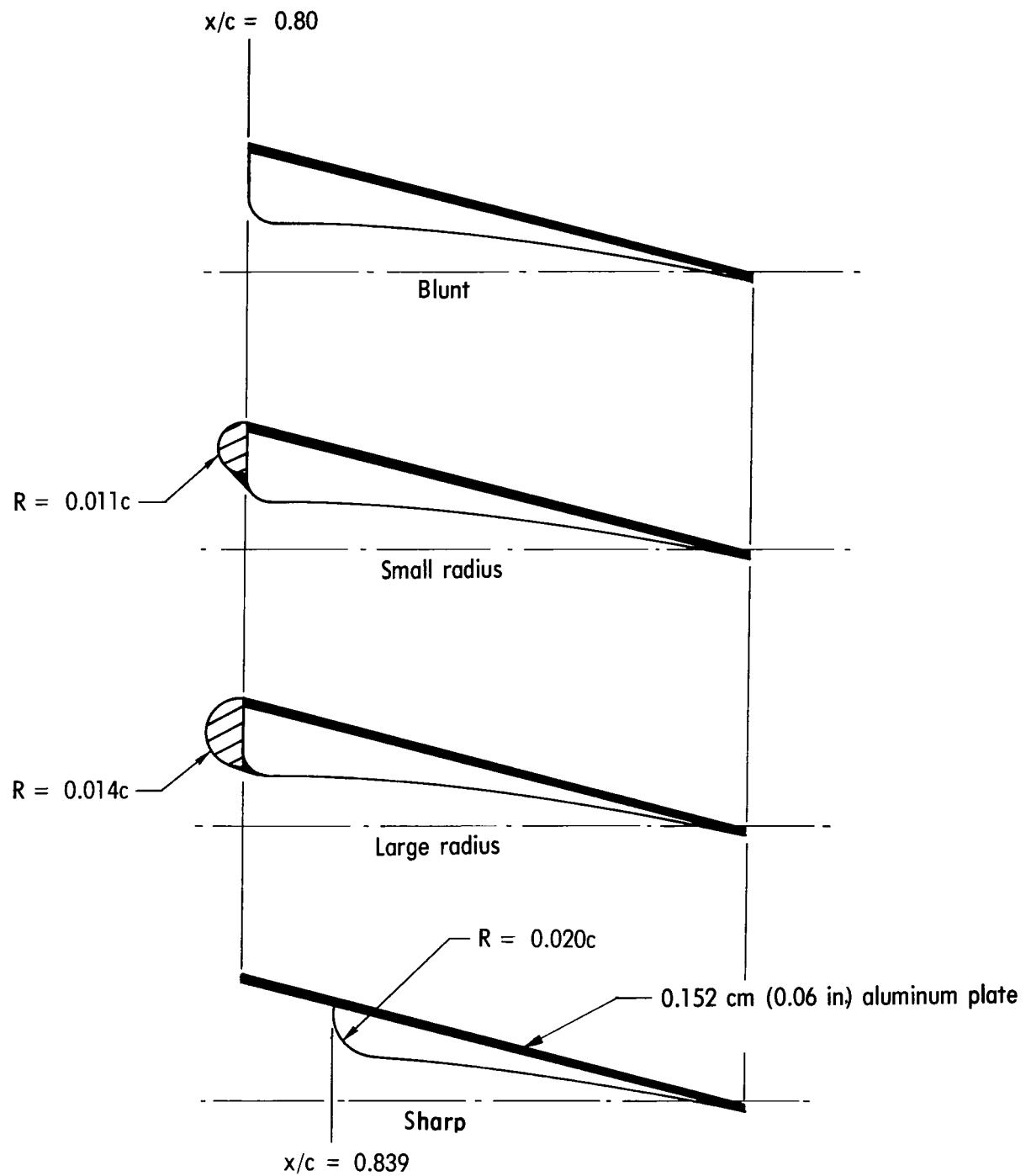
Figure 5.- Cross-section geometry of the four vent lips.
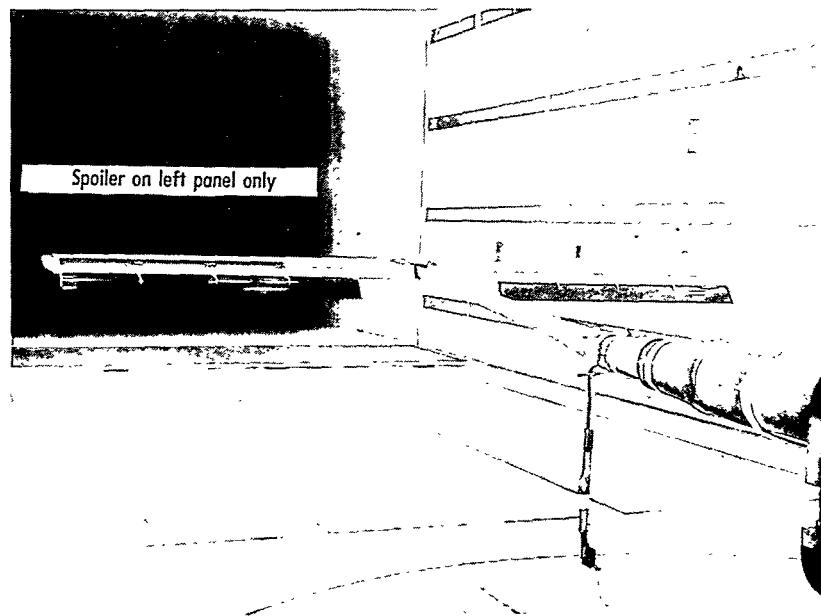
(a) Rear view.

(b) Front view.

L-76-191

Figure 6.- General aviation wing in Langley V/STOL tunnel test section.

Spoiler deflected 45⁰

Flap deflected 40⁰
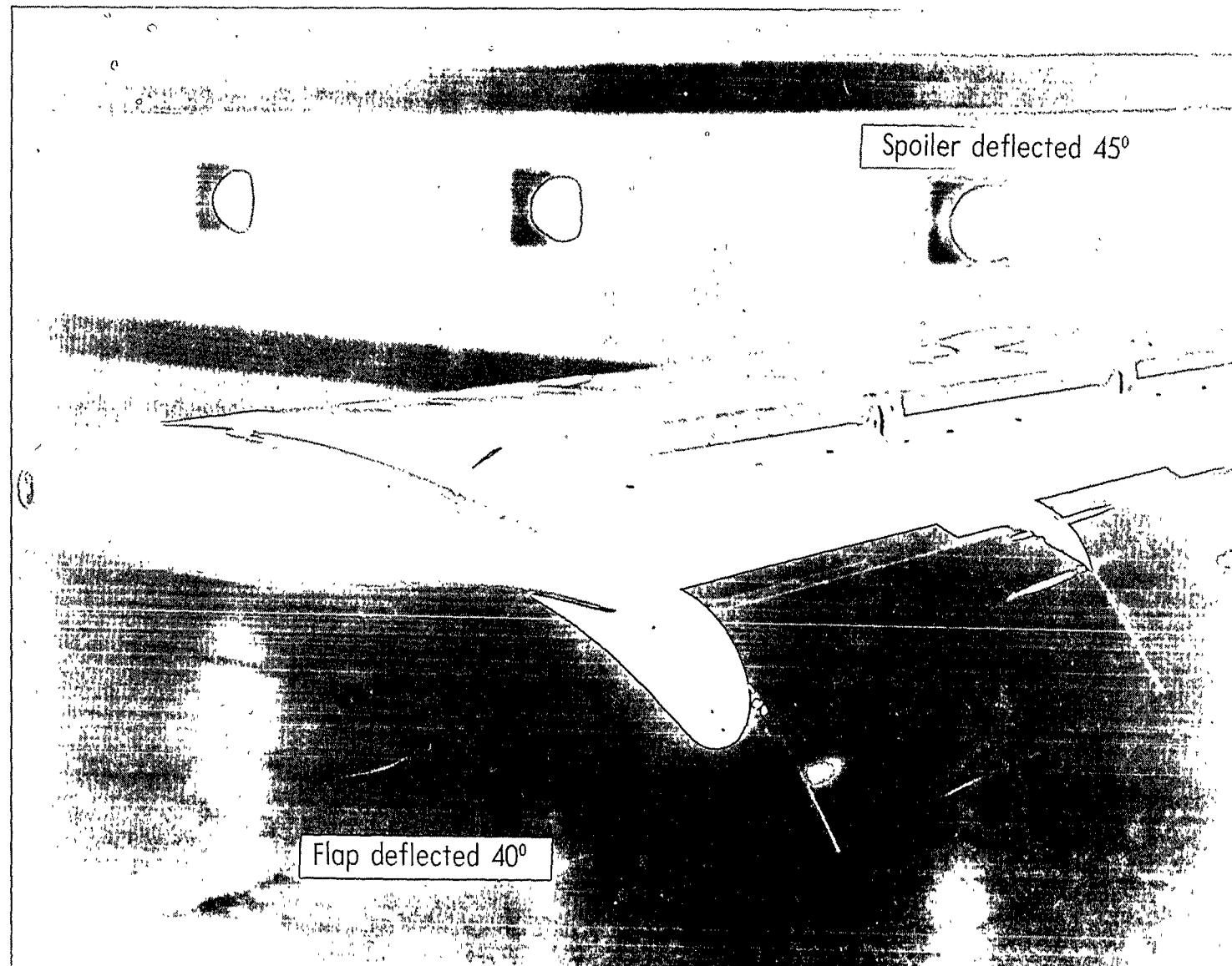
Figure 7.- Left wing tip of general aviation wing.

L-76-192
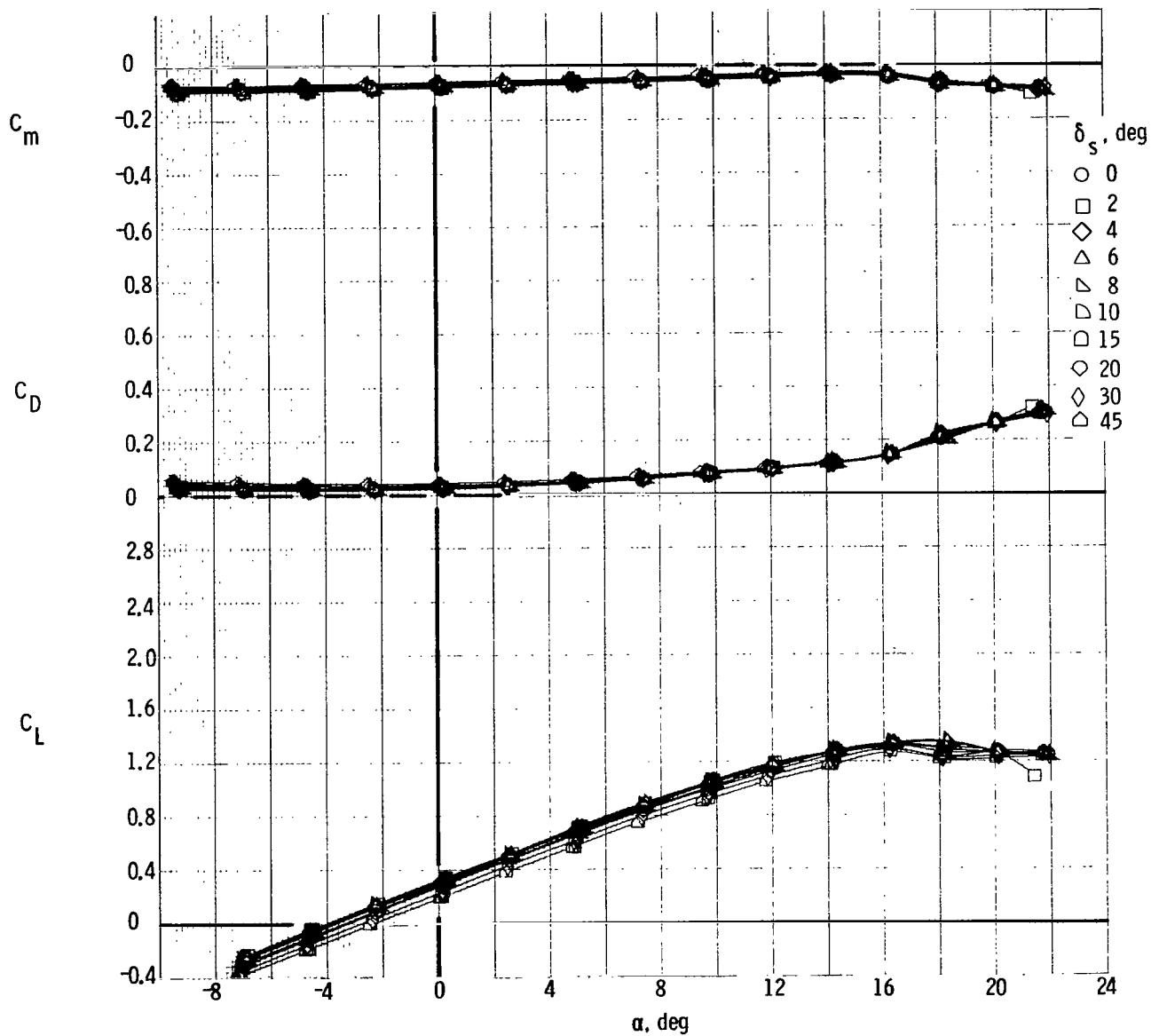
(a) Longitudinal characteristics; $\delta_f = 0^O$; $x/\bar{c} = 0.713$; blunt vent lip.

Figure 8.- Effects of flap position and deflection on spoiler B characteristics.
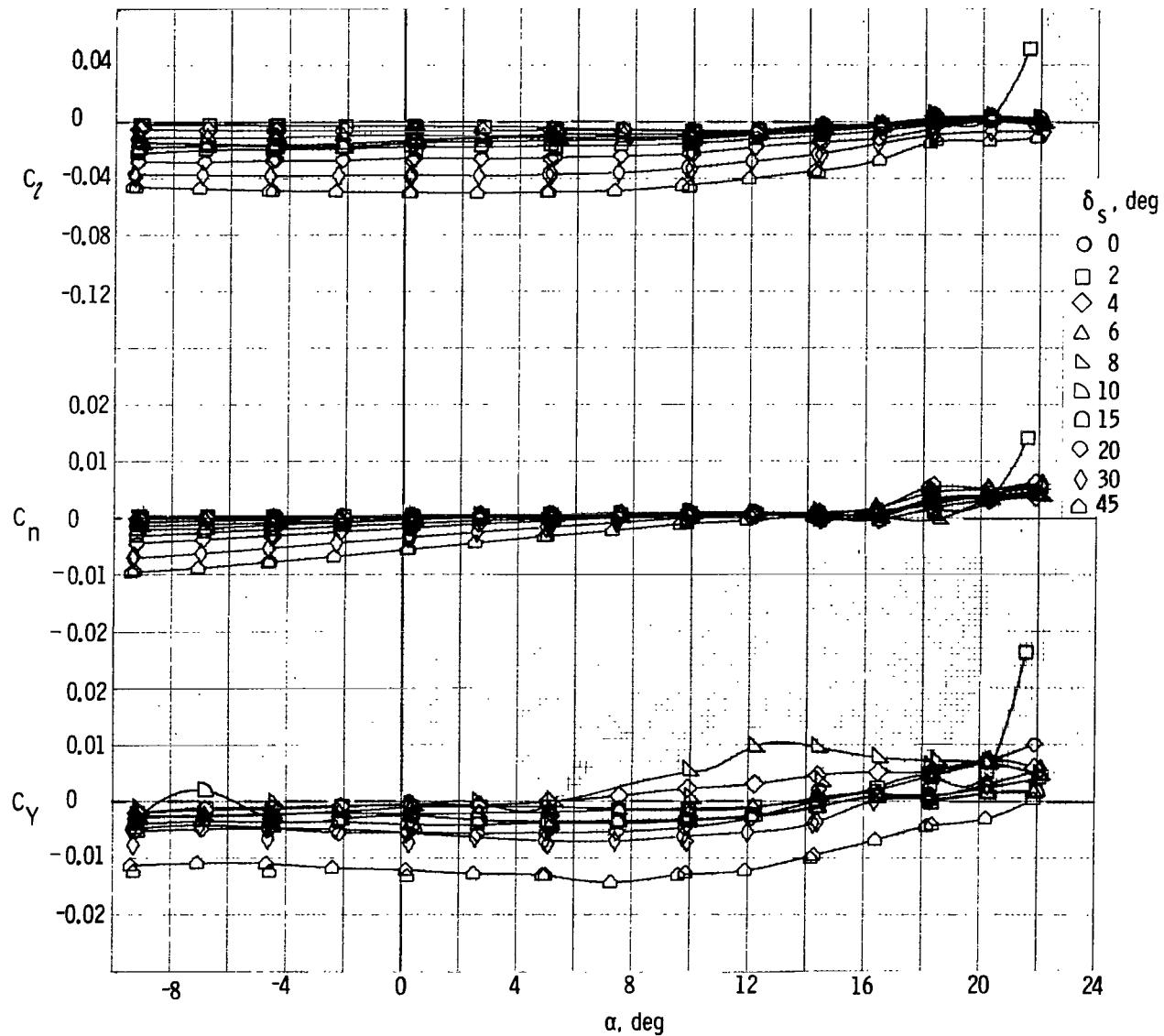
(b) Lateral characteristics; $\delta_f = 0^o$; $x/\bar{c} = 0.713$; blunt vent lip.

Figure 8.- Continued.

(c) Longitudinal characteristics; $\delta_f = 10^O$; $x/\bar{c} = 0.917$; large radius vent lip.
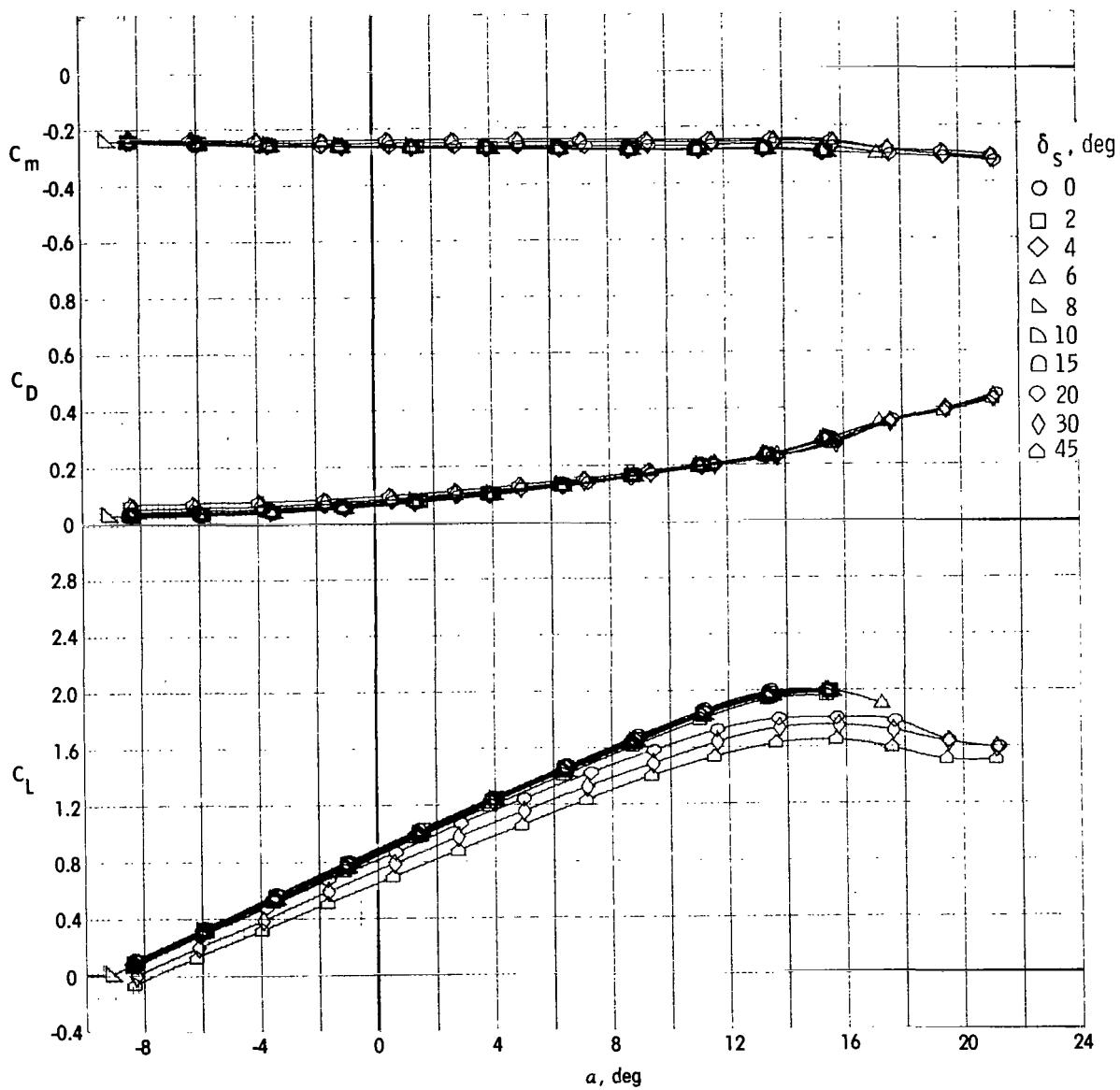
Figure 8.- Continued.

(d) Lateral characteristics; $\delta_f = 10^{\circ}$; $x/\bar{c} = 0.917$; large radius vent lip.
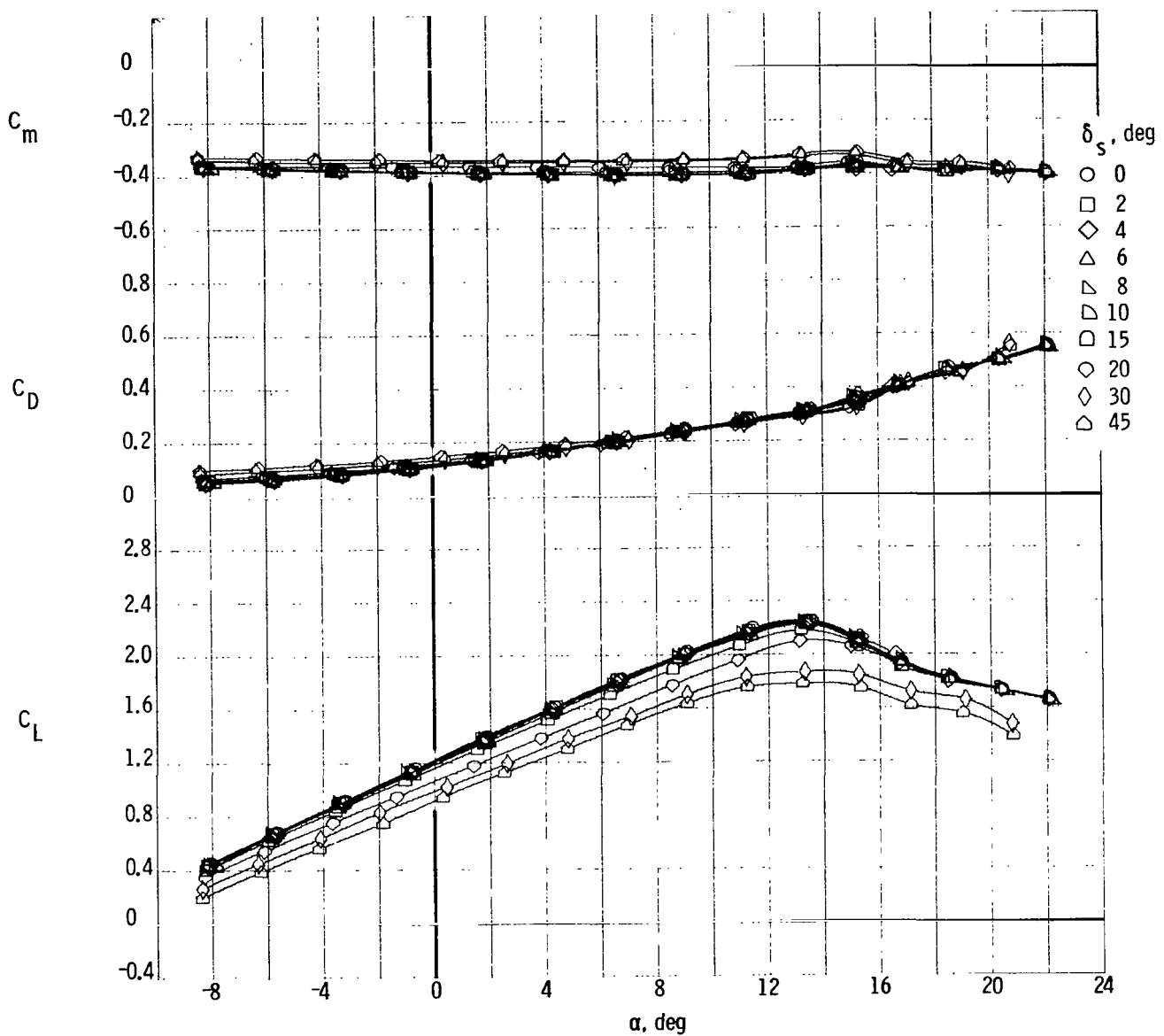
Figure 8.- Continued.

(e) Longitudinal characteristics; $\delta_f = 20^\circ$; $x/\bar{c} = 0.96$; blunt vent lip.

Figure 8.- Continued.

(f) Lateral characteristics; $\delta_f = 20^o$; $x/\bar{c} = 0.96$; blunt vent lip.

Figure 8.- Continued.
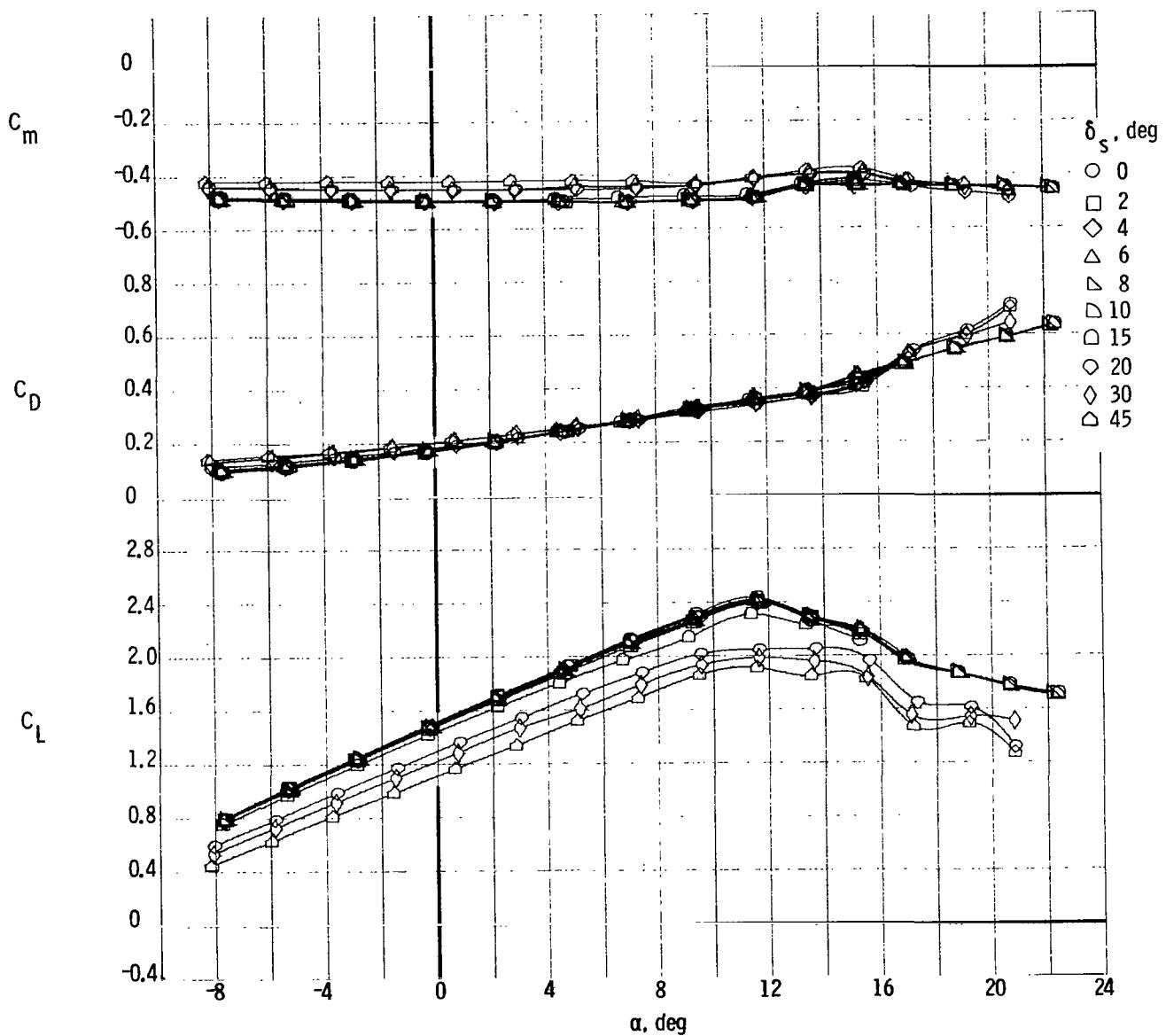
(g) Longitudinal characteristics; $\delta_f = 30^{o}$; $x/\bar{c} = 0.96$; large radius vent lip.
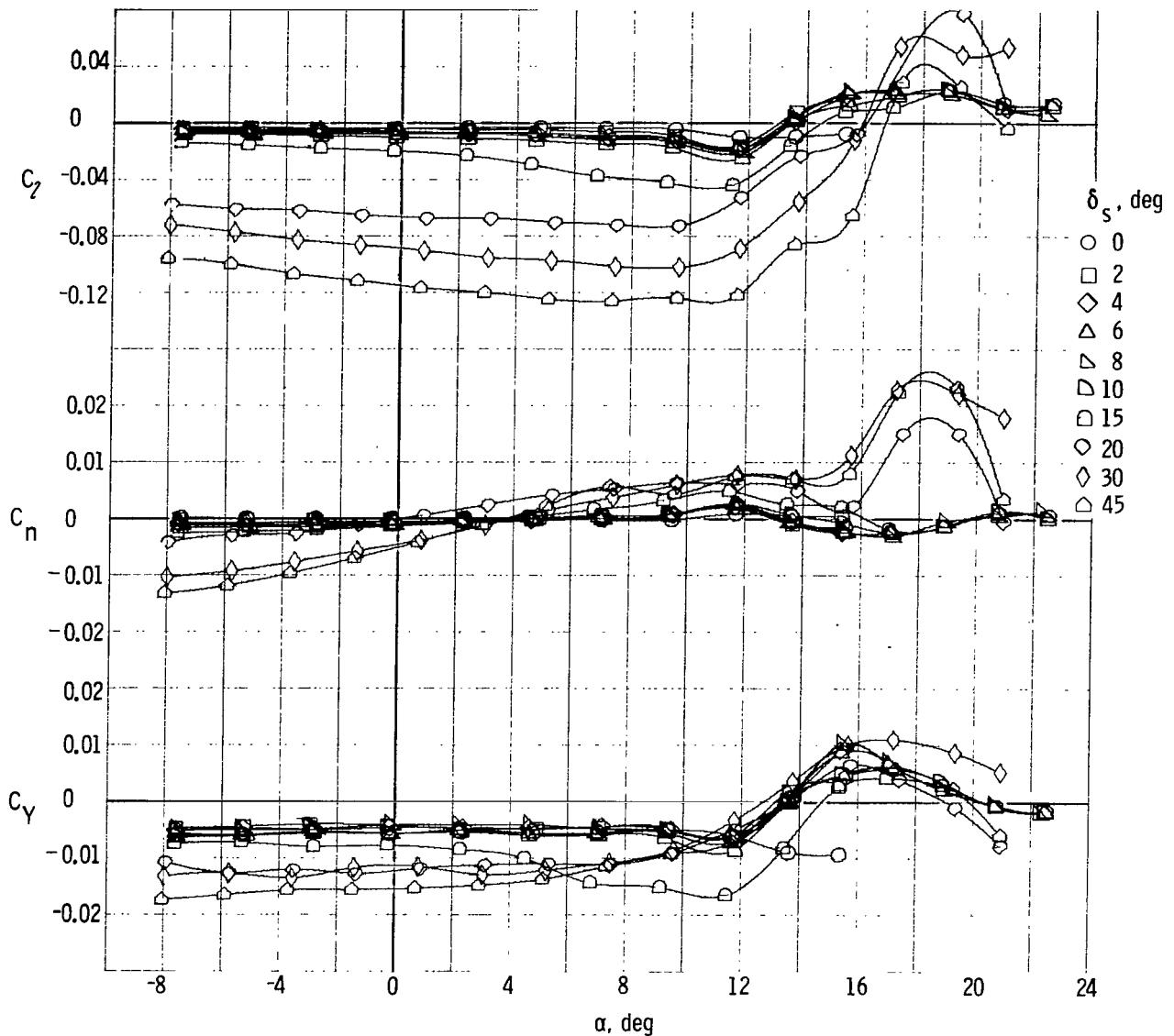
Figure 8.- Continued.

(h) Lateral characteristics; $\delta_f = 30°$; $x/\bar{c} = 0.96$; large radius vent lip.

Figure 8.- Continued.
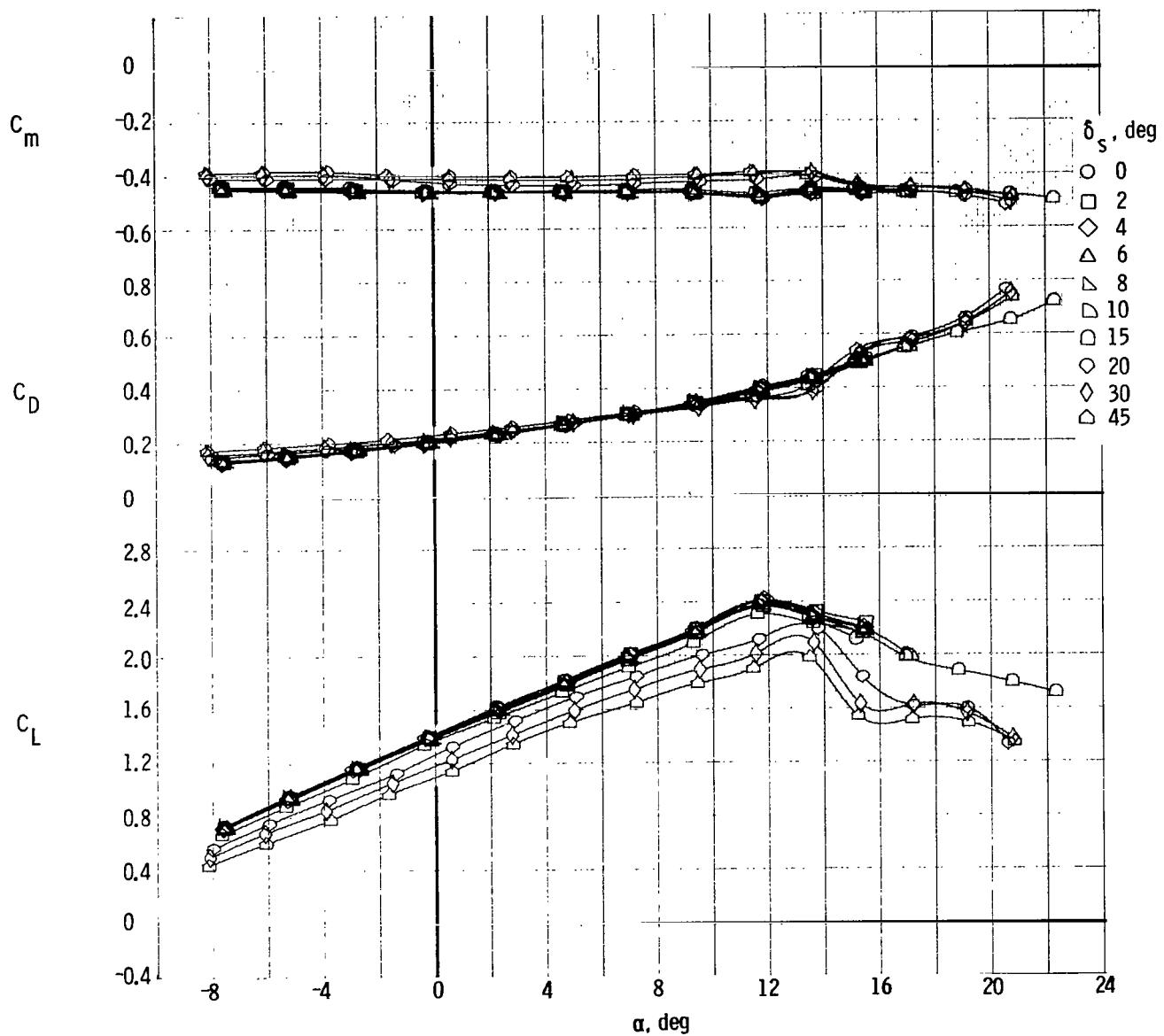
(i) Longitudinal characteristics; $\delta_f = 40^o$; $x/\bar{c} = 0.96$; blunt vent lip.

Figure 8.- Continued.
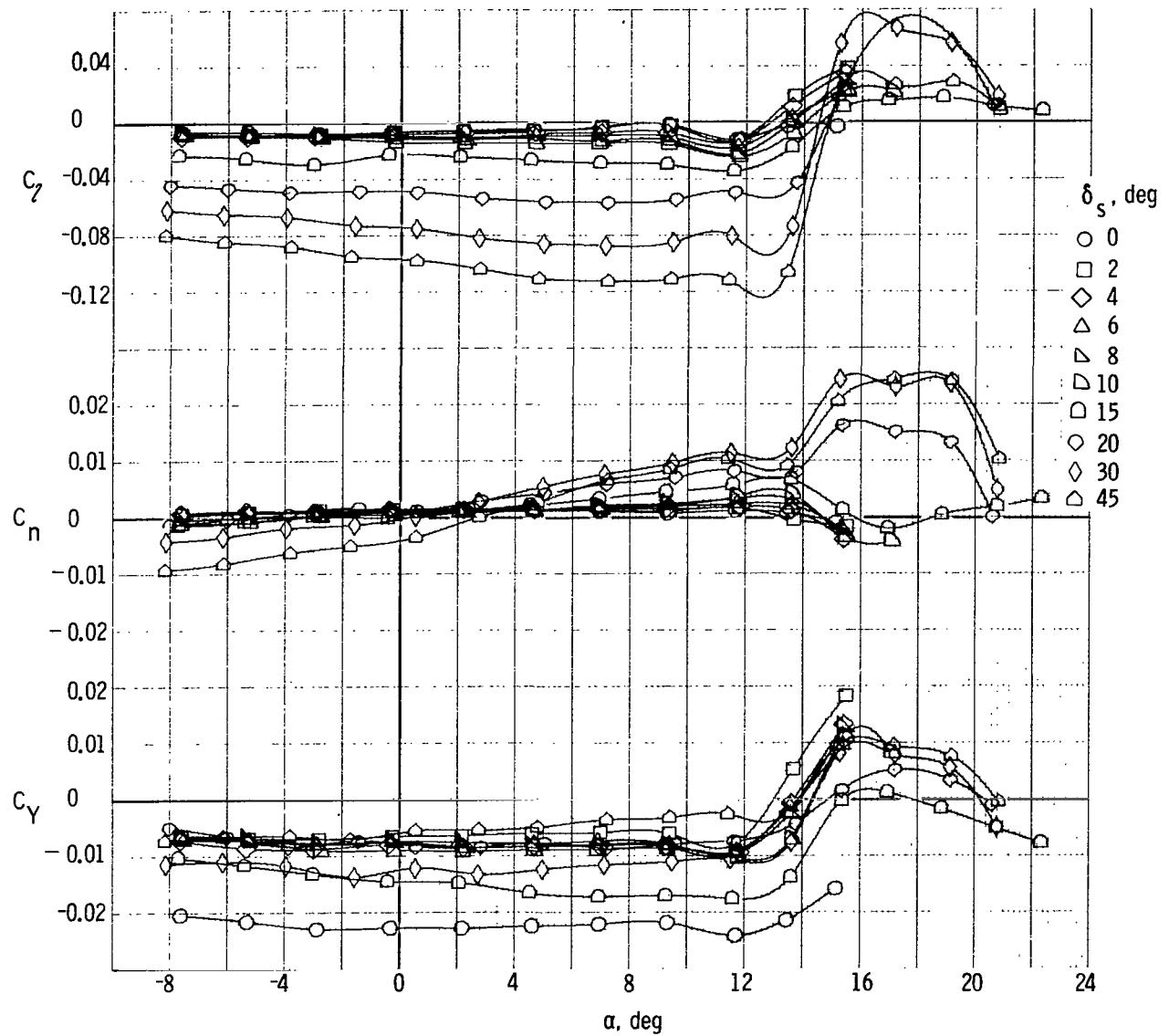
(j) Lateral characteristics; $\delta_f = 40^{\circ}$; $x/\bar{c} = 0.96$; blunt vent lip.

Figure 8.- Concluded.
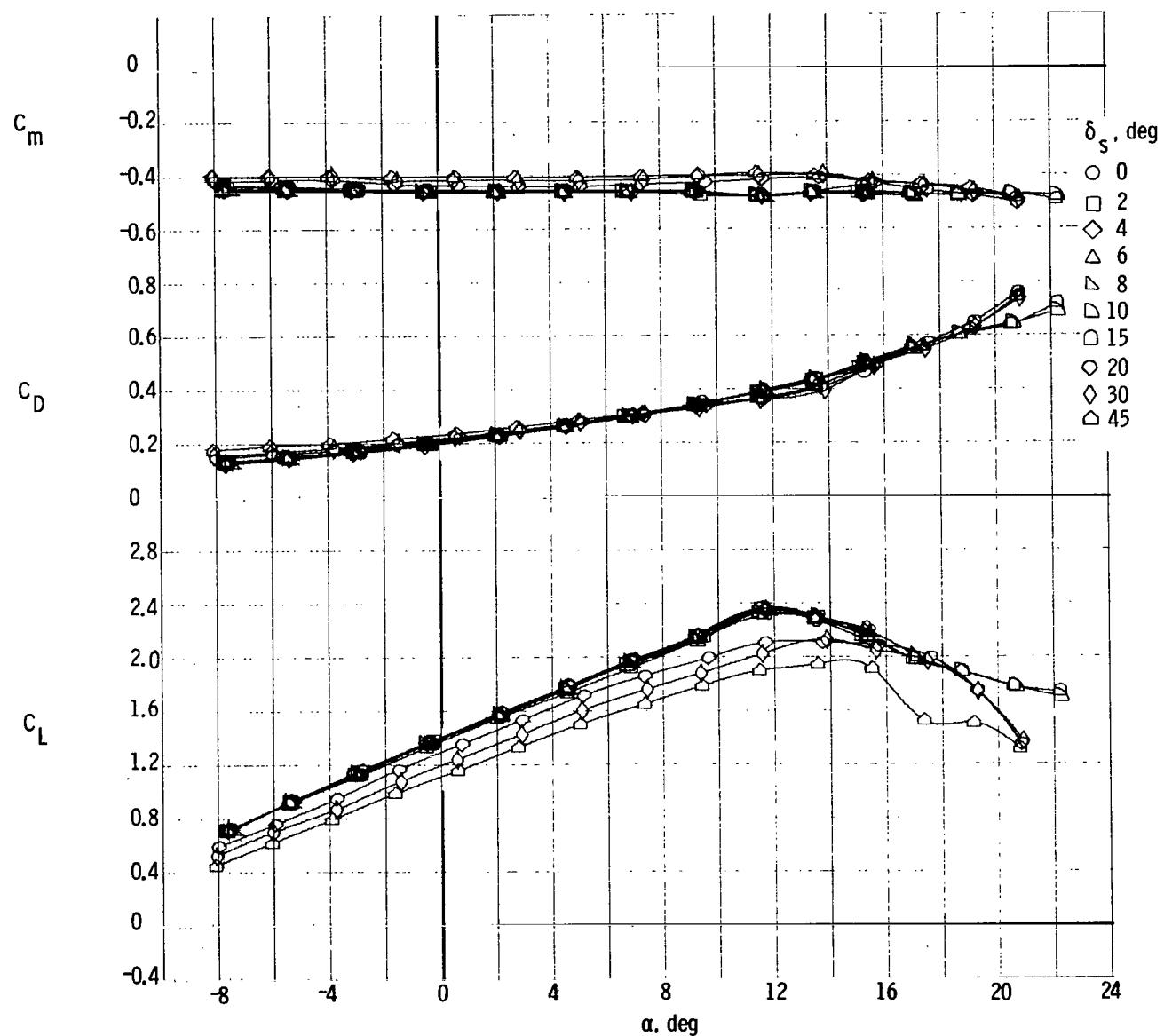
(a) Longitudinal characteristics; small radius vent lip.

Figure 9.- Effects of vent-lip geometry on spoiler B characteristics with $\delta_f = 40^o$ at $x/\bar{c} = 0.96$.
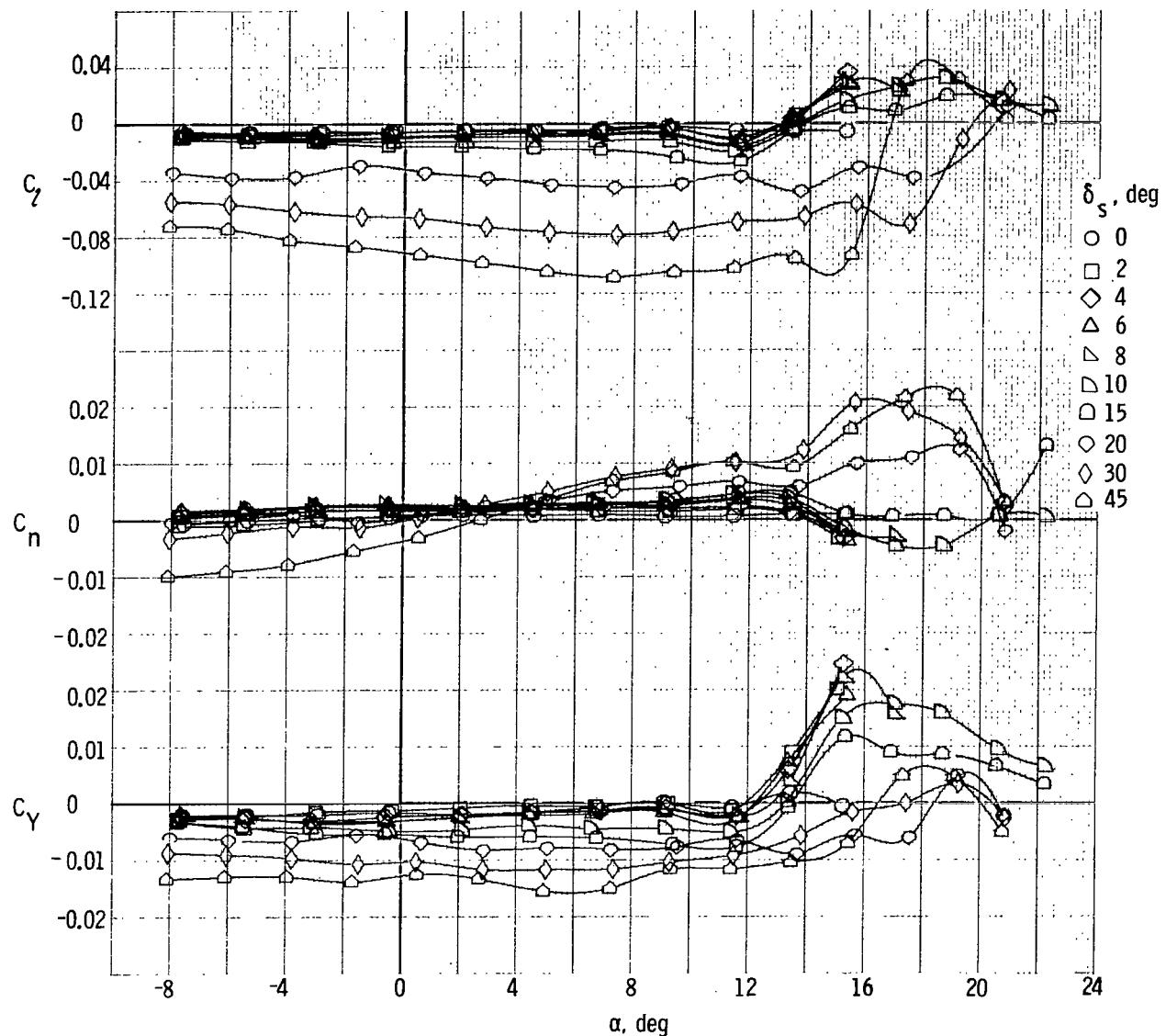
(b) Lateral characteristics; small radius vent lip.
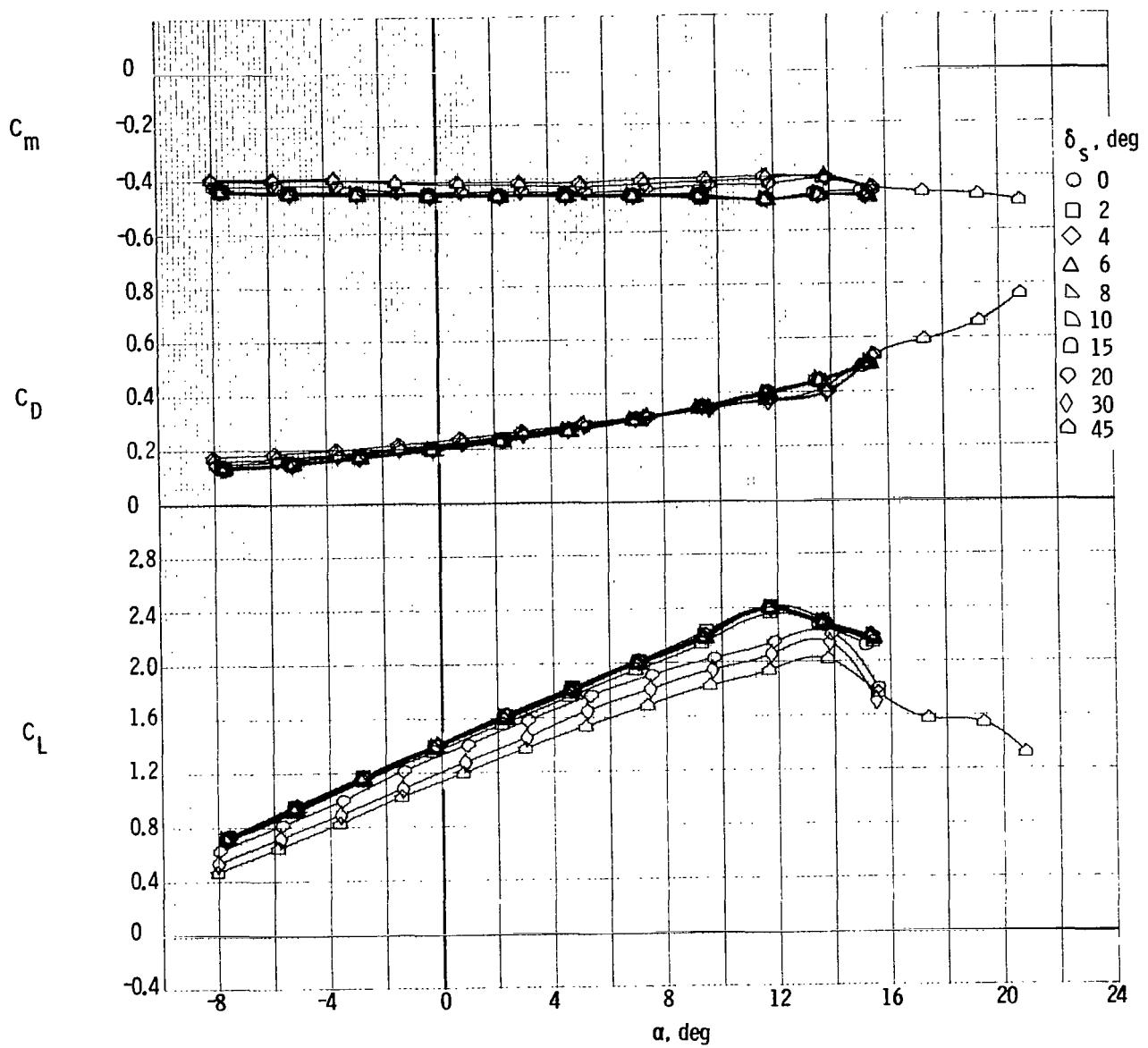
Figure 9.- Continued.

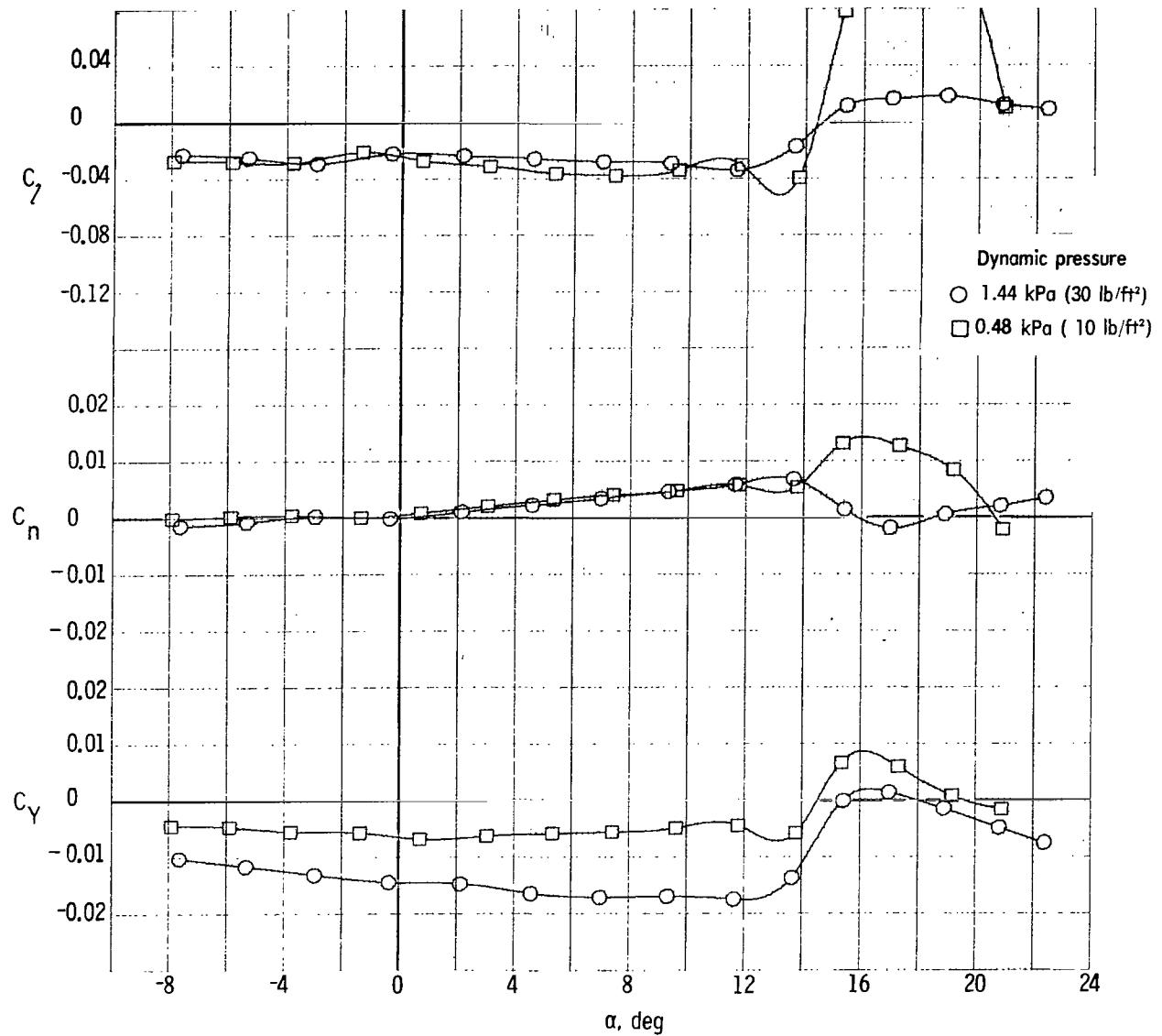(c) Longitudinal characteristics; large radius vent lip.

Figure 9.- Continued.
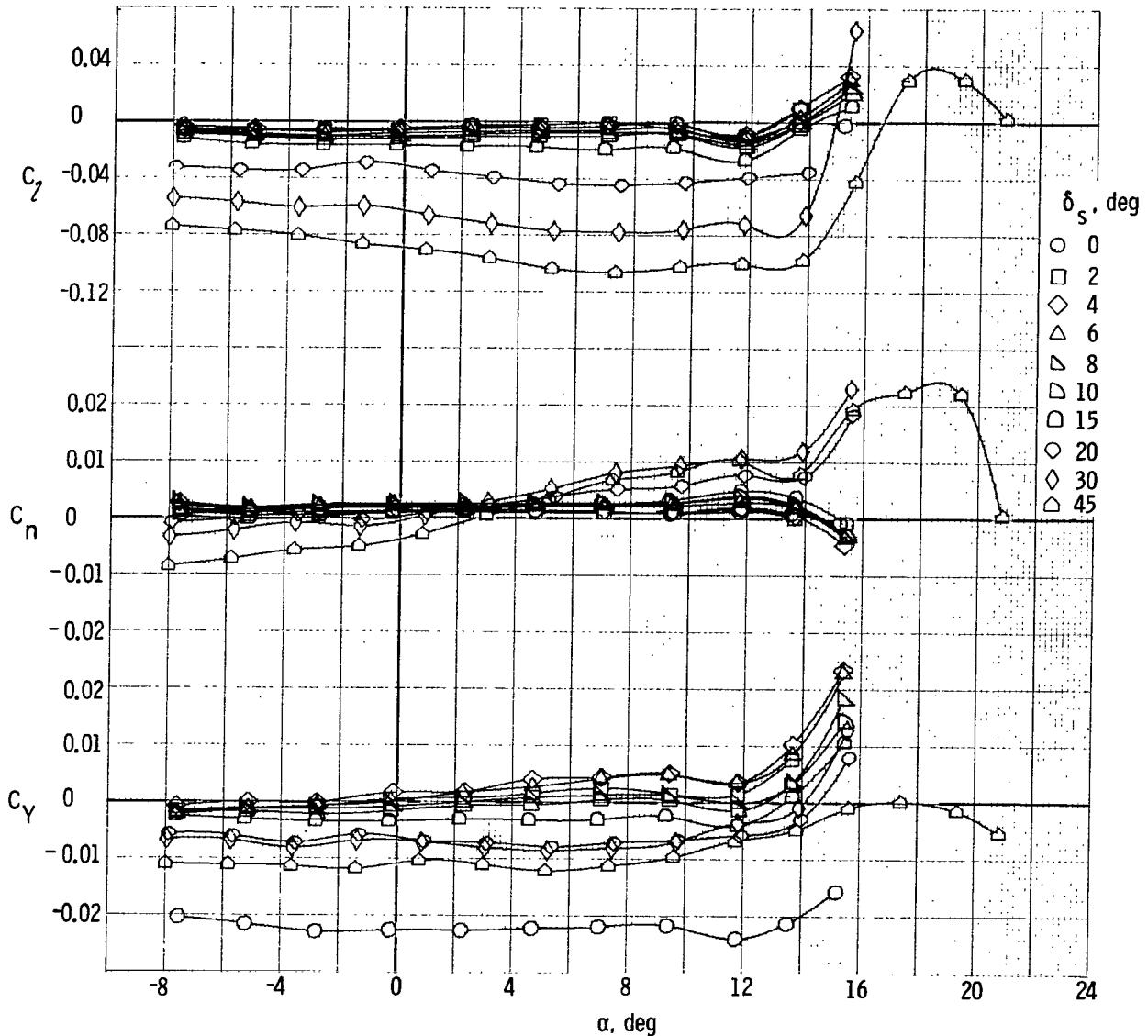
(d) Lateral characteristics; large radius vent lip.

Figure 9.- Concluded.
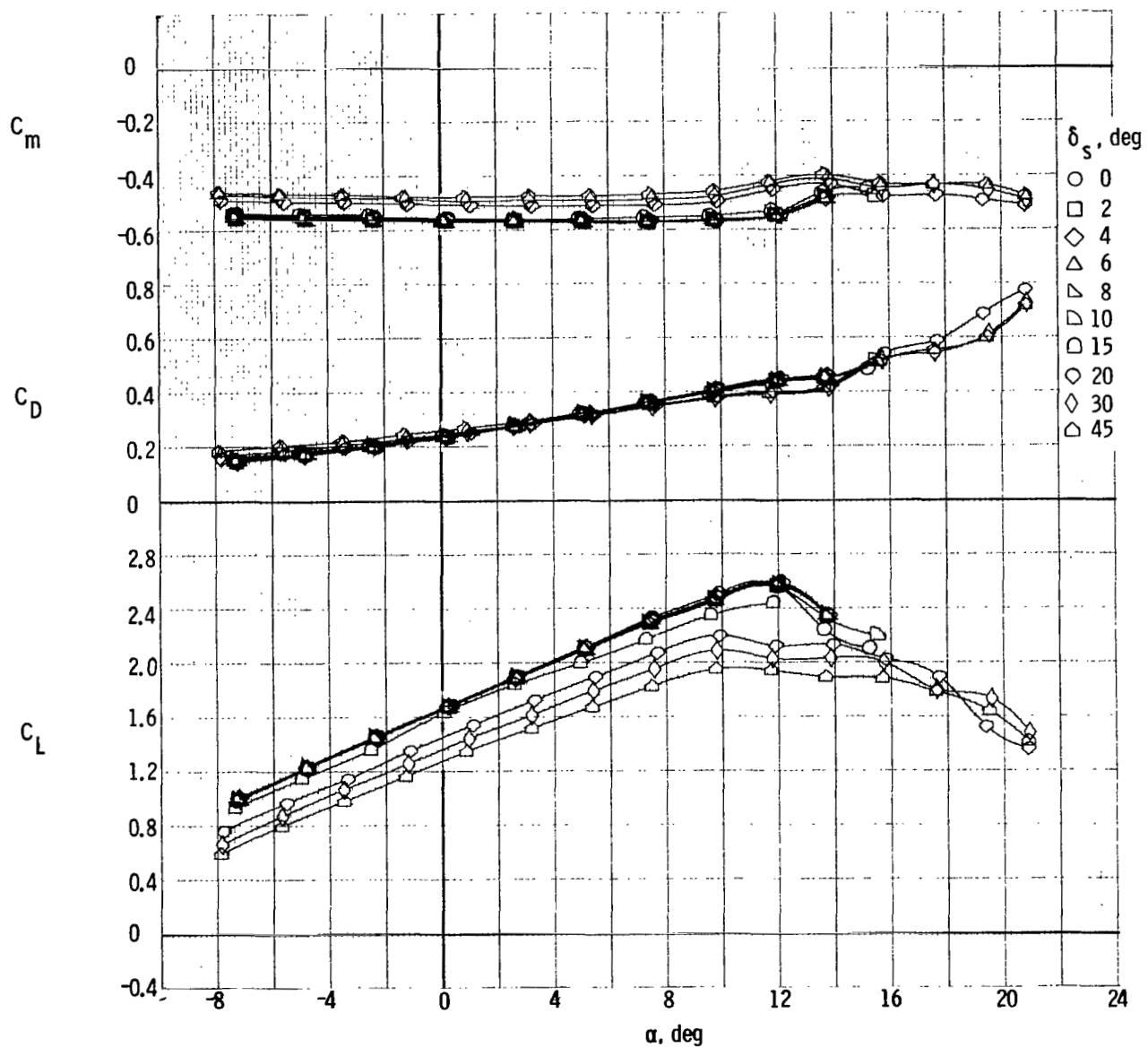
(a) Longitudinal characteristics; blunt vent lip.

Figure 10.- Effects of vent-lip geometry on spoiler B characteristics with $\delta_f = 40°$ at $x/\bar{c} = 1.00$.
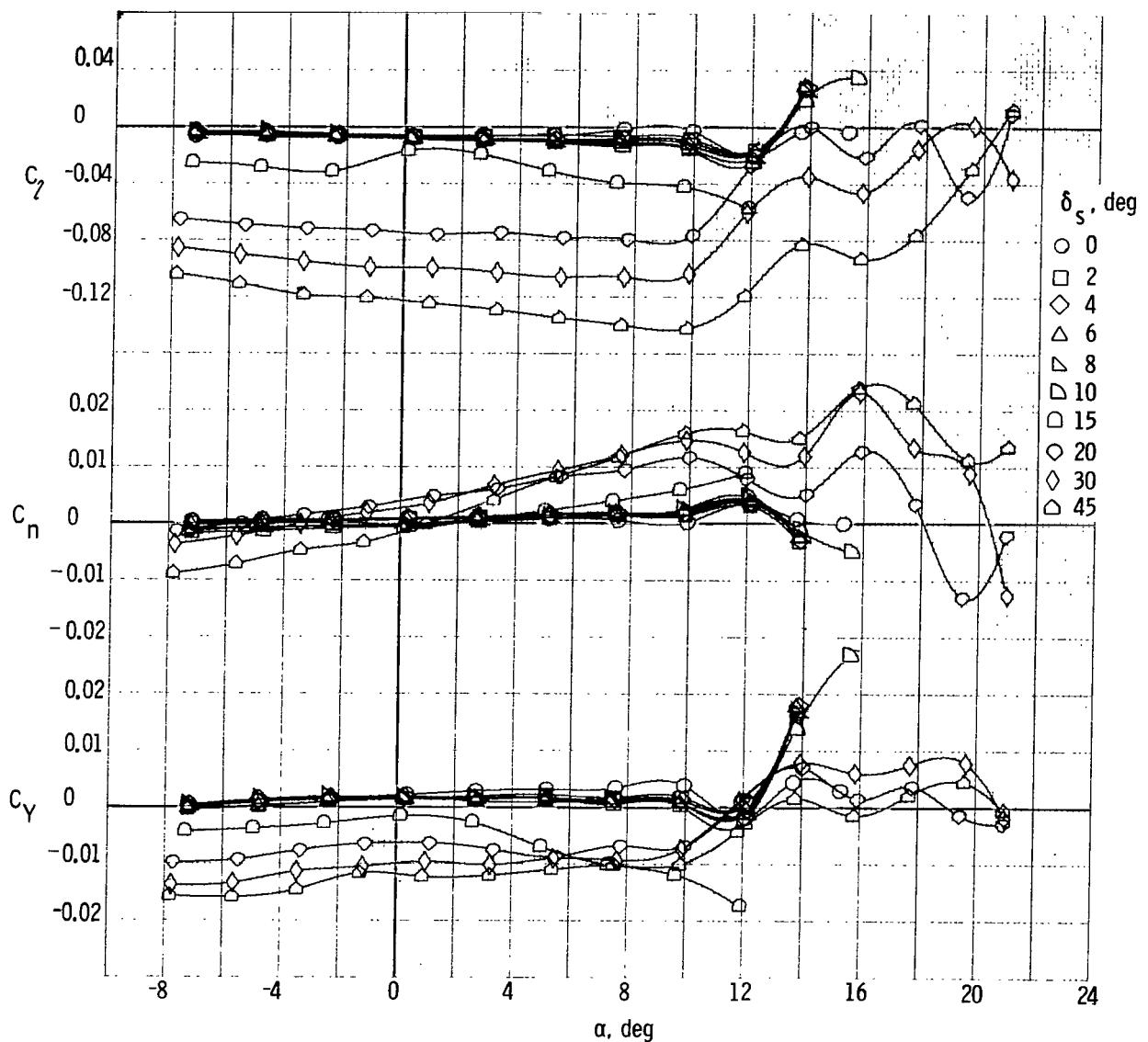
(b) Lateral characteristics; blunt vent lip.

Figure 10.- Continued.
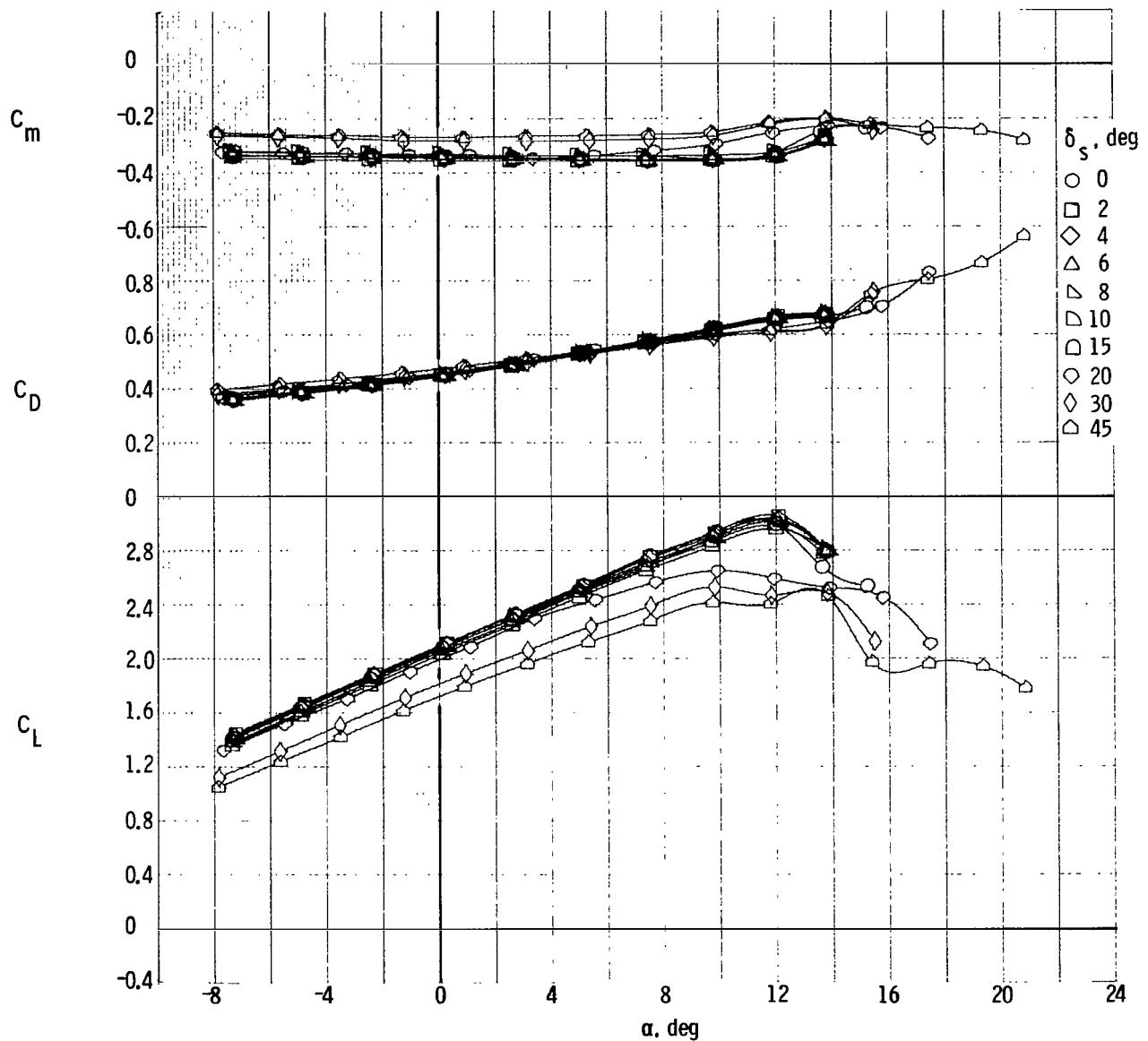
(c) Longitudinal characteristics; large radius vent lip.

Figure 10.- Continued.
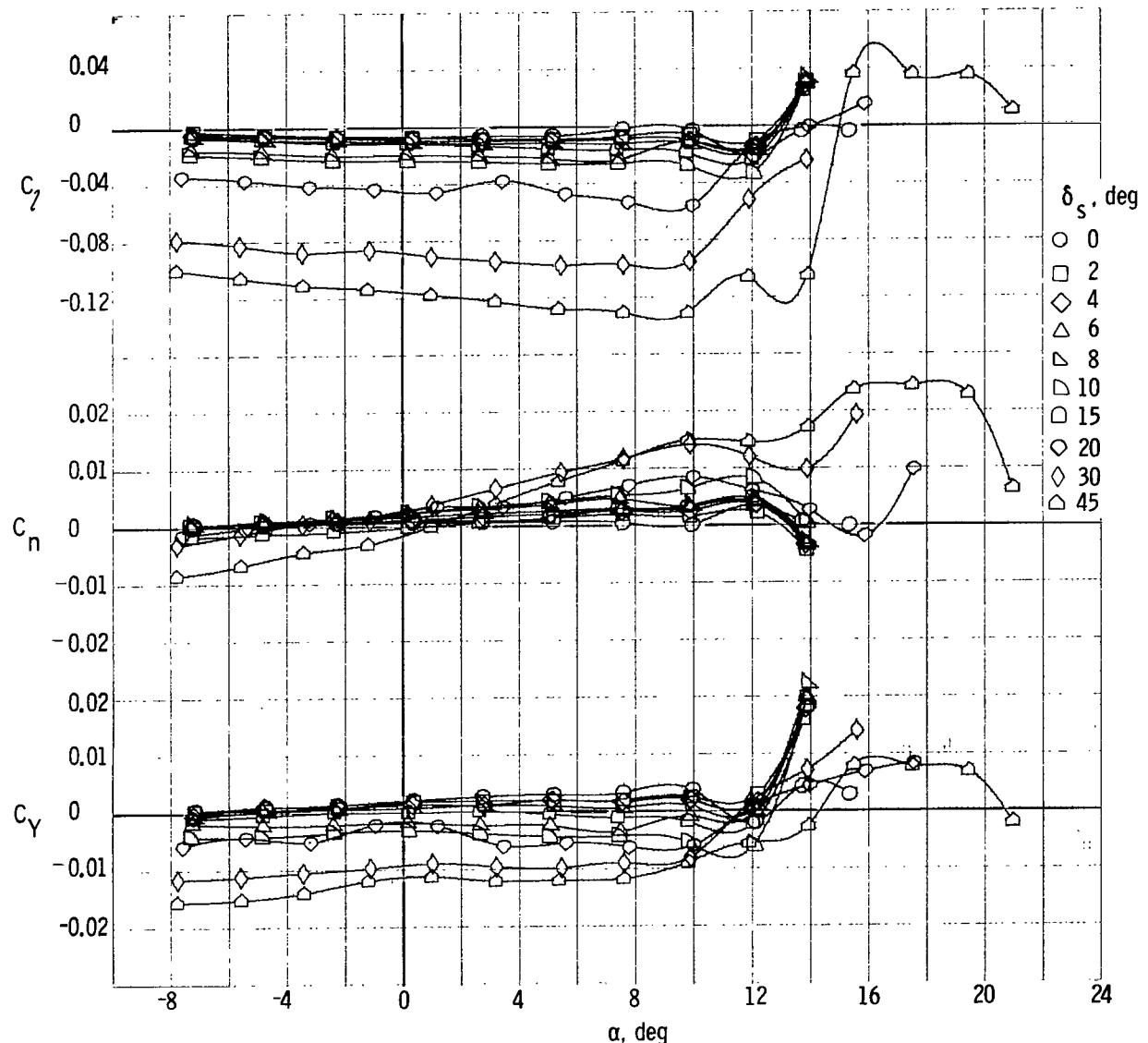
(d) Lateral characteristics; large radius vent lip.

Figure 10.- Continued.
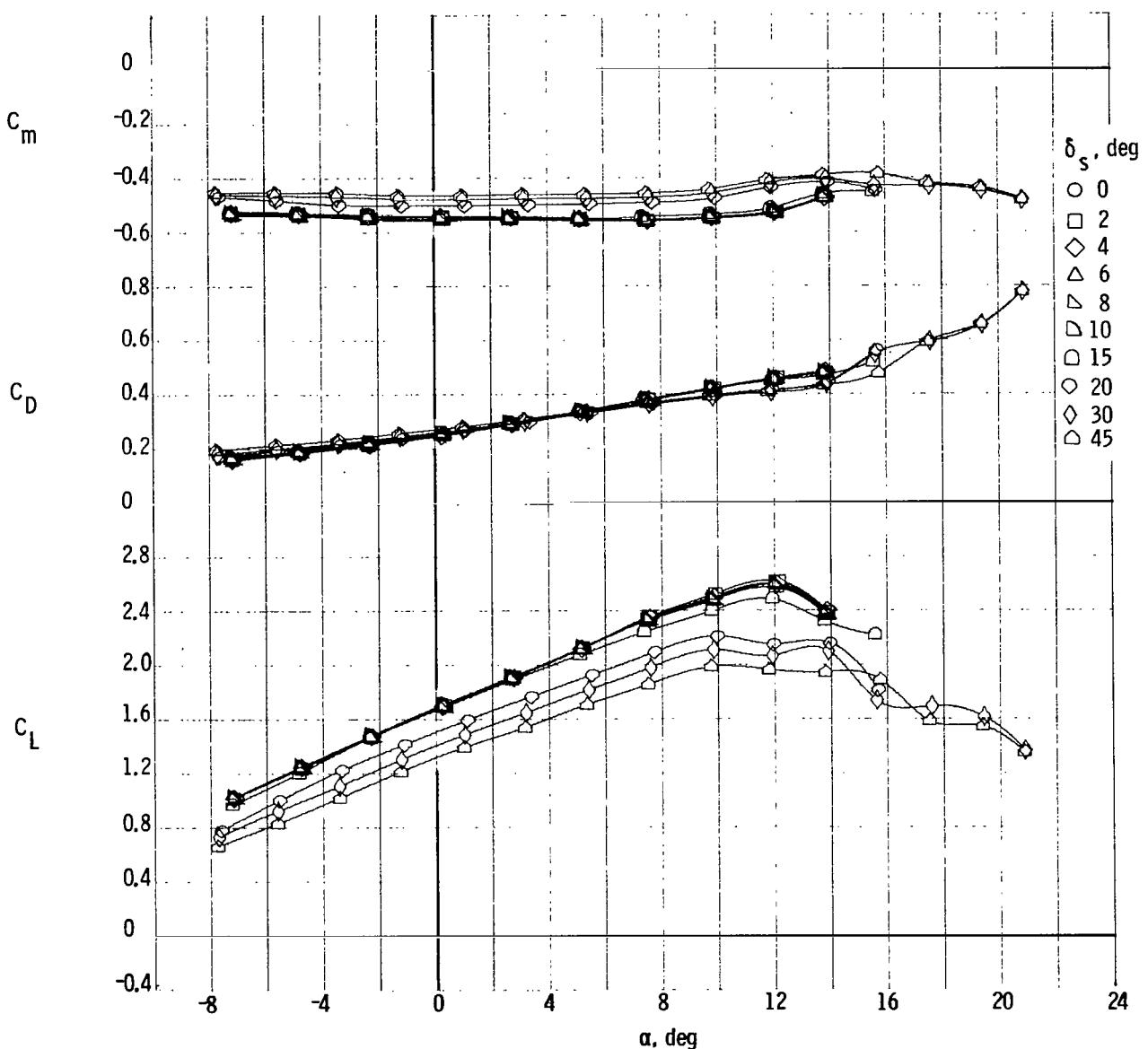
(e) Longitudinal characteristics; sharp vent lip.

Figure 10.- Continued.
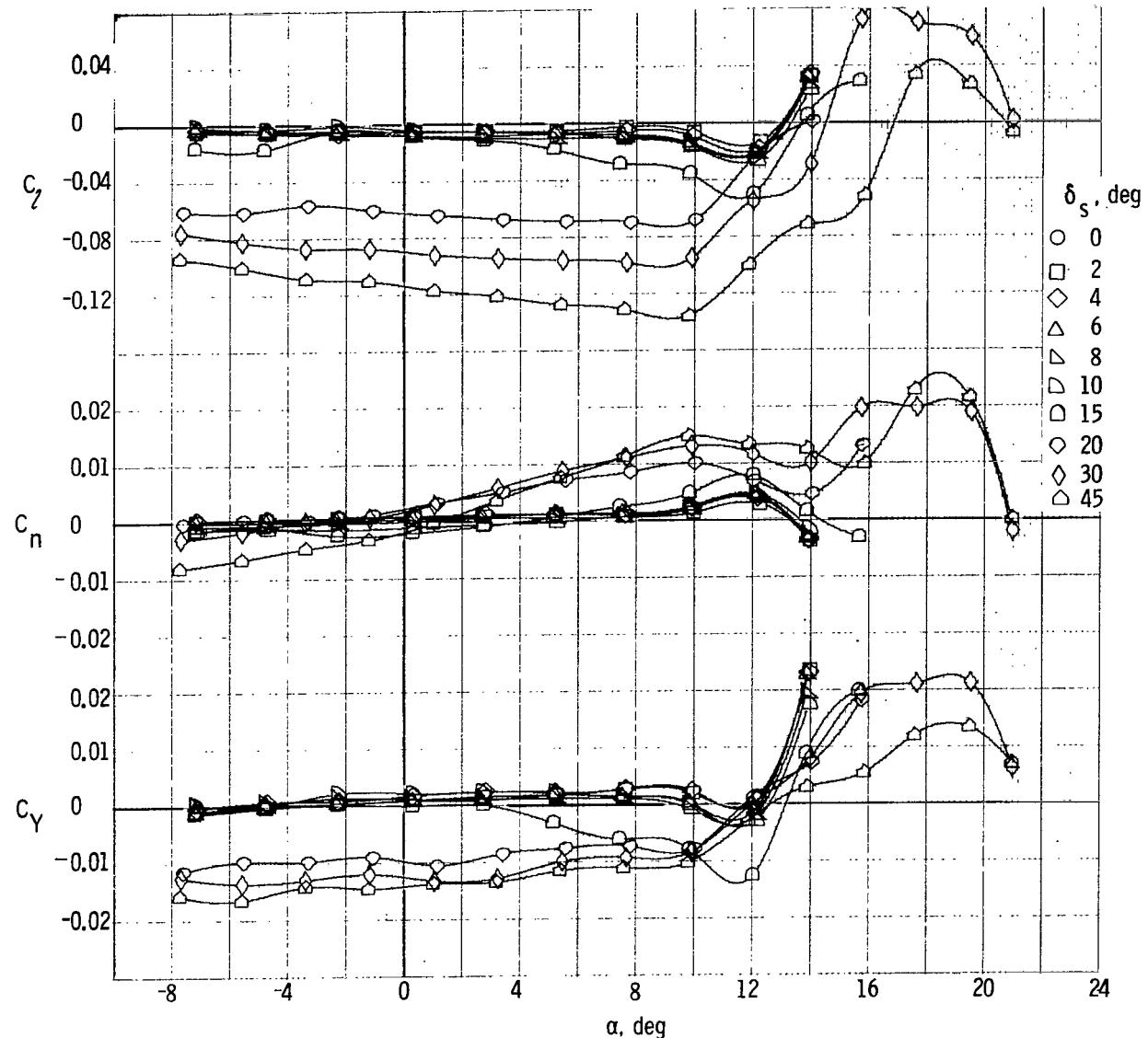
(f) Lateral characteristics; sharp vent lip.

Figure 10.- Concluded.
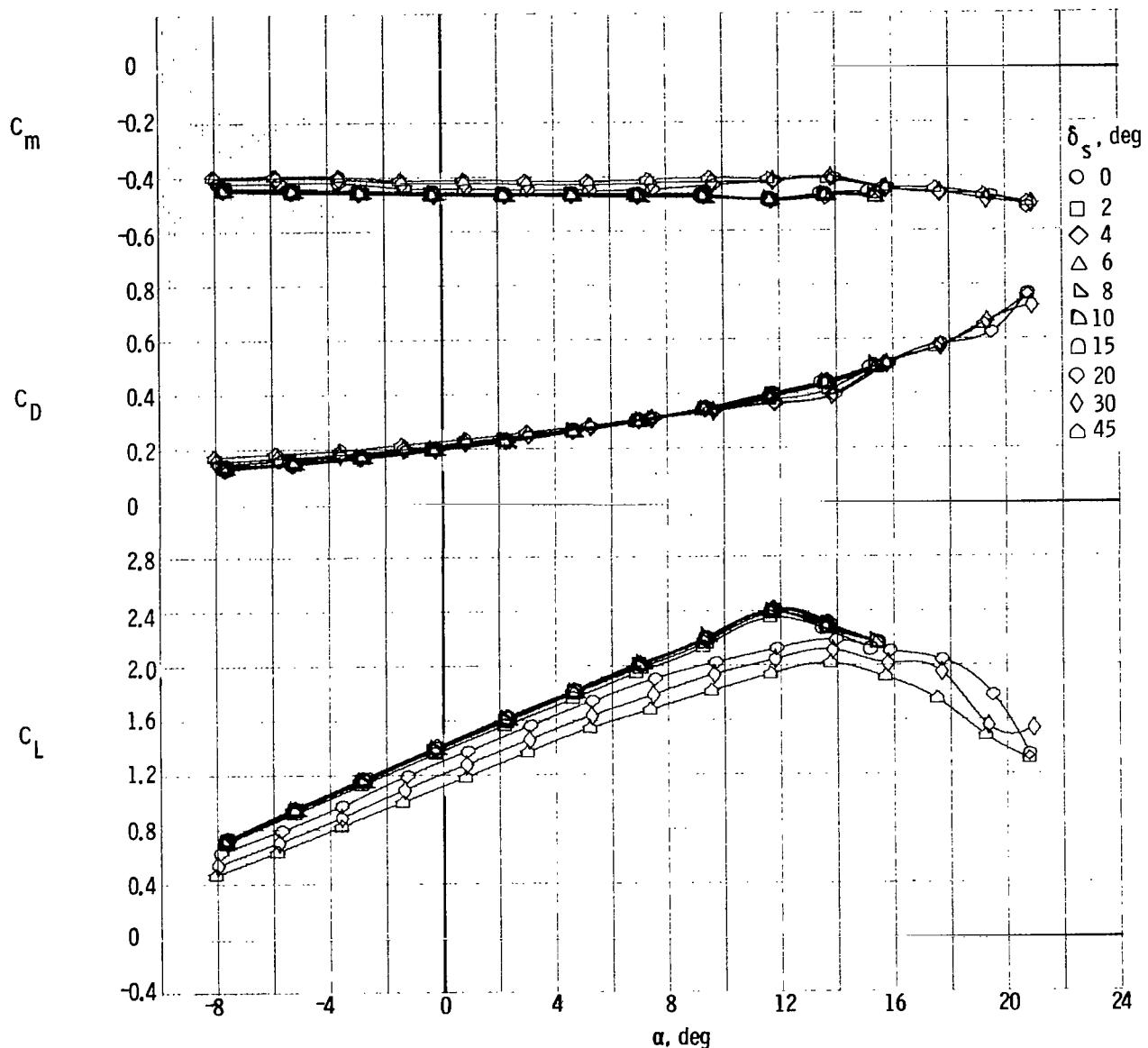
(a) Longitudinal characteristics; $\delta_f = 40^O$; $x/\bar{c} = 0.96$; small radius vent lip.

Figure 11.- Effects of vent-lip geometry on spoiler C characteristics.
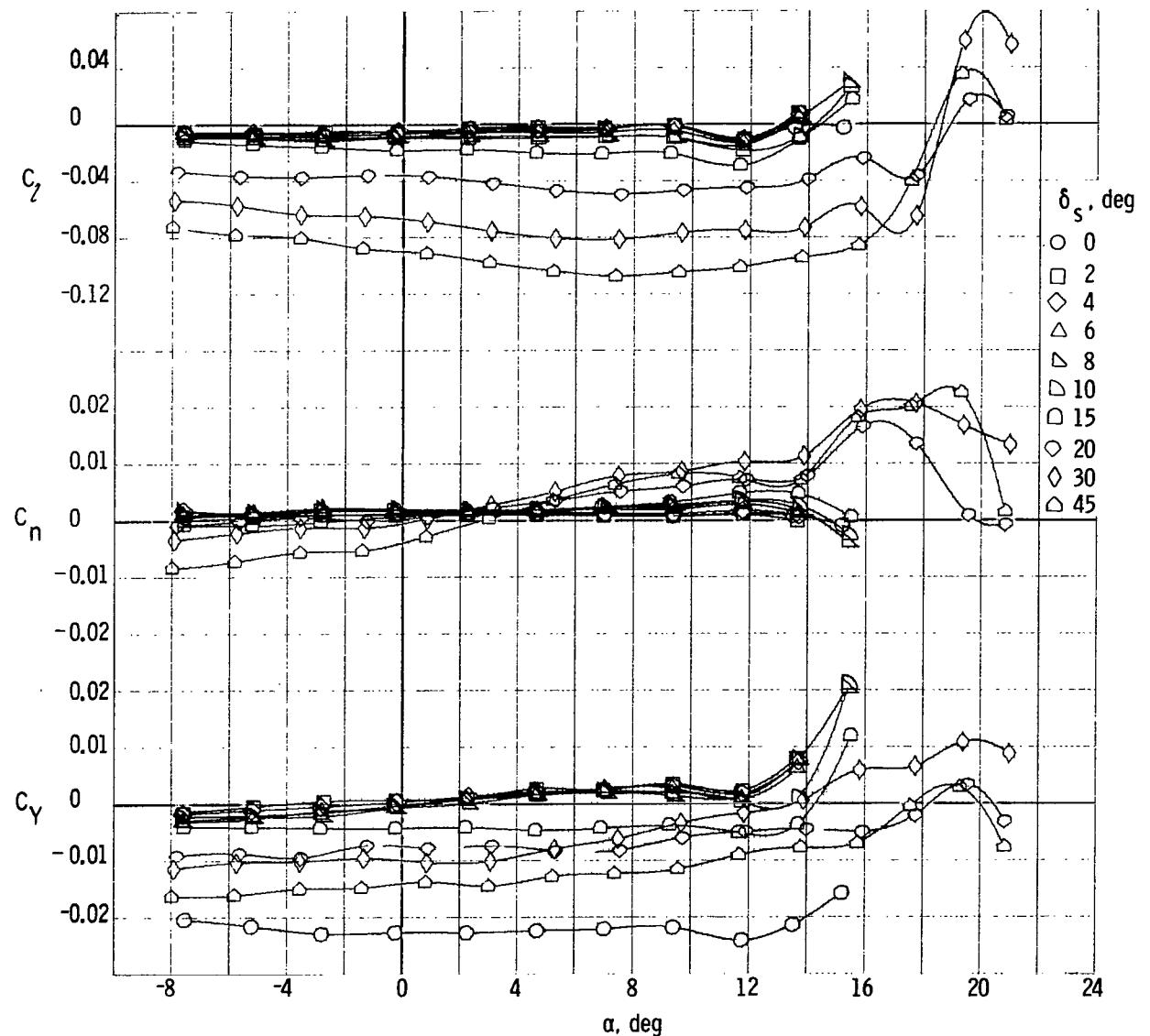
(b) Lateral characteristics; $\delta_f = 40^o$; $x/\bar{c} = 0.96$; small radius vent lip.
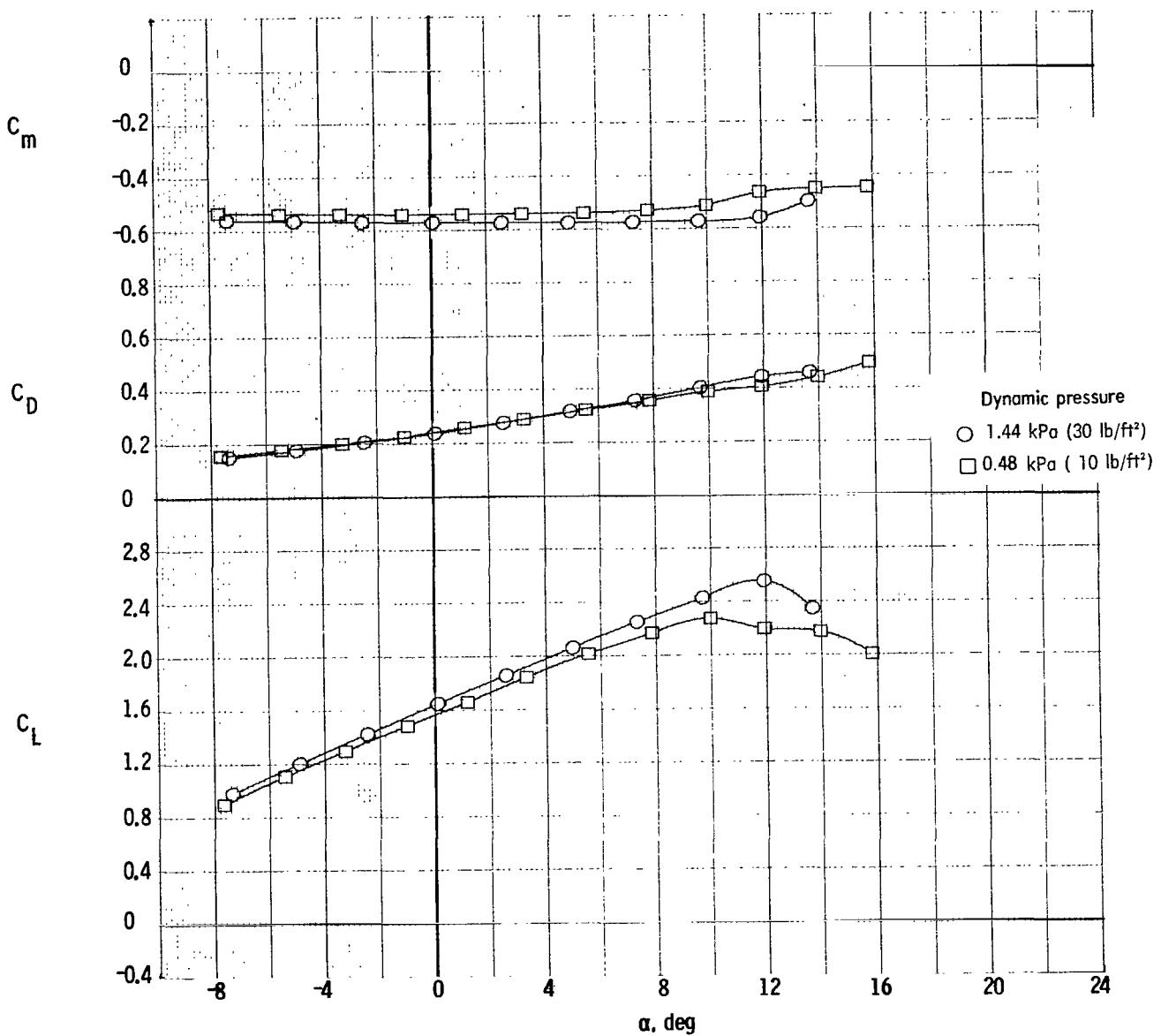
Figure 11.- Continued.
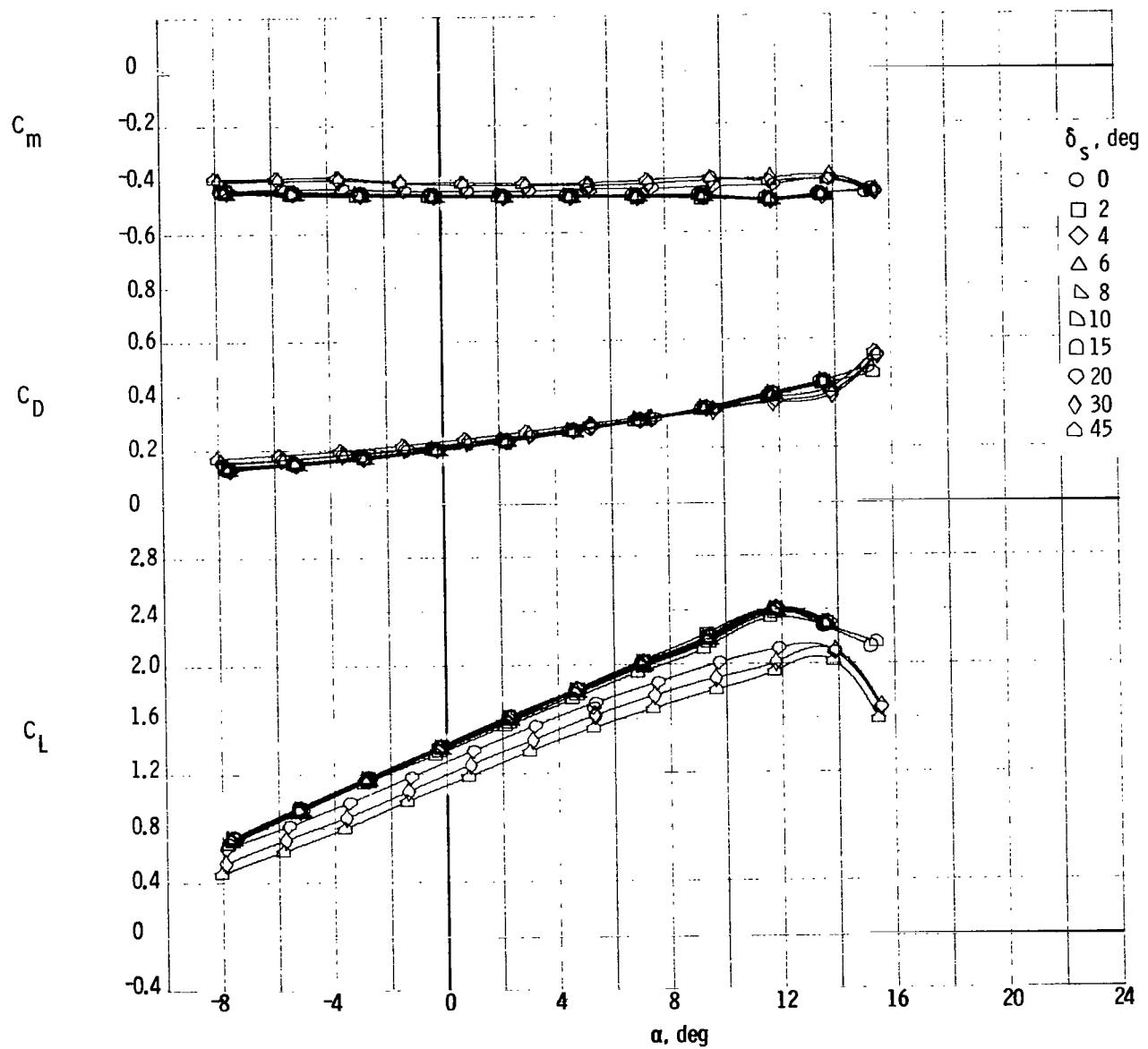
(c) Longitudinal characteristics; $\delta_f = 40^\circ$; $x/\bar{c} = 0.96$; large radius vent lip.
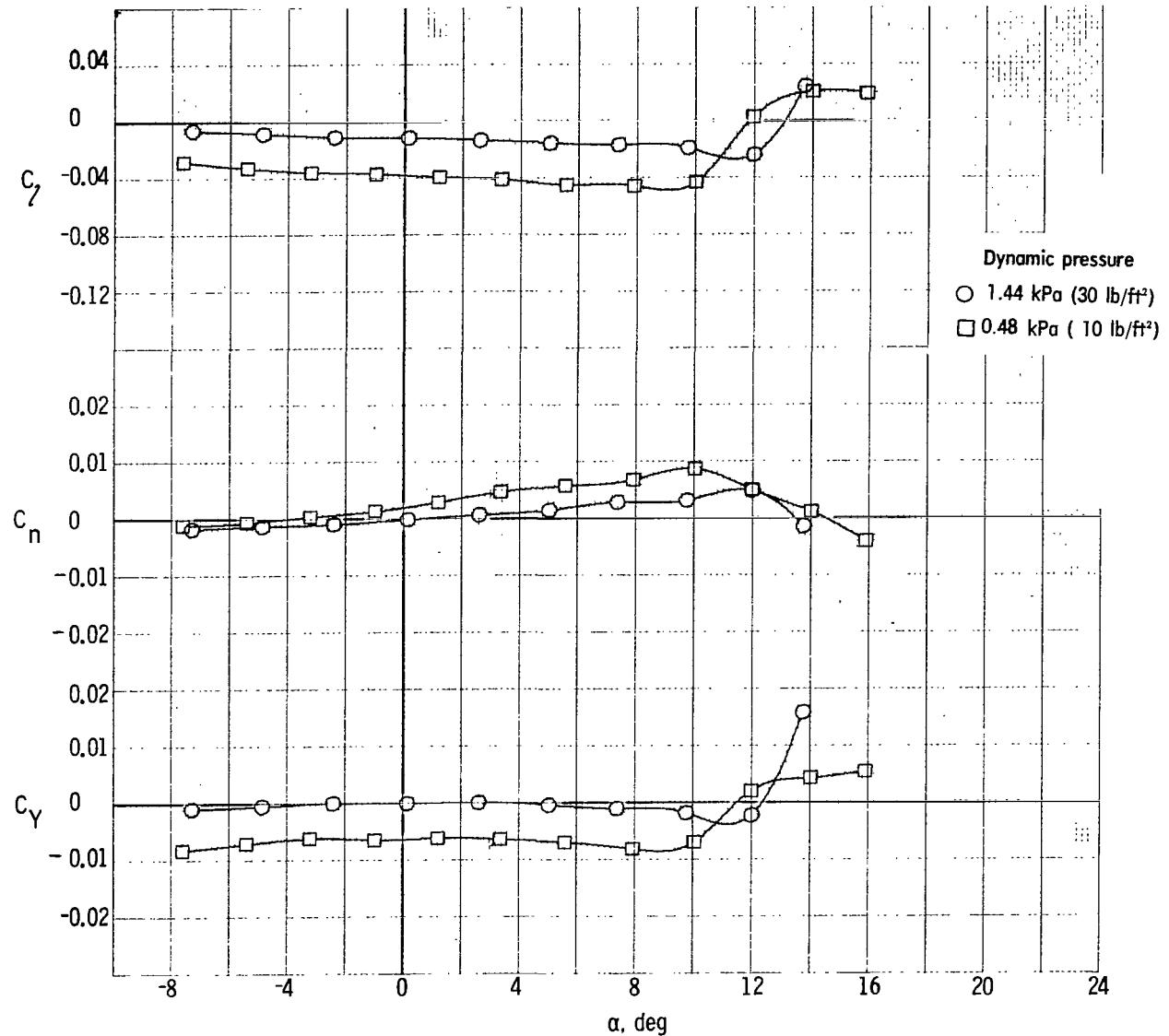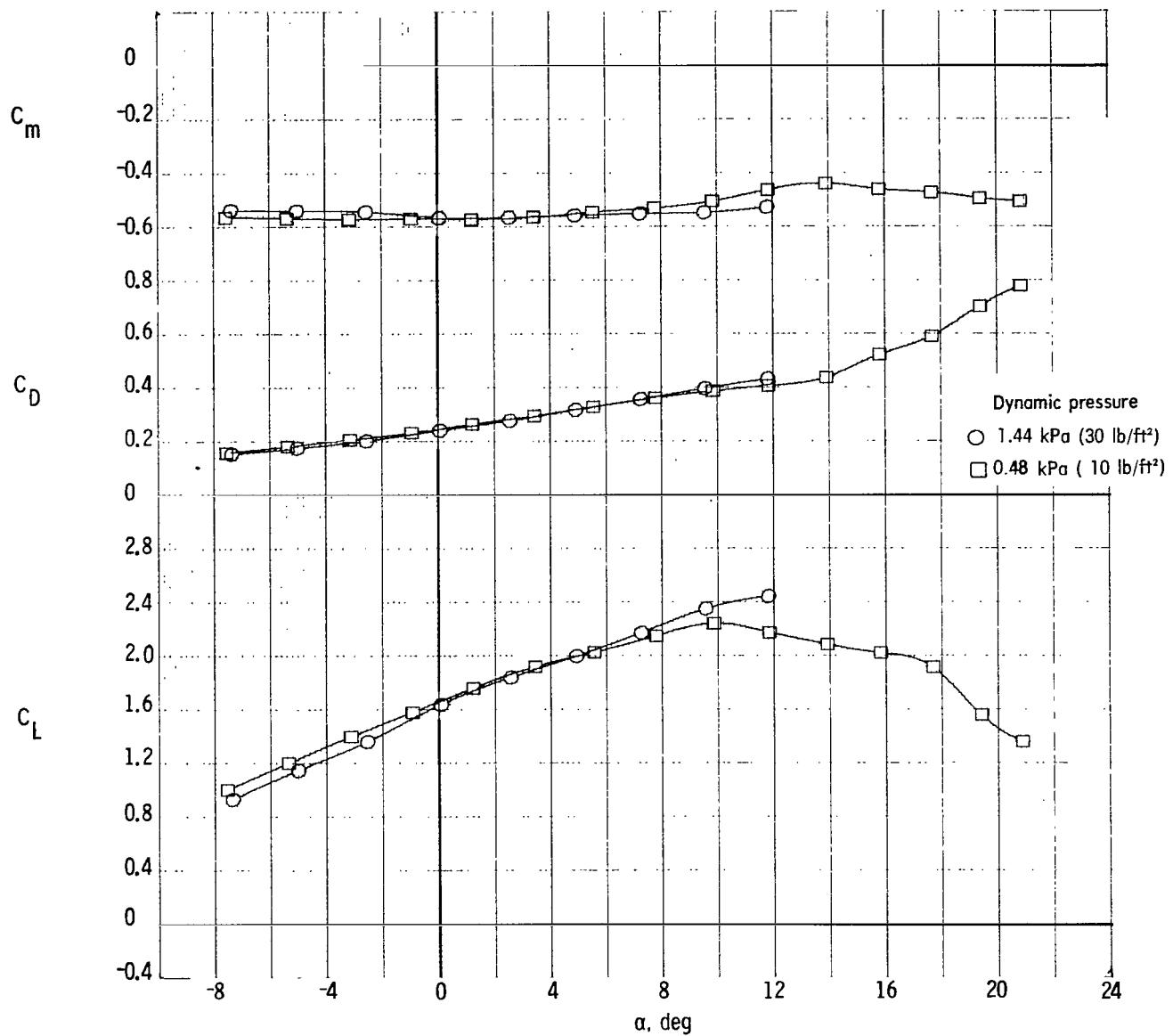
Figure 11.- Continued.
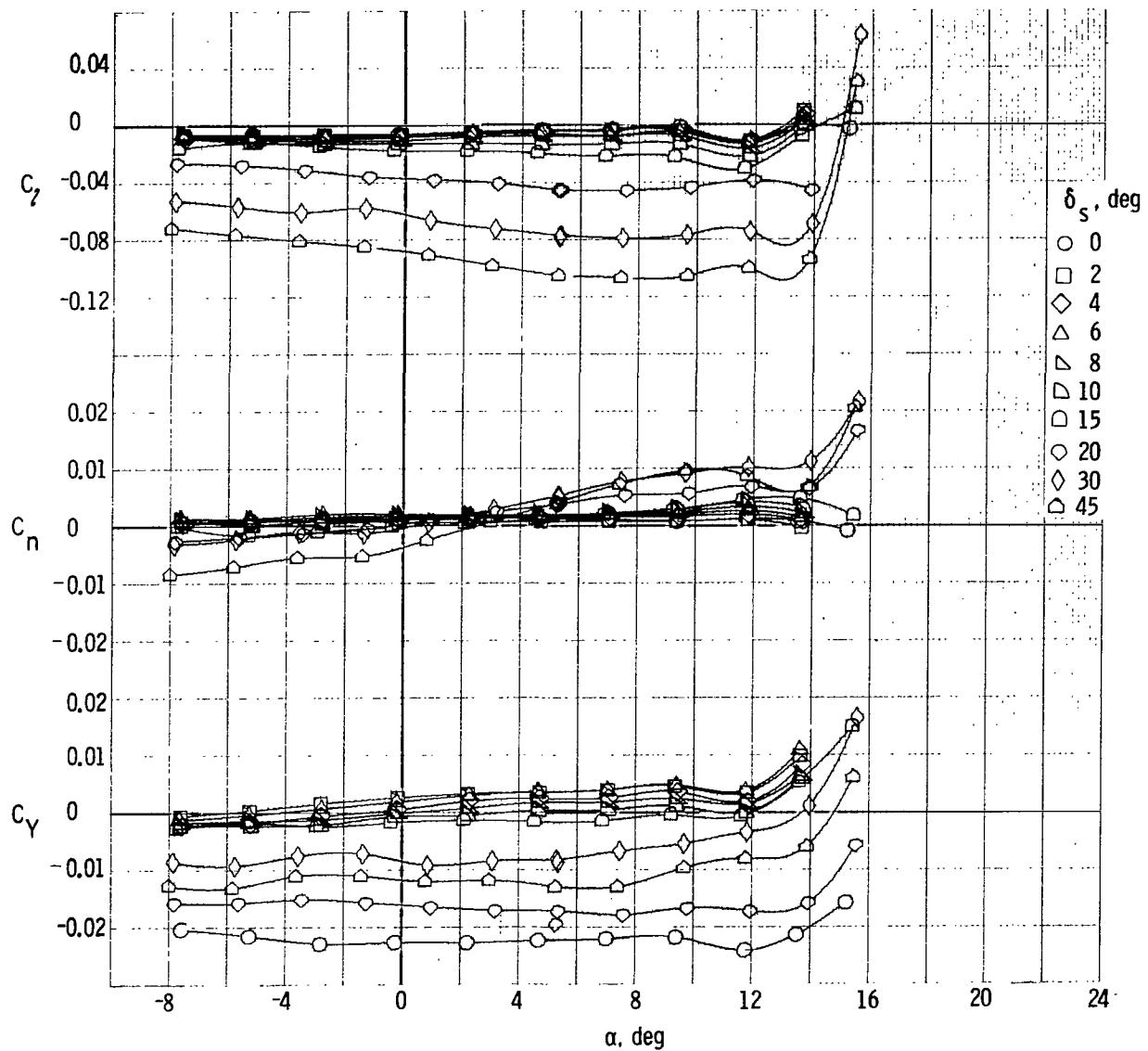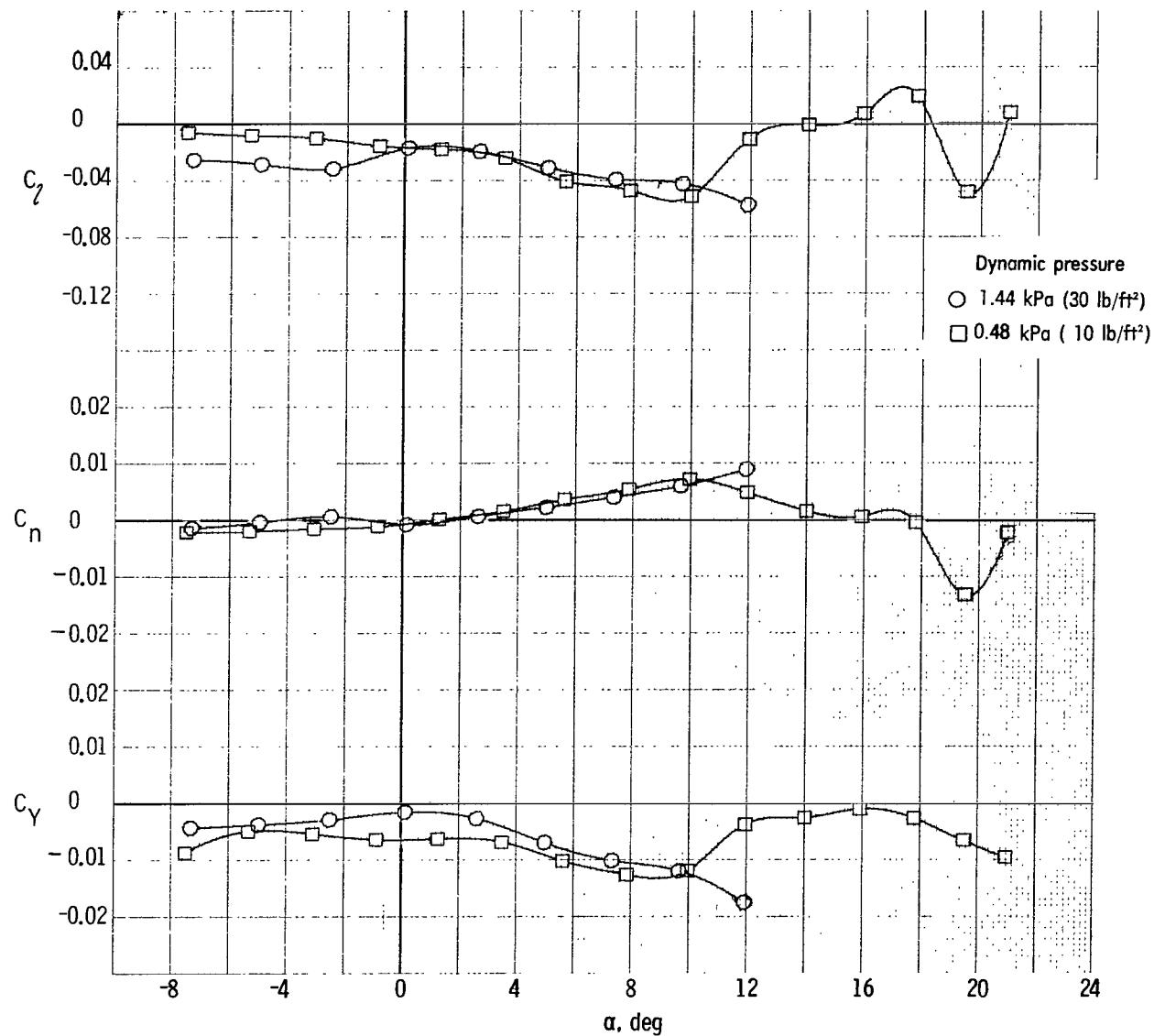
(d) Lateral characteristics; $\delta_f = 40^o$; $x/\bar{c} = 0.96$; large radius vent lip.

Figure 11.- Continued.
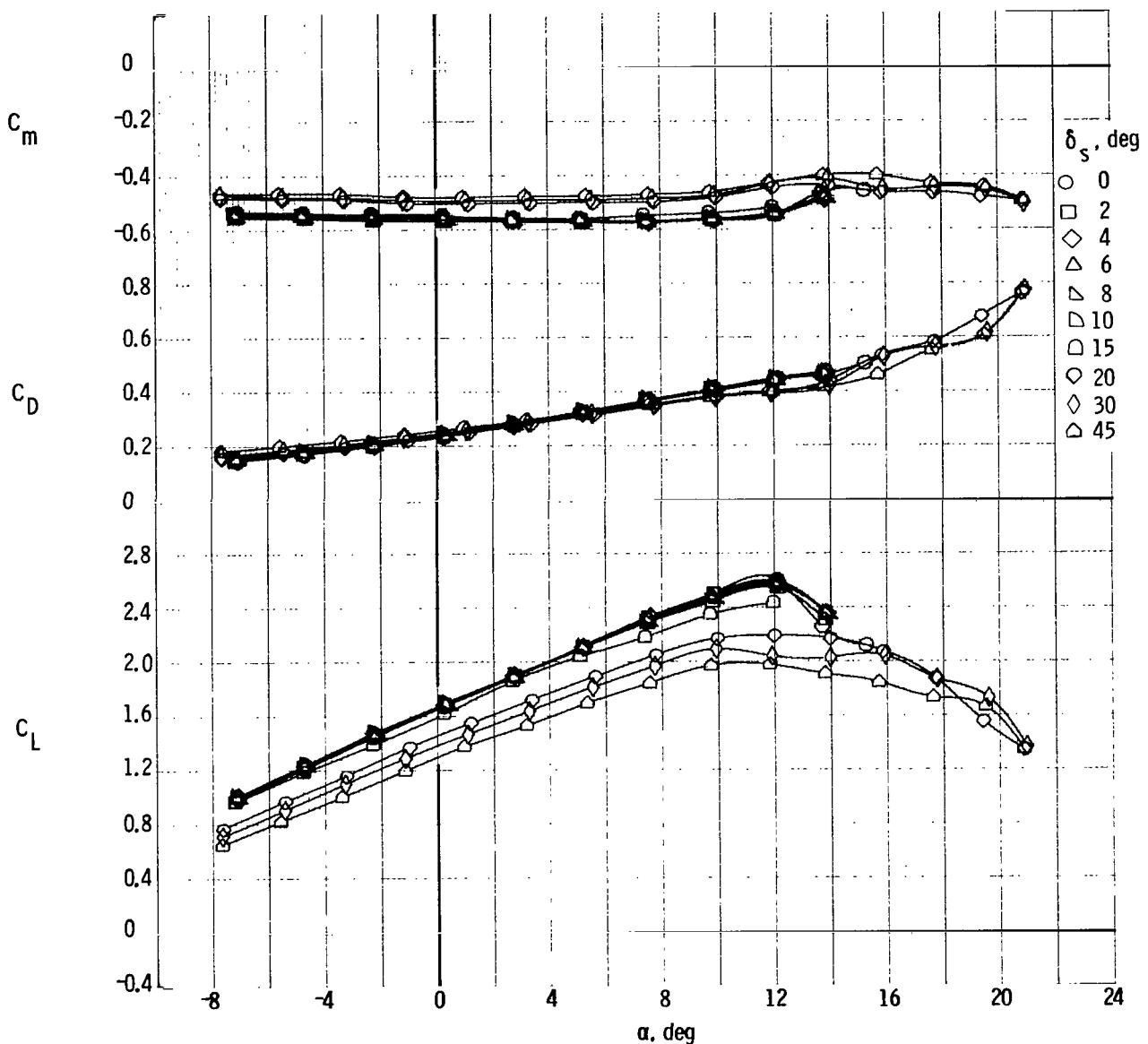
(e) Longitudinal characteristics; $\delta_f = 40^O$; $x/\bar{c} = 1.00$; sharp vent lip.

Figure 11.- Continued.
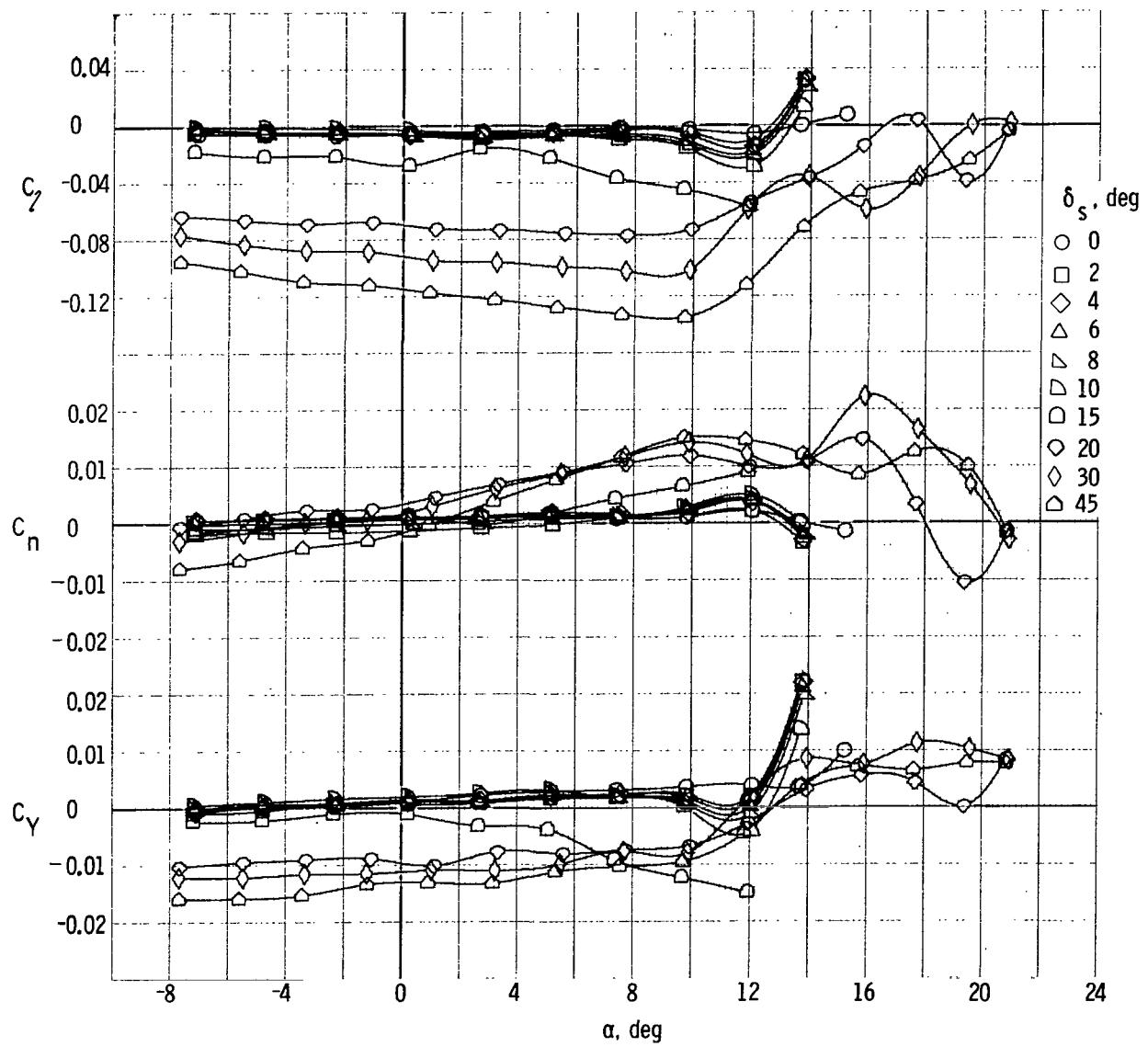
(f) Lateral characteristics; $\delta_f = 40^o$; $x/\bar{c} = 1.00$; sharp vent lip.

Figure 11.- Concluded.
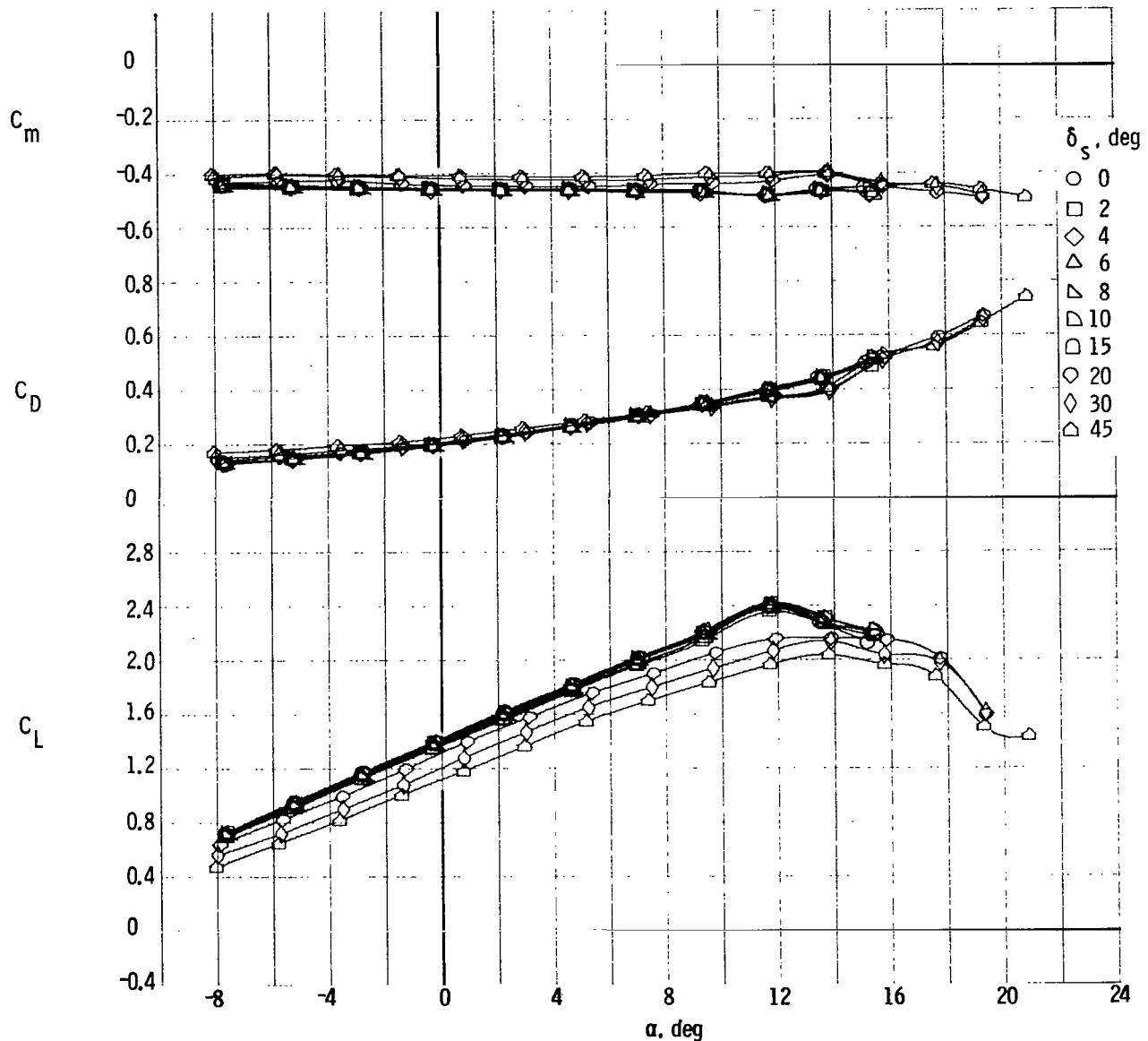
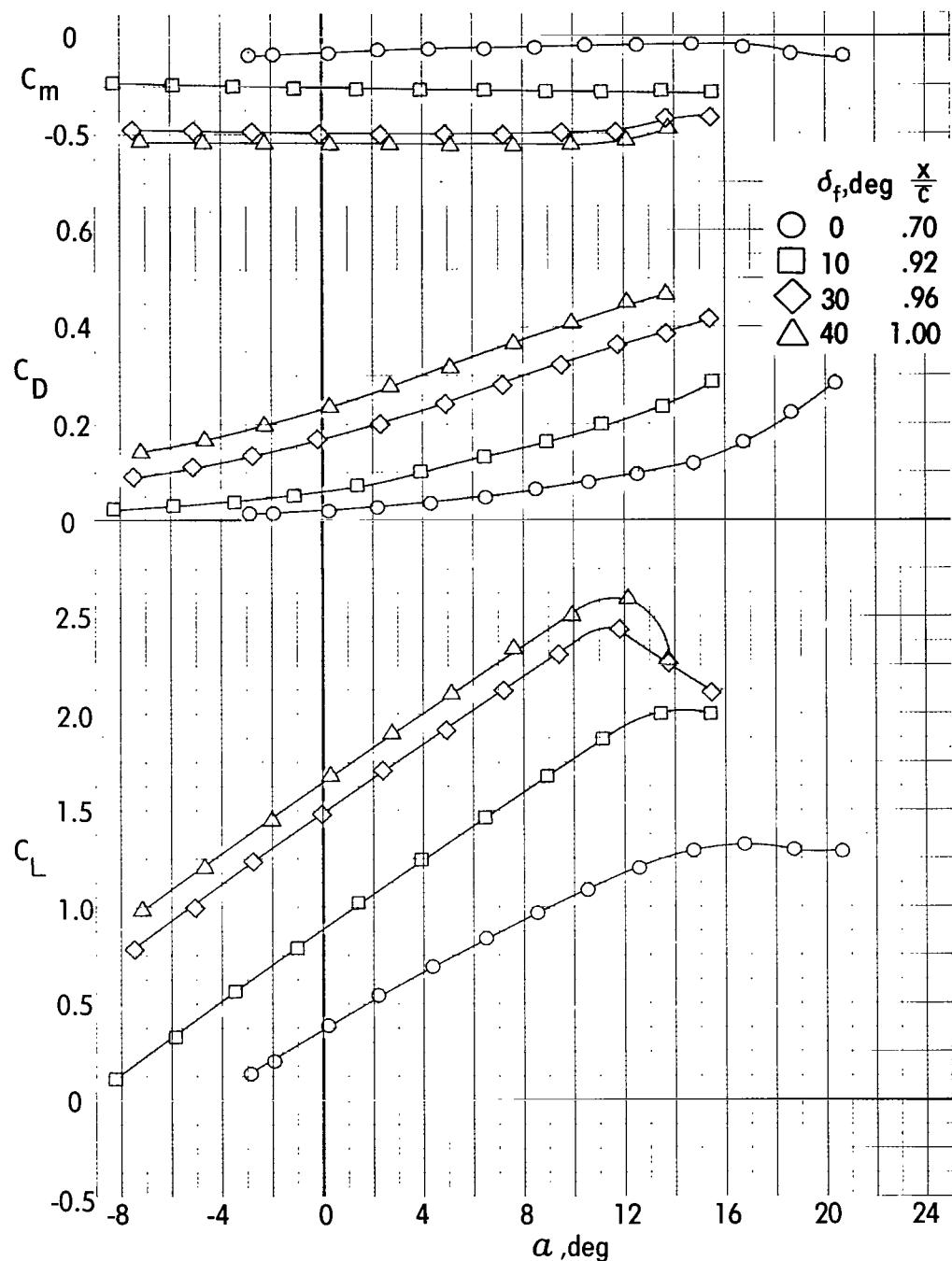(a) Longitudinal characteristics.

Figure 12.- Spoiler A characteristics with $\delta_f = 40^O$; $x/\bar{c} = 0.96$; large radius vent lip.
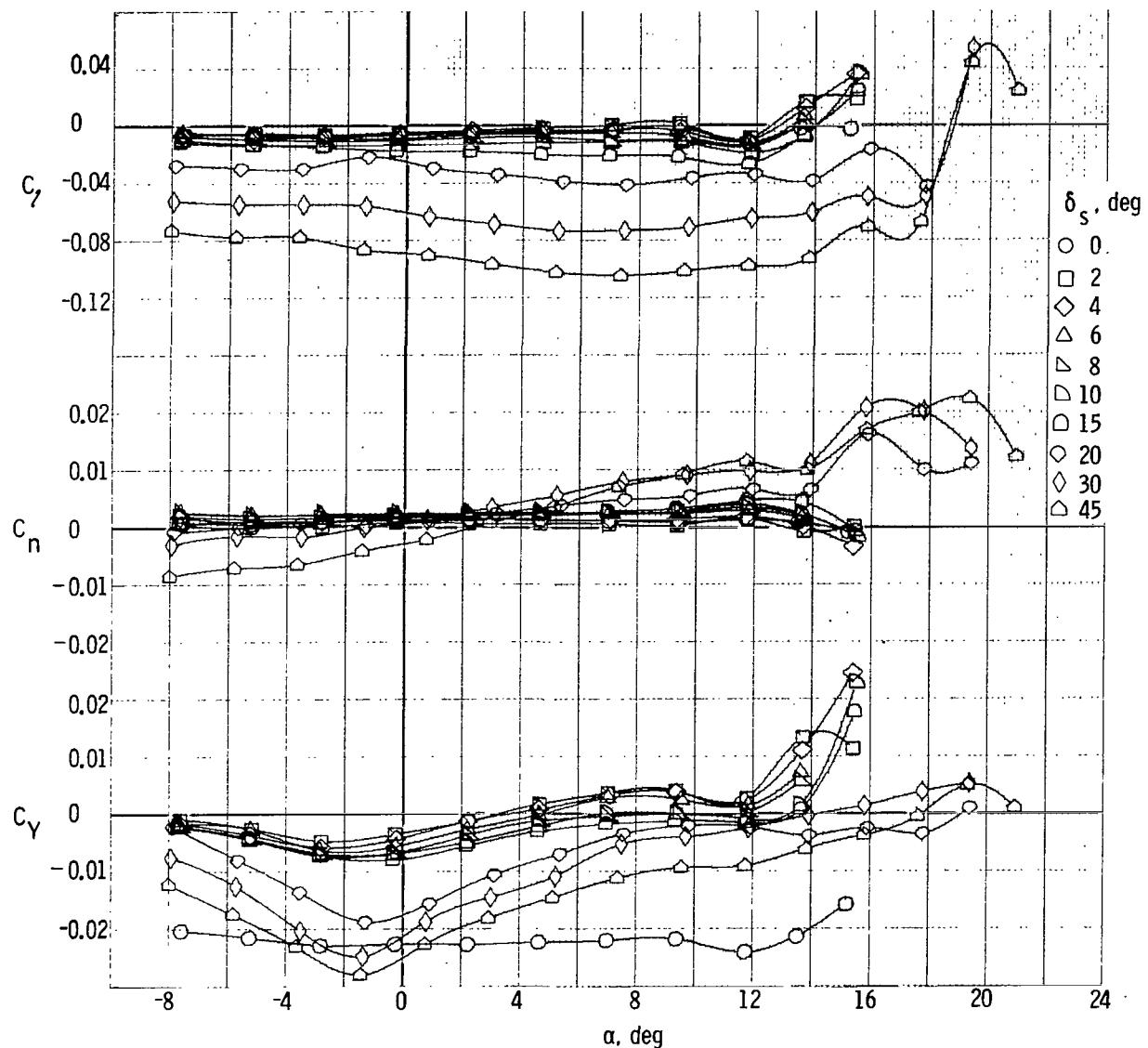
(b) Lateral characteristics.

Figure 12.- Concluded.
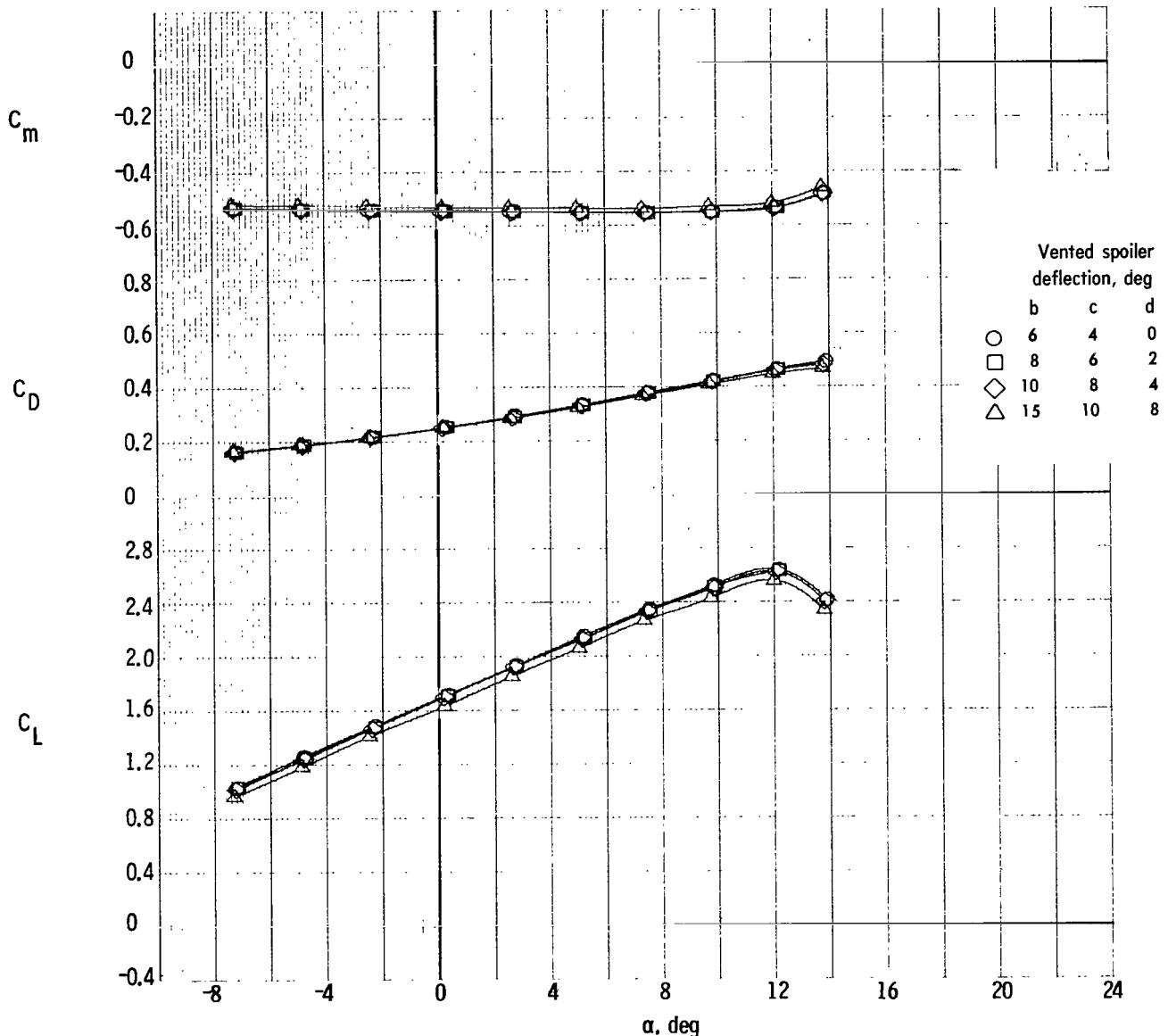
(a) Longitudinal characteristics, deflection sequence 1.

Figure 13.- Effects of sequential deflection of spoiler B elements b, c, and d
with $\delta_f = 40^O$; $x/\bar{c} = 1.00$; large radius vent lip.
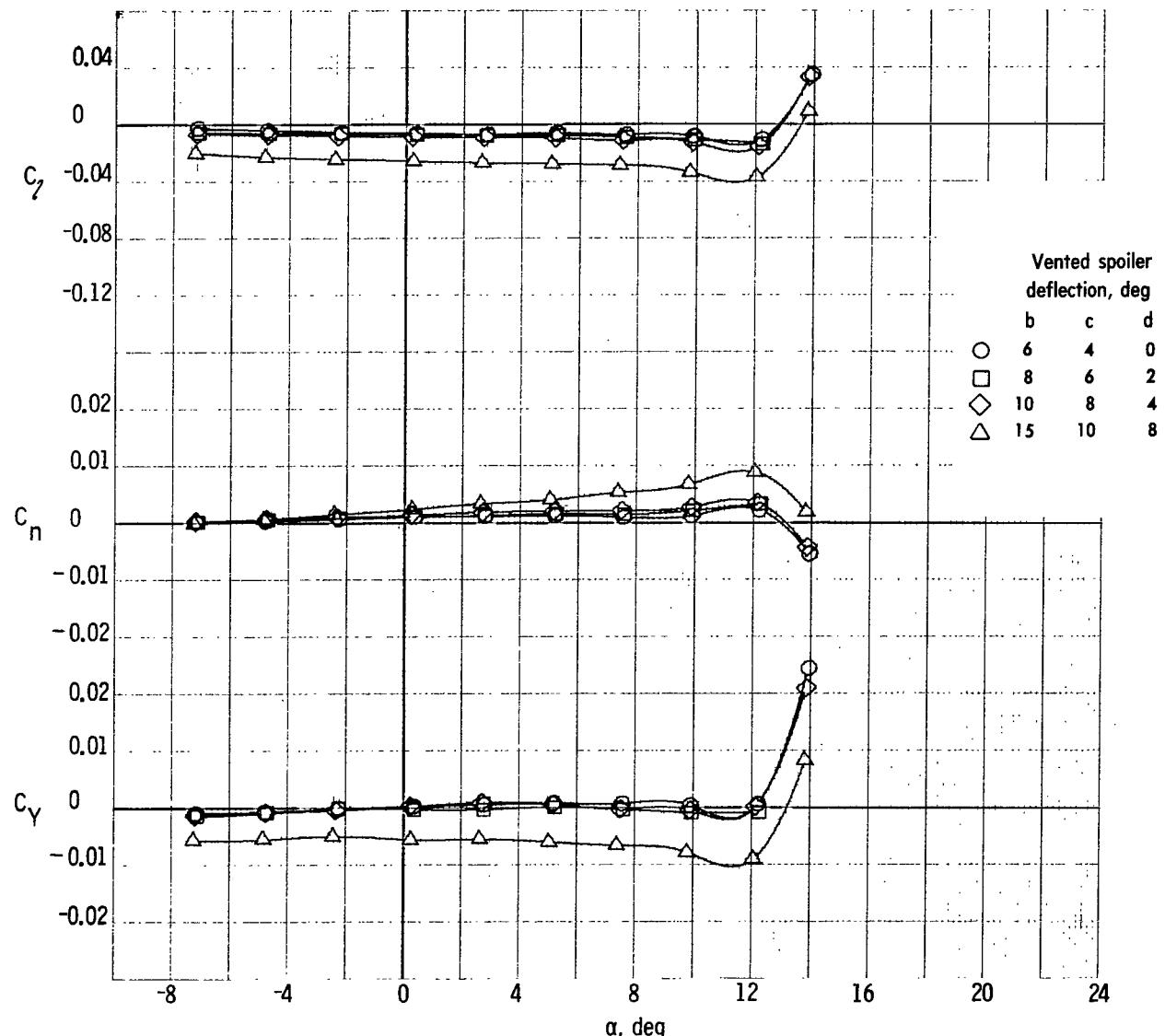
(b) Lateral characteristics, deflection sequence 1.

Figure 13.- Continued.
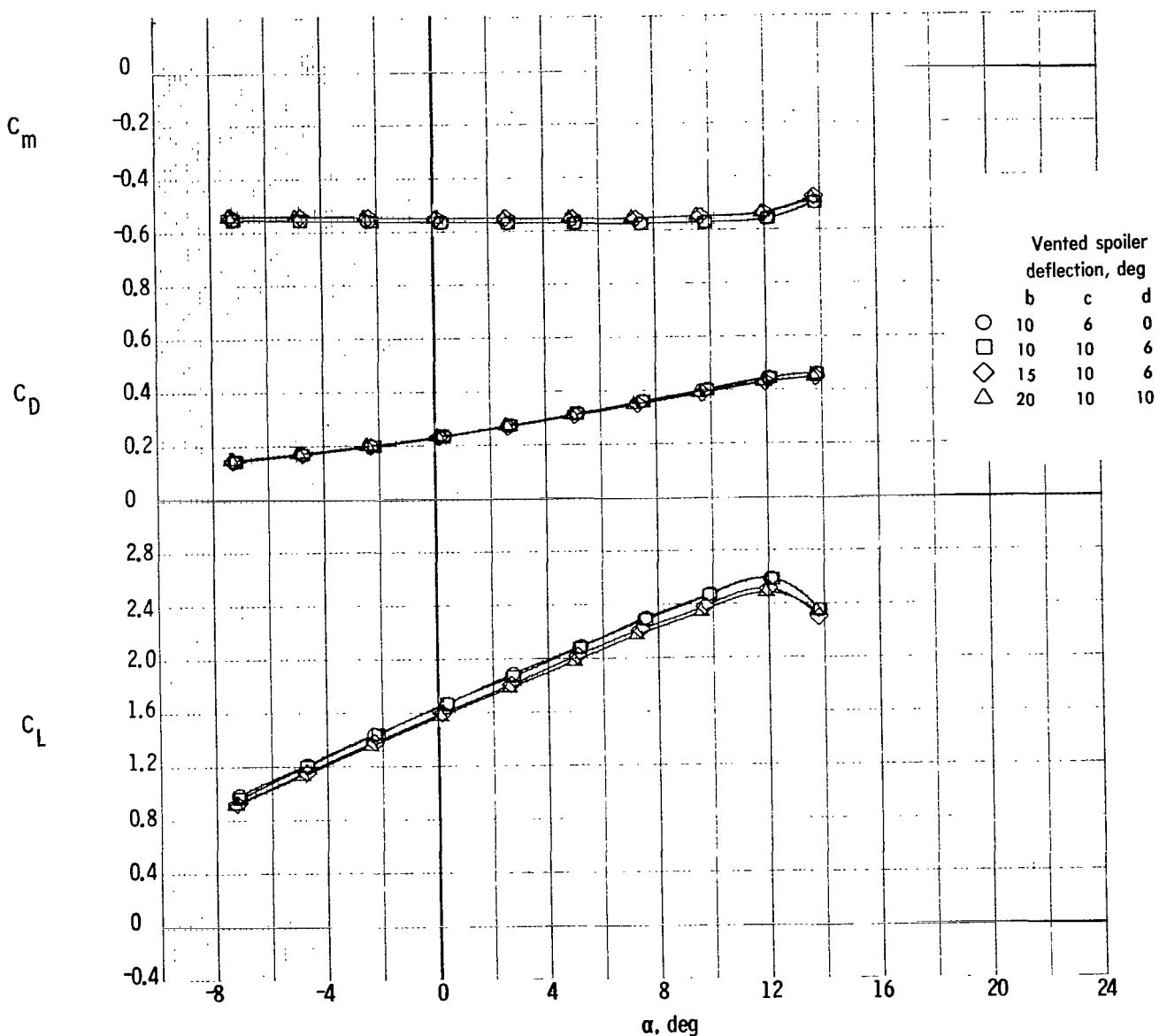
(c) Longitudinal characteristics, deflection sequence 2.

Figure 13.- Continued.
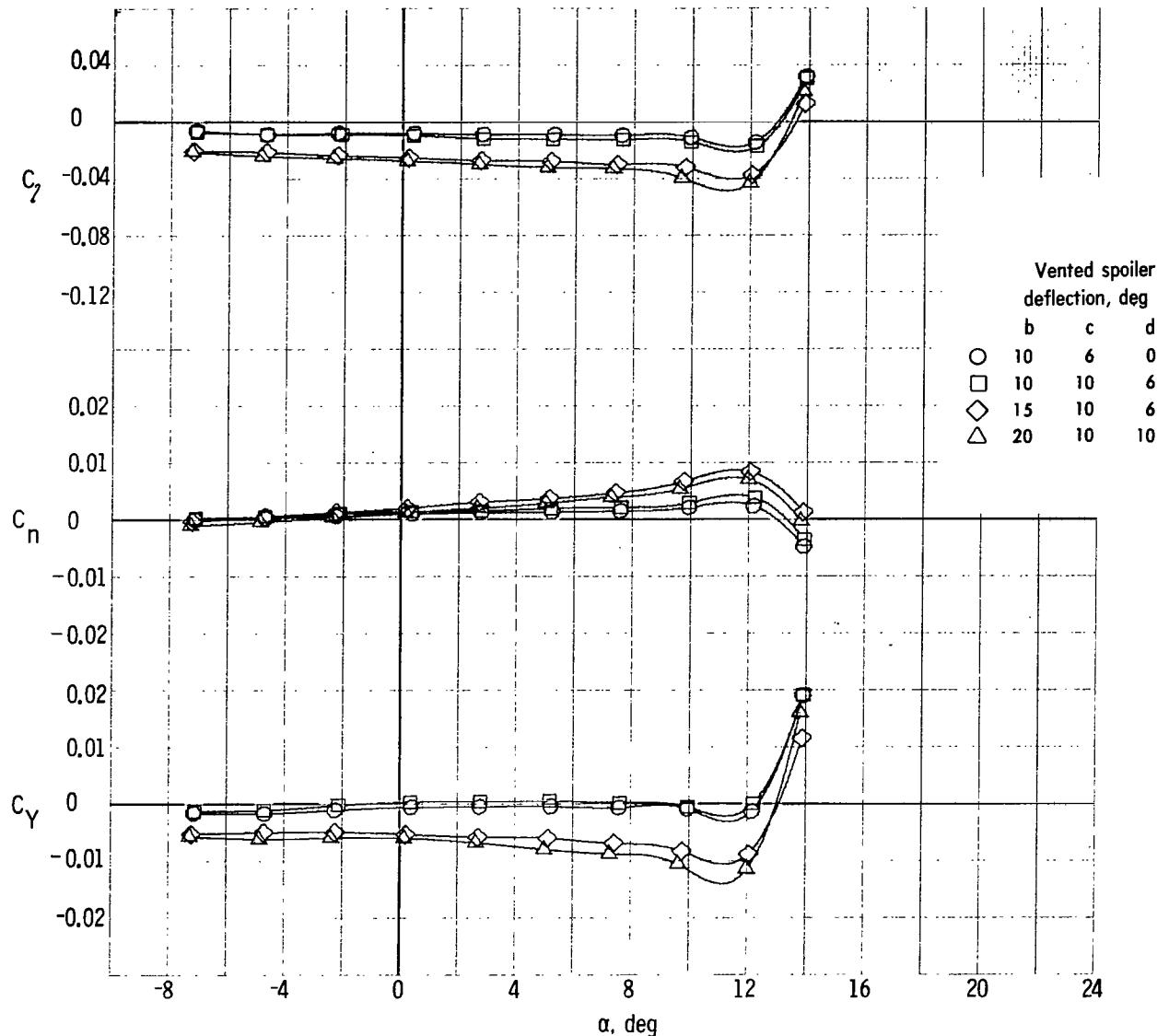
(d) Lateral characteristics, deflection sequence 2.

Figure 13.- Concluded.
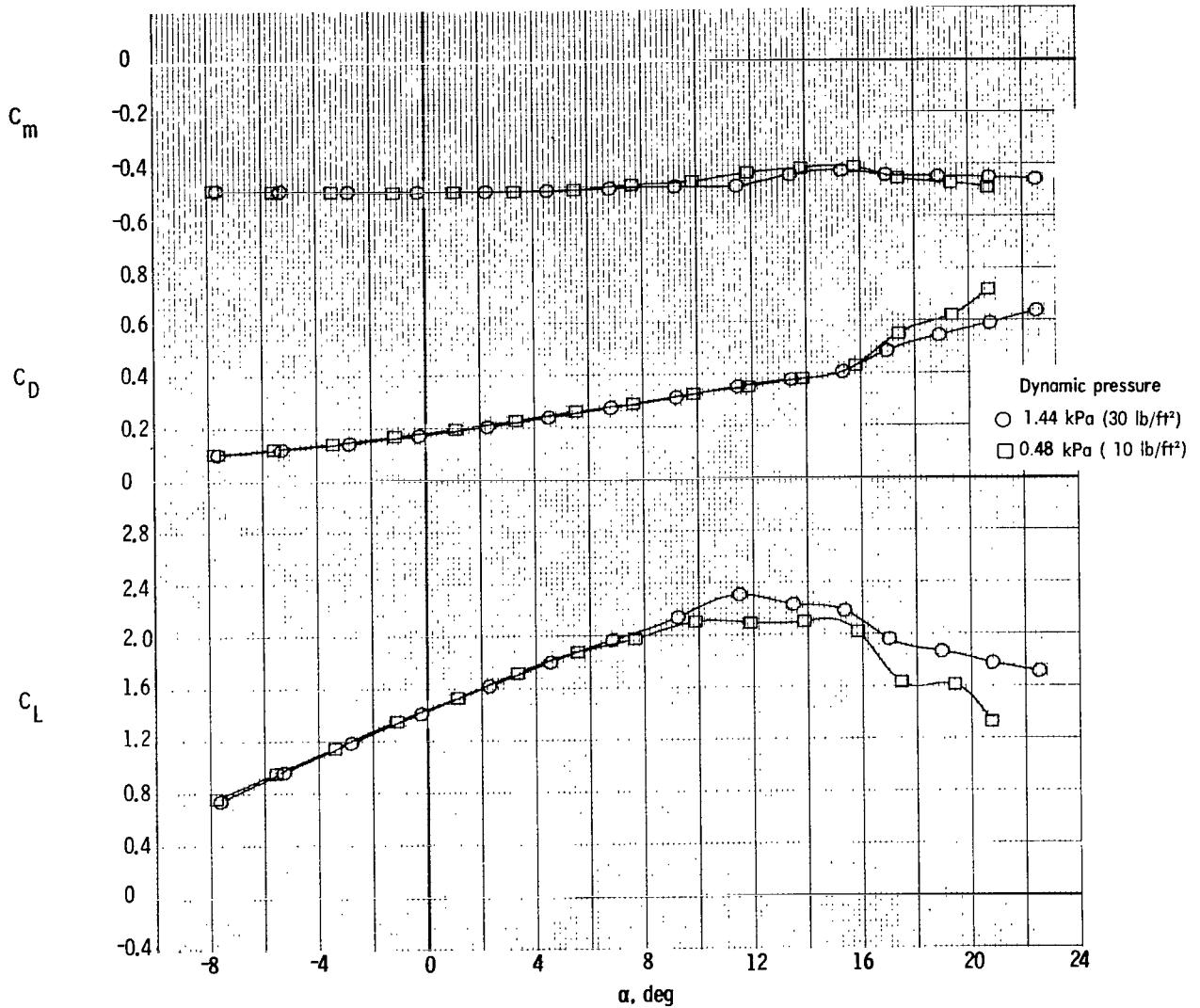
(a) Longitudinal characteristics; $\delta_f = 30°$; $x/\bar{c} = 0.96$; large radius vent lip.

Figure 14.- Effects of dynamic pressure on vented spoiler B characteristics.
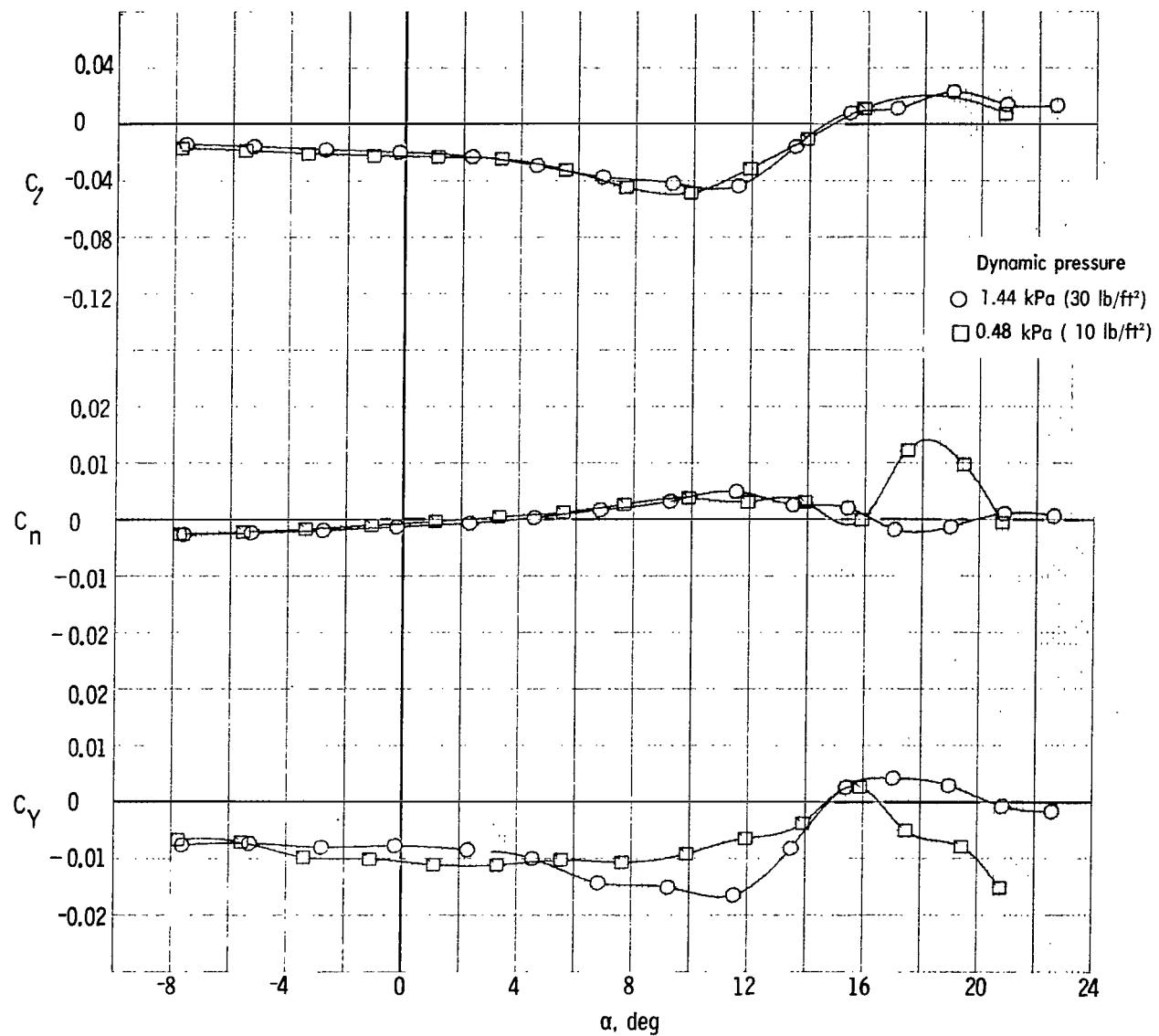
(b) Lateral characteristics; $\delta_f = 30^O$; $x/\bar{c} = 0.96$; large radius vent lip.

Figure 14.- Continued.
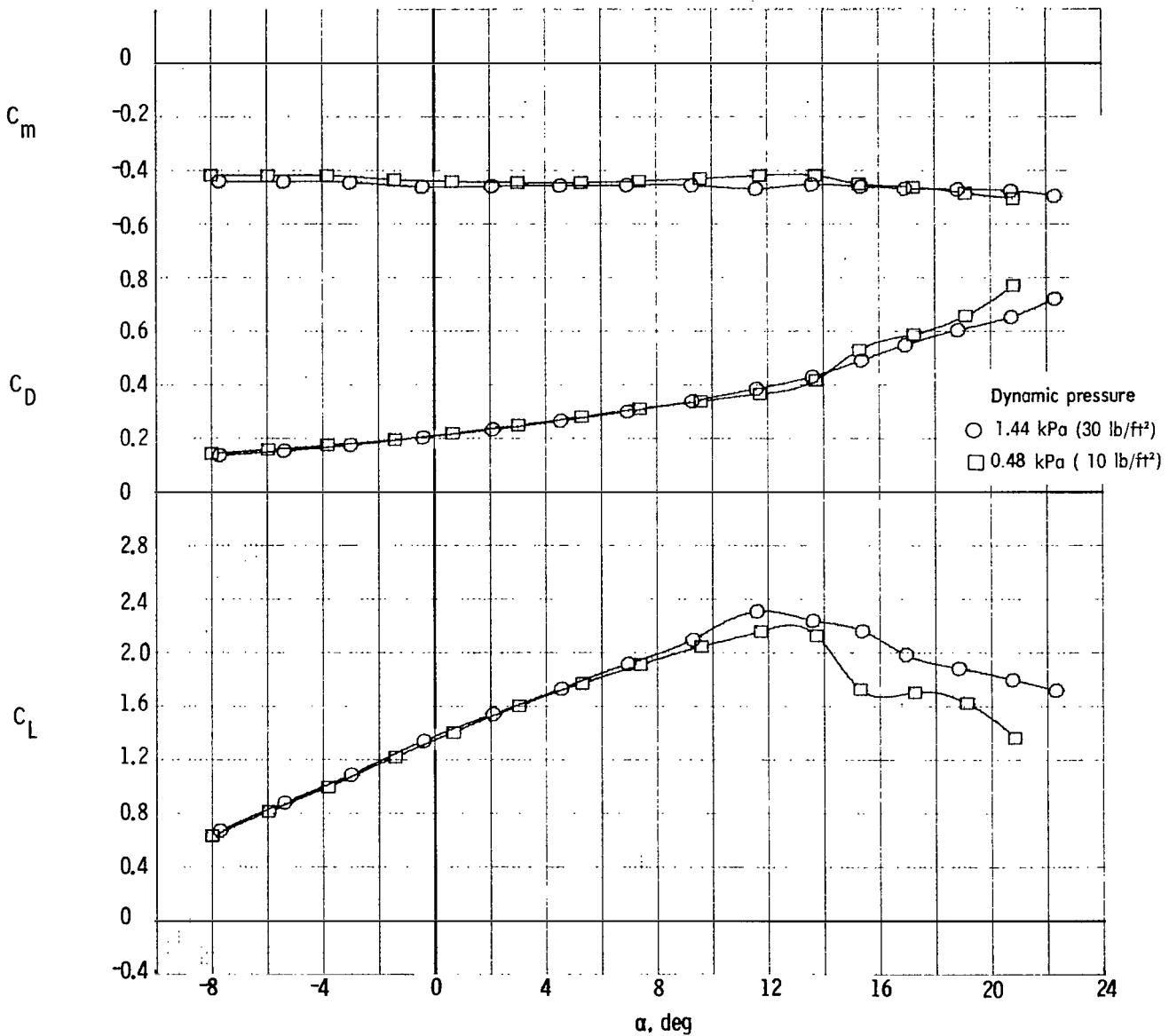
(c) Longitudinal characteristics; $\delta_f = 40^\circ$; $x/\bar{c} = 0.96$; blunt vent lip.

Figure 14.- Continued.

(d) Lateral characteristics; $\delta_f = 40^O$; $x/\bar{c} = 0.96$; blunt vent lip.

Figure 14.- Continued.
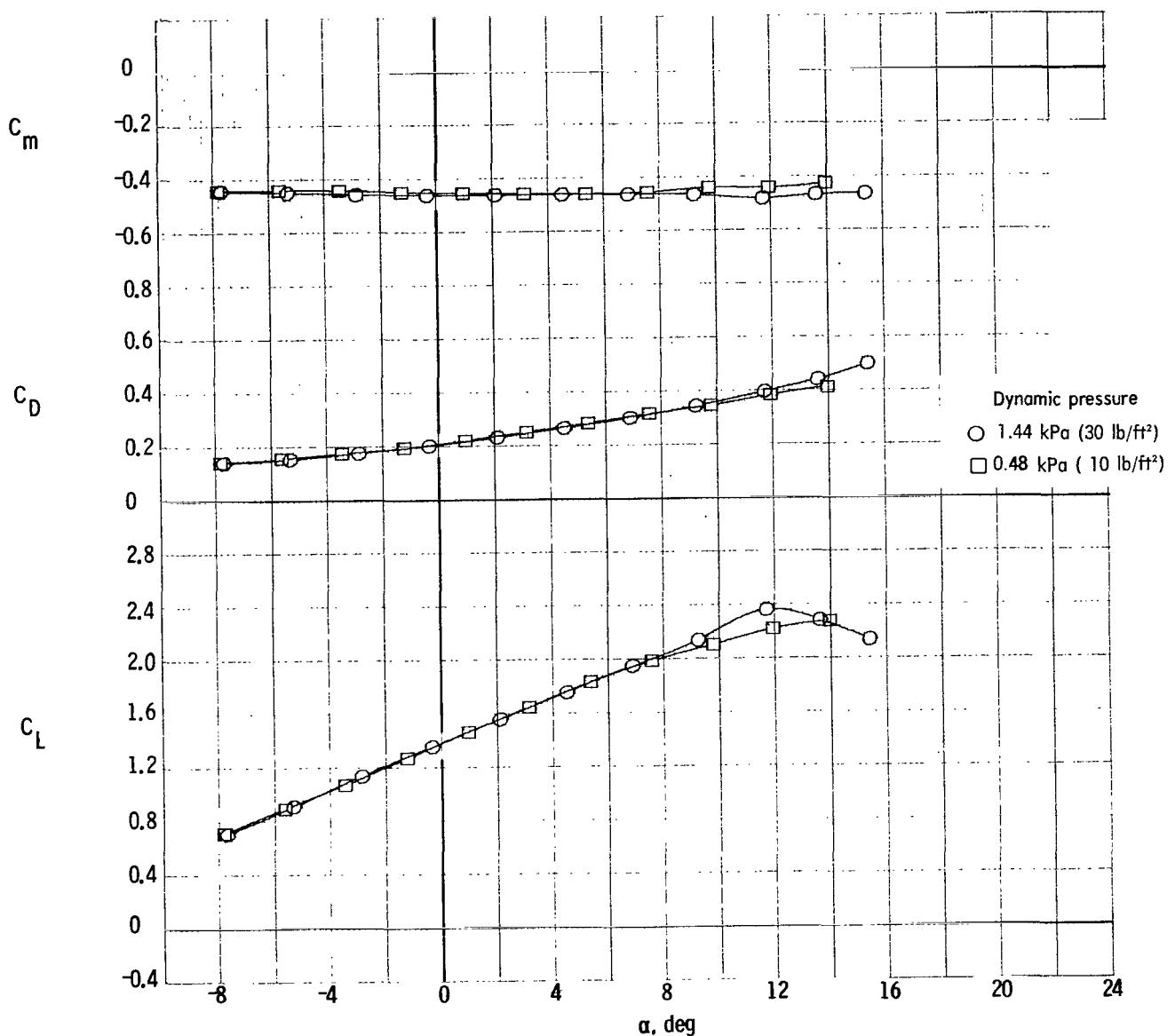
(e) Longitudinal characteristics; $\delta_f = 40^\circ$; $x/\bar{c} = 0.96$; large radius vent lip.

Figure 14.- Continued.
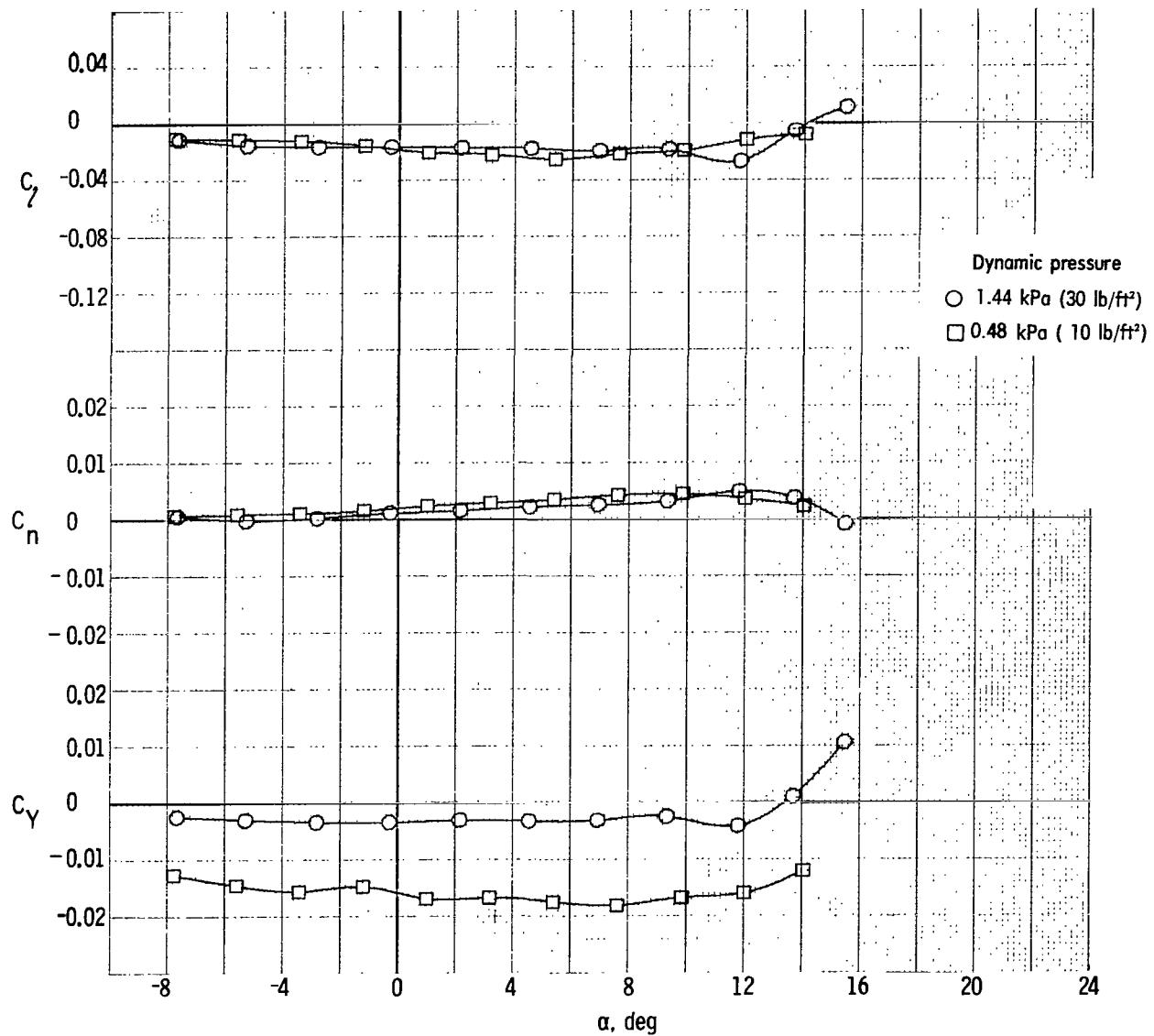
(f) Lateral characteristics; $\delta_f = 40^o$; $x/\bar{c} = 0.96$; large radius vent lip.

Figure 14.- Continued.

(g) Longitudinal characteristics; $\delta_f = 40^O$; $x/\bar{c} = 1.00$; large radius vent lip.

Figure 14.- Continued.

(h) Lateral characteristics; $\delta_f = 40^o$; $x/\bar{c} = 1.00$; large radius vent lip.

Figure 14.- Continued.

(i) Longitudinal characteristics; $\delta_f = 40°$; $x/\bar{c} = 1.00$;   blunt vent lip.

Figure 14.- Continued.

(j) Lateral characteristics; $\delta_f = 40^O$; $x/\bar{c} = 1.00$; blunt vent lip.

Figure 14.- Concluded.

Figure 15.- Effects of several flap positions and deflections on longitudinal characteristics of wing.
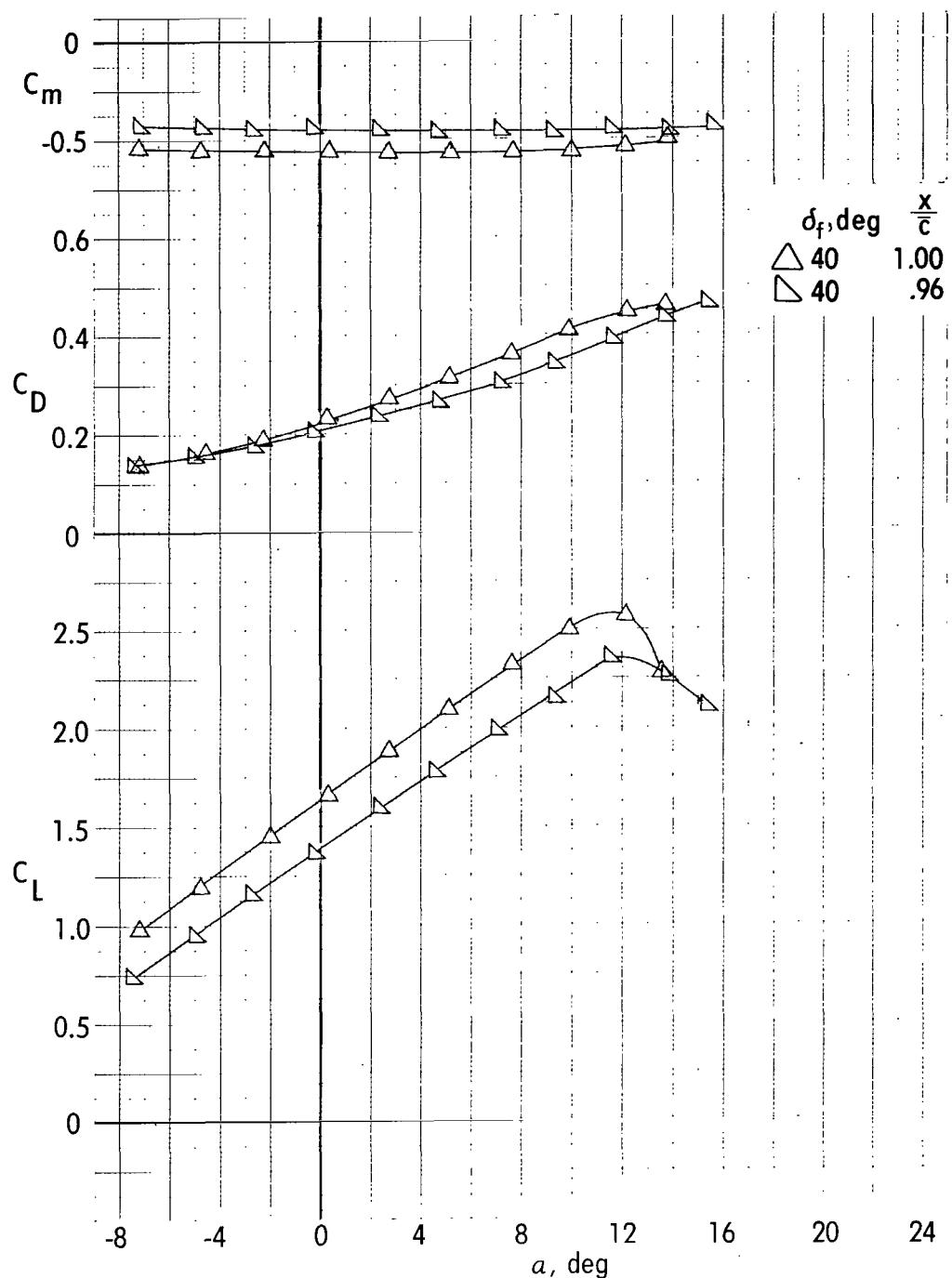
Figure 15.- Concluded.
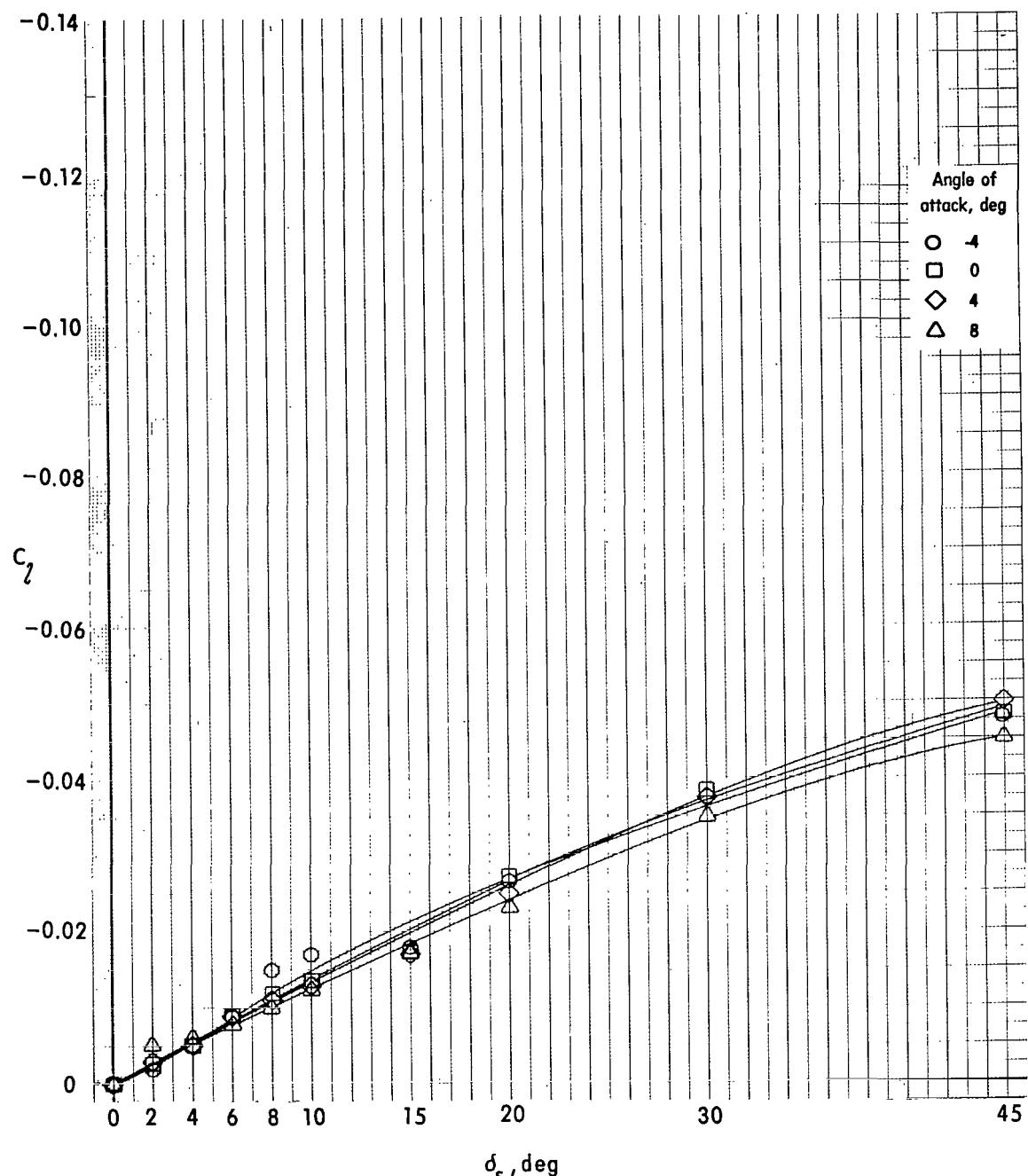
(a) $\delta_f = 0^O$; $x/\bar{c} = 0.713$.

Figure 16.- Effects of flap position and deflections and angle of attack on rolling moments generated by deflecting spoiler B with large radius vent lip.
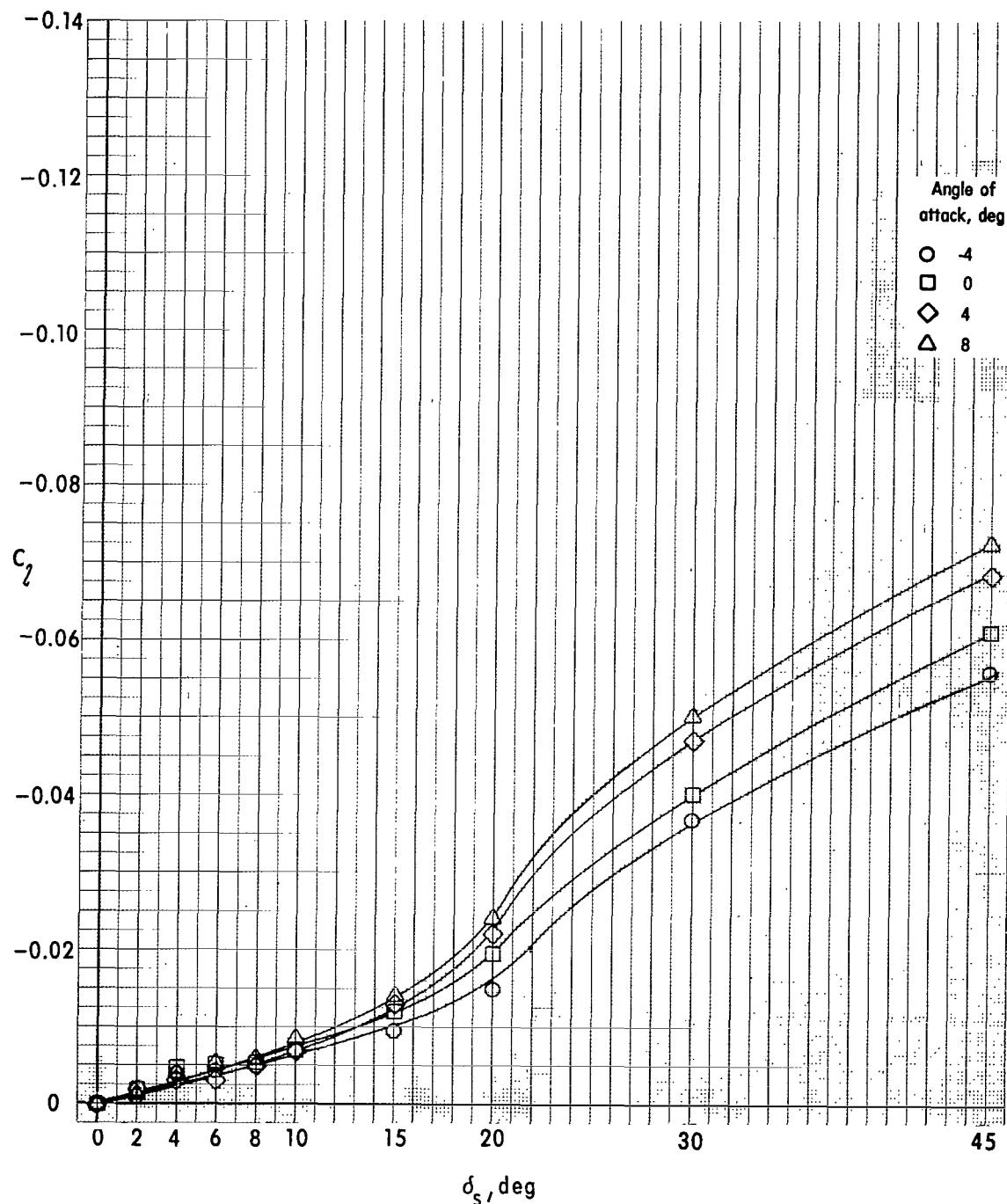
(b) $\delta_f = 10^O$; $x/\bar{c} = 0.917$.

Figure 16.- Continued.
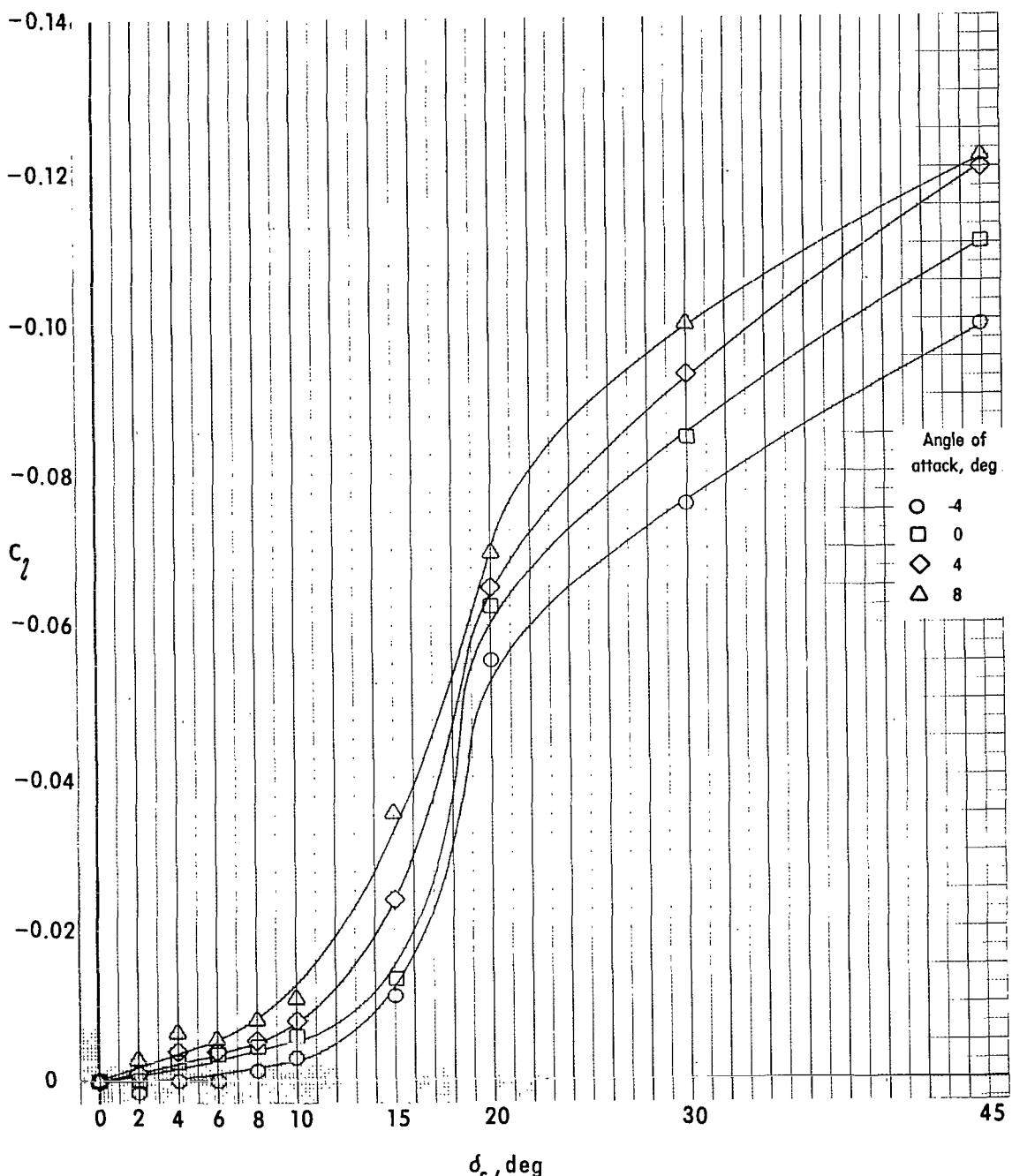
(c) $\delta_f = 30^O$; $x/\bar{c} = 0.960$.

Figure 16.- Continued.
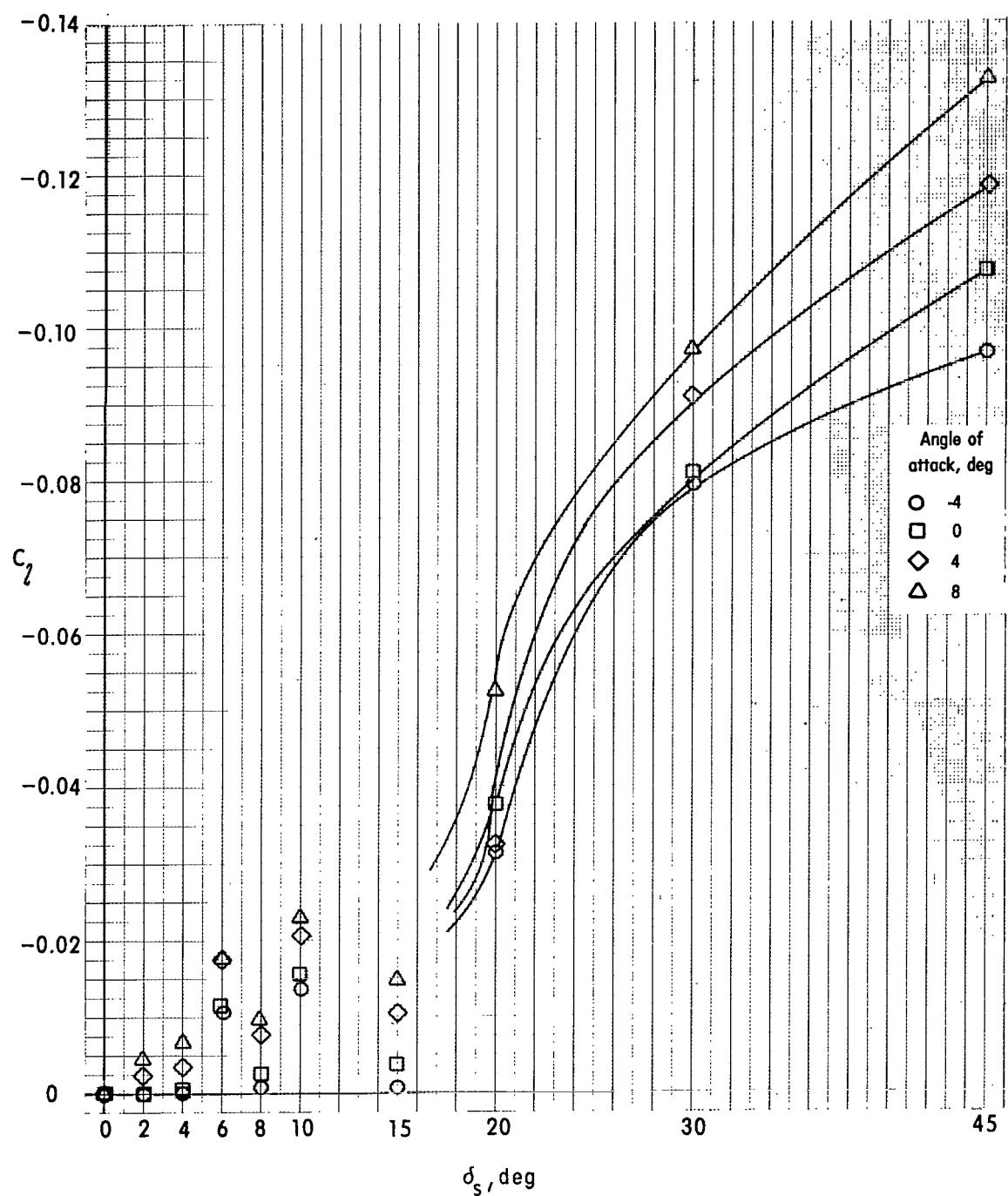
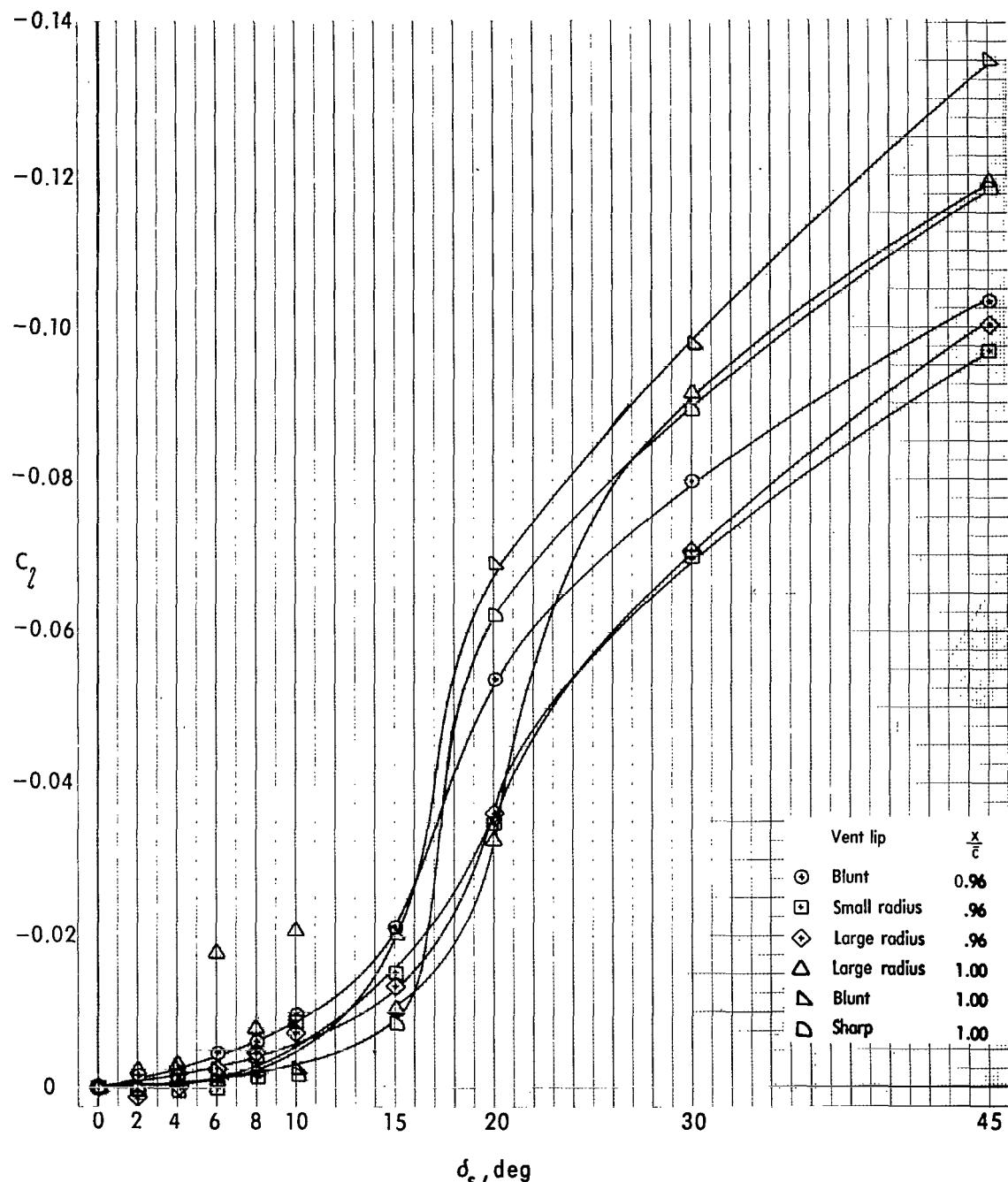(d) $\delta_f = 40^O$; $x/\bar{c} = 1.00$.

Figure 16.- Concluded.

(a) $\alpha = -4^{\mathrm{O}}$.
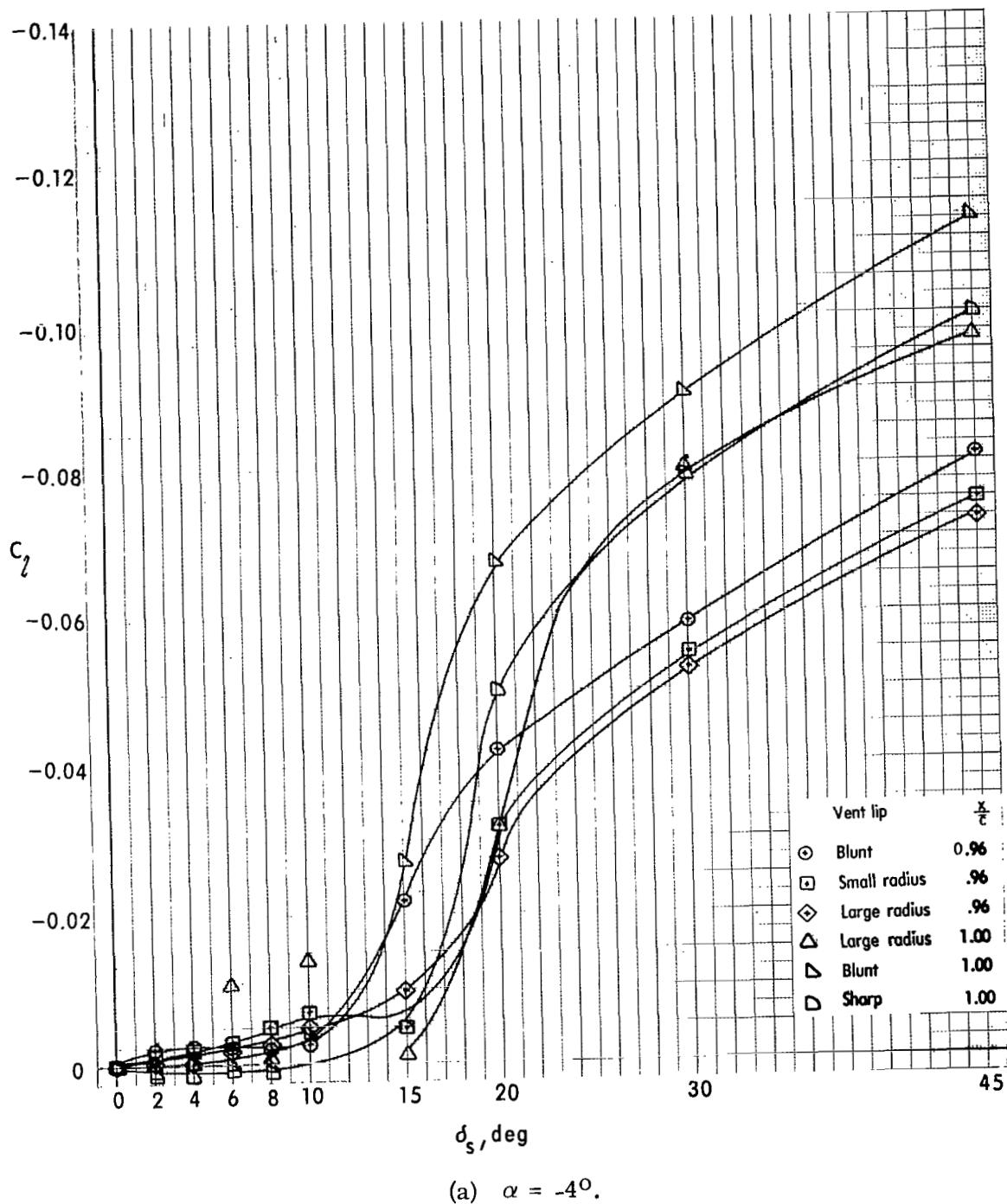
Figure 17.- Effects of vent-lip geometry and angle of attack on rolling moments generated by deflecting spoiler B with $\delta_f = 40^{\mathrm{O}}$ and $x/\bar{c} = 0.96$ and 1.00.
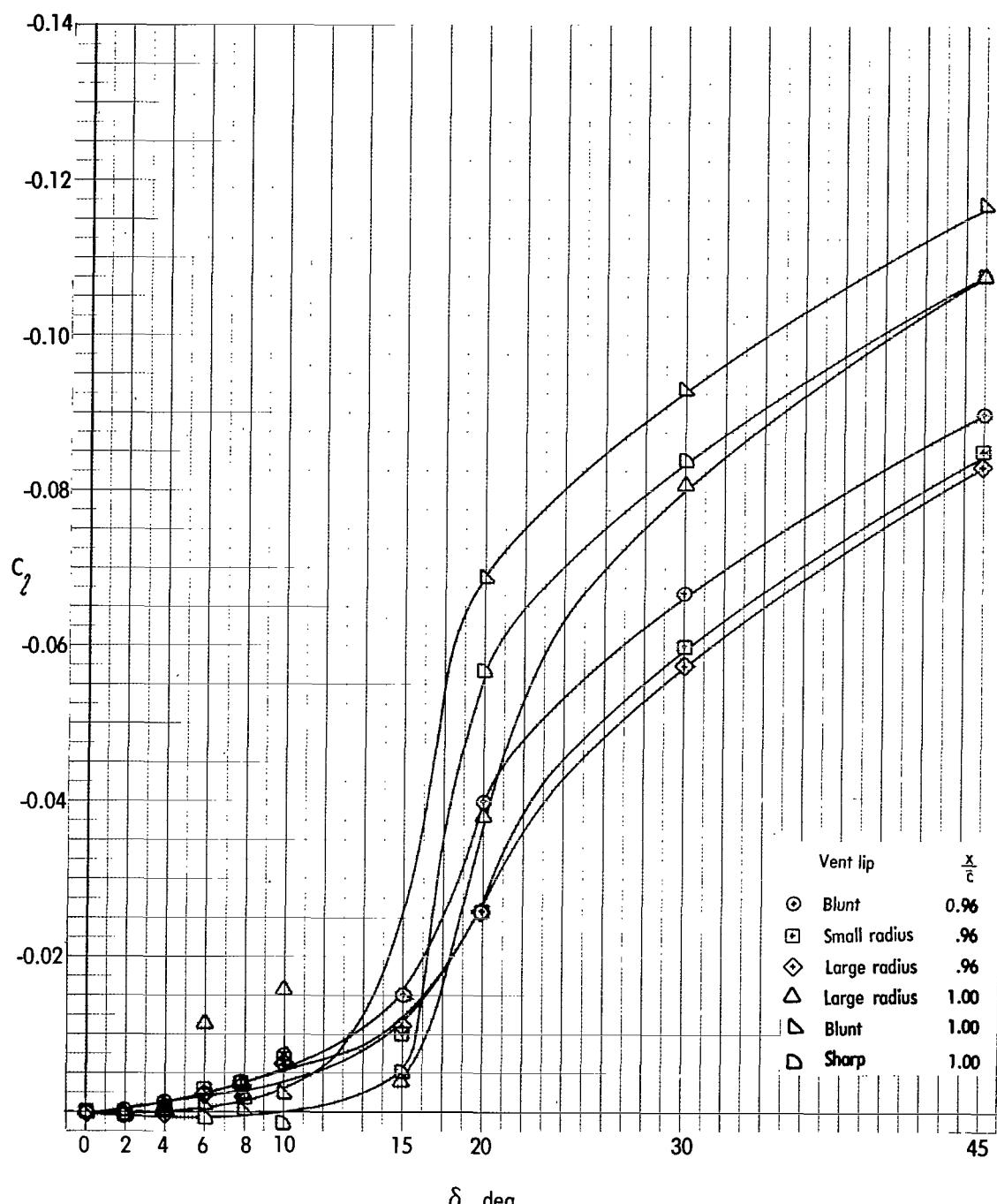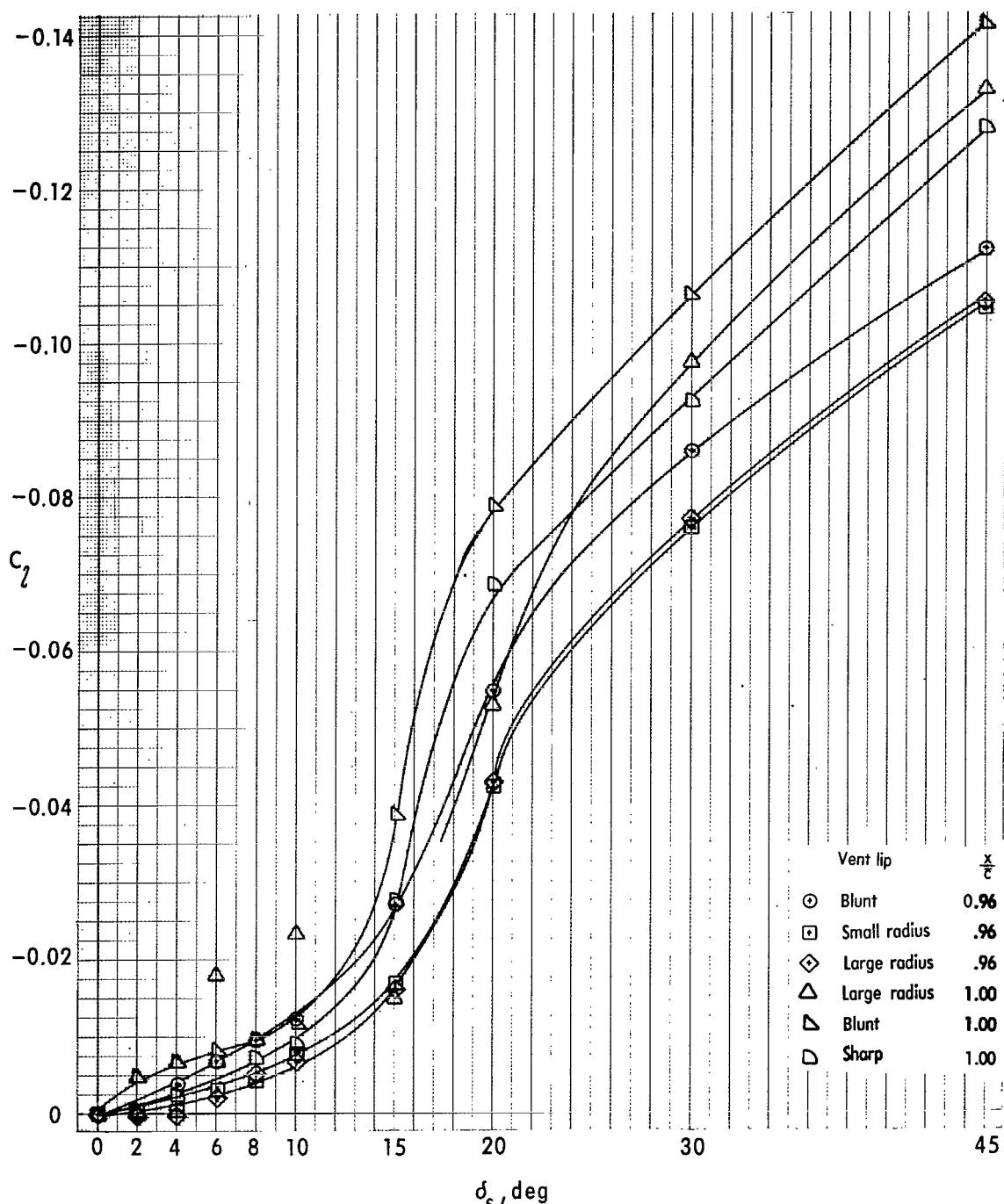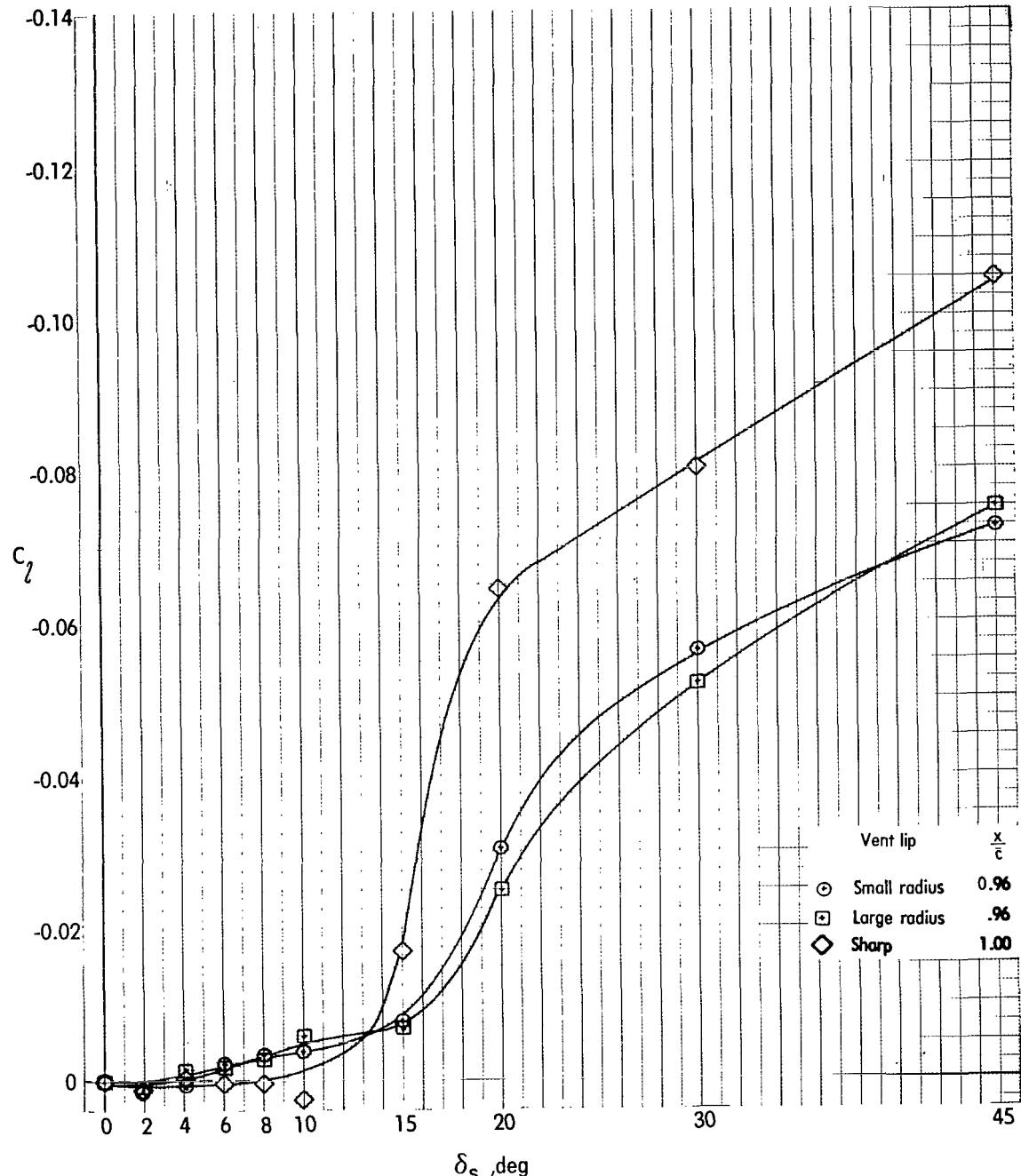
(b) $\alpha = 0^{\circ}$.

Figure 17.- Continued.

(c) $\alpha = 4^{\circ}$.

Figure 17.- Continued.

(d) $\alpha = 8°$.

Figure 17.- Concluded.

(a) $\alpha = -4^o$.

Figure 18.- Effects of vent-lip geometry and angle of attack on rolling moments generated by deflecting spoiler C with $\delta_f = 40^o$ and $x/\bar{c} = 0.96$ and 1.00.
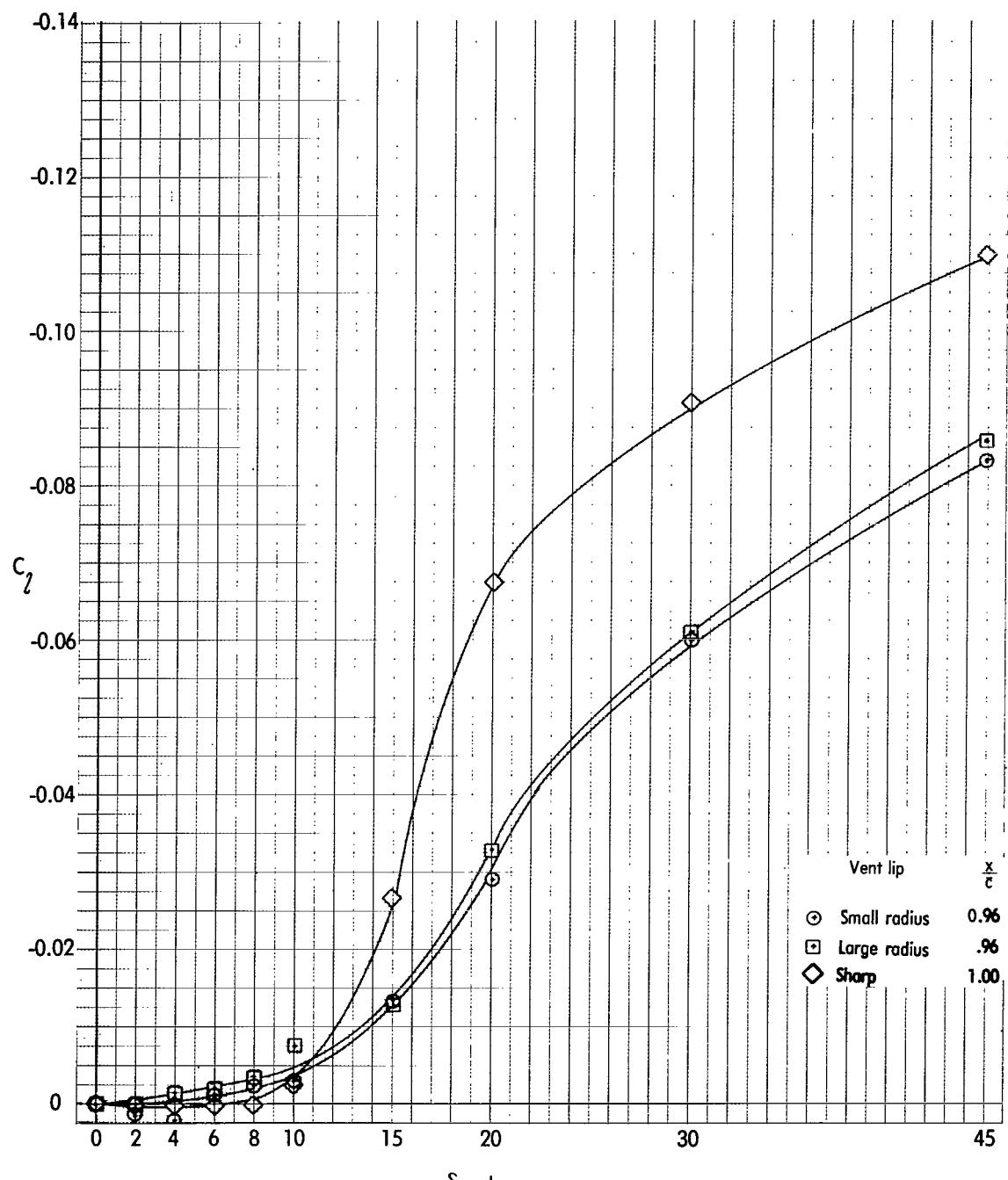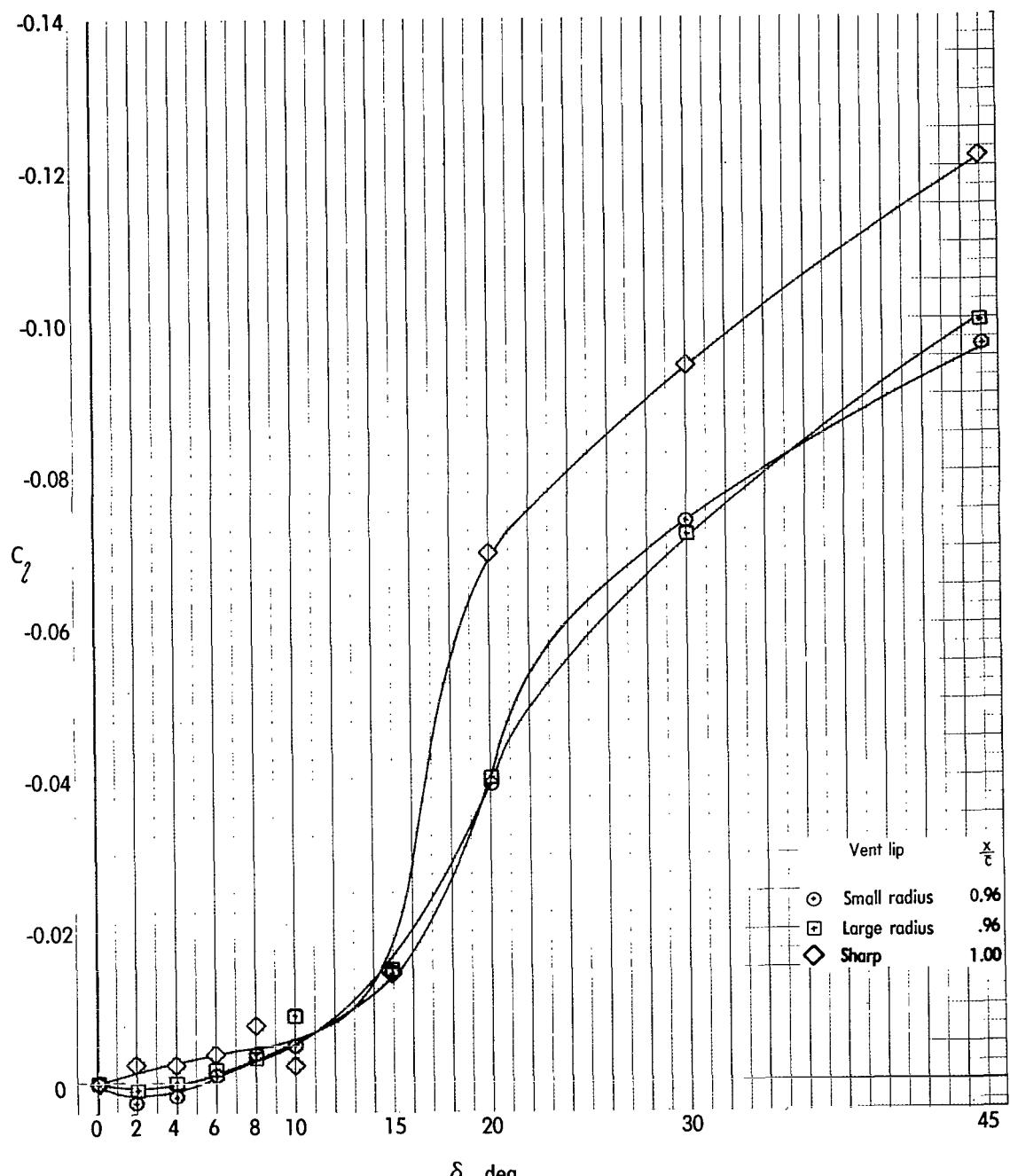
(b) $\alpha = 0^O$.

Figure 18.- Continued.

(c) $\alpha = 4^{\circ}$.

Figure 18.- Concluded.
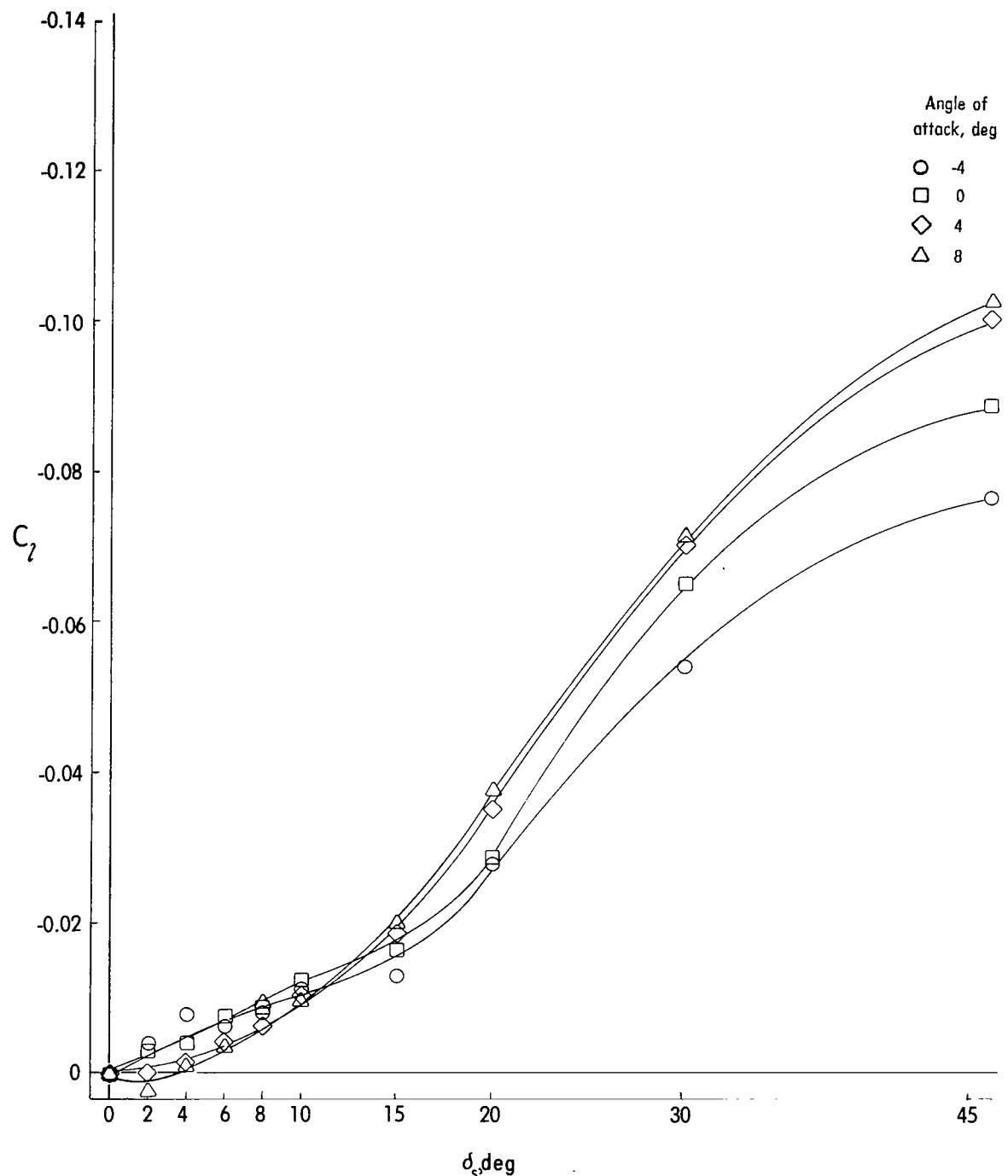
Figure 19.- Effect of angle of attack on rolling moments generated by deflecting spoiler A; $\delta_f = 40^O$ and $x/\bar{c} = 0.96$.

"The aeronautical and space activities of the United States shall be conducted so as to contribute . . . to the expansion of human knowledge of phenomena in the atmosphere and space. The Administration shall provide for the widest practicable and appropriate dissemination of information concerning its activities and the results thereof."
—NATIONAL AERONAUTICS AND SPACE ACT OF 1958

NASA SCIENTIFIC AND TECHNICAL PUBLICATIONS

TECHNICAL REPORTS: Scientific and technical information considered important, complete, and a lasting contribution to existing knowledge.

TECHNICAL NOTES: Information less broad in scope but nevertheless of importance as a contribution to existing knowledge.

TECHNICAL MEMORANDUMS: Information receiving limited distribution because of preliminary data, security classification, or other reasons. Also includes conference proceedings with either limited or unlimited distribution.

CONTRACTOR REPORTS: Scientific and technical information generated under a NASA contract or grant and considered an important contribution to existing knowledge.

TECHNICAL TRANSLATIONS: Information published in a foreign language considered to merit NASA distribution in English.

SPECIAL PUBLICATIONS: Information derived from or of value to NASA activities. Publications include final reports of major projects, monographs, data compilations, handbooks, sourcebooks, and special bibliographies.

TECHNOLOGY UTILIZATION PUBLICATIONS: Information on technology used by NASA that may be of particular interest in commercial and other non-aerospace applications. Publications include Tech Briefs, Technology Utilization Reports and Technology Surveys.

Details on the availability of these publications may be obtained from:

SCIENTIFIC AND TECHNICAL INFORMATION OFFICE

NATIONAL AERONAUTICS AND SPACE ADMINISTRATION

Washington, D.C. 20546